Faculty of Engineering

Department of Electrical, Computer and Telecommunications Engineering

VERTICAL CAVITY SURFACE EMITING LASER FOR OPTICAL COMMUNICATION SYSTEMS.

by

OGOMODITSE ODUETSE MOATLHODI

Student ID number: 13001490

BEng (Telecommunications) (BIUST)

A Dissertation/Thesis Submitted to the Faculty of Engineering in Partial Fulfilment of the Requirements for the Award of the Degree of Master of Engineering in Electrical and Electronics, BIUST.

Supervisor(s): Dr. Nonofo M. J. Ditshego

Prof. Ravi Samikannu

Department of Electrical, Computer and Telecommunications.

Faculty of Engineering, BIUST

Declaration of Authorship

I Ogomoditse O. MOATLHODI, declare that this missive titled, "VERTICAL CAVITY SURFACE EMITTING LASER FOR OPTICAL COMMUNICATION SYSTEMS" and the work presented in it are authored by me. I confirm that:

1. This work was done wholly or mainly while in candidature for a research degree at this University.
2. I am aware that the thesis in digital form can be examined for the habituate of unauthorised aid and in order to ad measure whether the thesis as whole or parts Incorporated in it may be deemed as copy right infringement.
3. This paper has never been submitted elsewhere to any board for consideration.
4. All direct or indirect sources used are acknowledged as references.
5. I have acknowledged all main sources of help.
6. Where the thesis is based on work done by myself jointly with the supervision of help of others, I have made clear exactly what was done by others and what I have contributed myself.

Signed: 

Date: February 3, 2022

"...In as much as the nation has got policies, vision and mission, constitution as well as different ministries that contribute to the successful running of the nation, so is the family supposed to subscribe to the same order of operation. In fact such should be seen in intentional application at a family setup. Look around my guy, look at how many people have forsaken and have been forsaken by their families. It has become an order of life now in many communities that a family member can lack something which a brother who sleeps in the next room has in excess but wouldn't care to help. Buddy I don't know what the world is running into, but living life in this continued trajectory will further divide our efforts and our chances of maximizing our potentials. I have come to realise that the diversity of consolidation of resources to ensure great execution of dreams, family mission and positive national impact...."

Tumelo Sitayelo

BOTSWANA INTERNATIONAL UNIVERSITY OF SCIENCE & TECHNOLOGY

Abstract

Faculty of Engineering & Technology
Department of Electrical, Computer and Telecommunications

Master of Engineering, Electrical and Electronics

VERTICAL CAVITY SURFACE EMITTING LASER FOR OPTICAL COMMUNICATION SYSTEMS

by Ogomoditse O. MOATLHODI

The minimal cost, high efficiency and low power consumption of the Vertical Cavity Surface Emitting Laser (VCSEL) gives it an additional advantage when used in applications like fibre optical communication systems to meet the growth of data communication traffic. However, development of VCSELs working at longer wavelengths (1.3- 1.55 μm) has been limited by the inherent material problem making VCSELs longitudinal single-modes emitters. These problems among commonly used fibre optic transmitters (Light Emitting Diodes) include: limited efficiency, limited power output and incoherent light. Emitted power, threshold current and voltage are the main device characteristics studied in this research. The basic functionality of semiconductor lasers with improved output power performance is the main aim of this work. Comparisons of growth techniques and material selection gives the best material performance for nano optical sources used in optical communication systems. A seven Quantum Well Indium Gallium Arsenide Phosphide (InGaAsP) VCSEL structure that emits at 1550 nm is simulated and the following characteristics are analysed: Direct current and voltage (I-V) characteristics, light power against electrical bias, optical gain against electrical bias, light distribution over the structure, output power, threshold current and gain profiles. The specification of the material characteristics, the ordinary physical model settings, the initial VCSEL biasing, the mesh declarations, declaration of laser physical models, their optical and electrical parameters were defined using Atlas syntax. Mirror ratings and Quantum Wells are the two main parameters that were studied and analysed. Proper selection of the emission wavelength and choice of material was done and a VCSEL with an output power of 9.5 mW was simulated and compared with other structures.

Acknowledgements

I would like to express my gratitude to my primary supervisors, Dr Nonofo Ditshego and Prof Ravi Samikannu, who guided me throughout this research. I would also like to thank my friends, family, the department of Electrical, Computer and Telecommunications and the Botswana International University of Science and Technology who supported me, offered deep insight and provided me with such a great opportunity to my studies.

Contents

Declaration of Authorship **i**

Abstract **iii**

Acknowledgements **iv**

List of Figures **viii**

List of Tables **x**

List of Abbreviations **xi**

Physical Constants **xiii**

List of Symbols **xiv**

1 Introduction **1**
1.1 Background of optical communication 2
1.2 Problem statement 4
1.3 Overall research aim 5
1.3.1 Research objectives 5
1.4 Justification of study 5
1.5 Chapter summary 5
1.6 Research questions 6

2 Literature review **7**
2.1 Fibre optic system 7
2.1.1 Optical fibre basis 8
Parameters affecting fibre performance 9
2.2 Fibre optic cables merits 11
2.3 Typical optical fibre communication system 11
Types of optical fibre cables 12
2.4 Types of optical sources 13
2.4.1 Light Emitting Diode (LED) 14

2.4.2 Types of LEDs . . . 16
2.4.3 Laser v.s LED . . . 17
2.5 Light Amplification by Stimulated Emission of Radiation (LASER) . 18
2.5.1 Types of lasers . . . 18
2.5.2 Laser applications . . . 19
2.5.3 Basic laser operation . . . 20
Population distribution. . . . 21
Stimulated absorption. . . . 21
Spontaneous emission. . . . 22
Stimulated emission. . . . 22
2.5.4 Einstein coefficients. . . . 23
2.5.5 Life time. . . . 24
2.5.6 Optical absorption. . . . 25
2.5.7 Population inversion. . . . 26
2.5.8 Cavity construction. . . . 27
2.5.9 Threshold gain. . . . 28
2.6 Rate equations . . . 29
2.6.1 Two level system. . . . 29
2.6.2 Three level system. . . . 31
2.6.3 Four level system. . . . 34
2.7 Semiconductor laser structures . . . 36
2.7.1 Carrier Distribution of Structures. . . . 38
2.8 Materials For VCSEL realisation . . . 39
2.8.1 Light emitting materials and choice of material . . . 41
2.8.2 VCSEL structure. . . . 43
2.8.3 Dynamics of the Structure. . . . 44
2.9 Growth Techniques . . . 46
2.9.1 Lattice matching. . . . 47
Vapour Phase Epitaxy (VPE) . . . 47
Molecular Beam Epitaxy (MBE) . . . 48
2.10 State of art of VCSELs . . . 49
2.11 Related research results . . . 50
2.11.1 Methods used by different groups to realise VCSELs used today refer to table 2.6 and 2.7. . . . 53

3 Methodology **58**
3.1 Research methodology . . . 58
3.2 Design methodology . . . 59

3.2.1 Flowchart development process 61
3.3 Simulation development 63
3.4 Final VCSEL structure 64
3.4.1 Seven quantum well active region 65
3.4.2 Light distribution over the device structure 66
3.4.3 Chapter summary 68

4 Results and Discussions **69**
4.1 Third window emission P-I-V characteristics 69
4.2 Optical wavelength emission analysis 71
4.3 1550nm - 1600 nm VCSEL results 76
4.3.1 Power v.s optical wavelength results 77
4.3.2 Absorption v.s optical wavelength results 79
4.3.3 Reflectivity and transmission results 80
4.3.4 P-I-V characteristics for the 1500 nm - 1600 nm wavelength emission 83
4.4 Chapter summary 87

5 Conclusion **88**

A Final code **90**

B List of publications **95**

List of Figures

2.1 Optical fibre cable typical sketch [1]. 9
2.2 Attenuation V.S wavelength for a fused silica optical fibre [2]. 10
2.3 Pulse Spreading Caused by Dispersion. 11
2.4 Schematic of a fibre communication system showing amplifiers and repeaters [2]. 12
2.5 Fibre types [2]. 13
2.6 energy v.s K relationship for (a) conduction band and (b) valence band with parabolic curves and E (k) centred about = 0 15
2.7 (a) direct band gap semiconductor showing electron-hole recombination sketch. (b) indirect band gap electron-hole semiconductor sketch. 15
2.8 Types of LEDs 17
2.9 Classifications of lasers. 19
2.10 Laser applications. 20
2.11 Boltzmann's law schematic on multilevel systems. 21
2.12 Illustrations on conditions for laser operation. 23
2.13 Population inversion illustration. 27
2.14 Cavity construction. 28
2.15 Three level system. 34
2.16 Four level system. 36
2.17 Junction laser structures. 37
2.18 Quantum Well laser structures (a) showing a single quantum (b) Multiple Quantum Wells. 38
2.19 Carrier distribution across a homo junction. 38
2.20 Homo junction before contact. 39
2.21 Homo junction after contact, before and after biasing. 39
2.22 Band Gaps of some semiconductors. 41
2.23 Conduction band energies of GaAsP. 43
2.24 Typical VCSEL structure. 44
2.25 Steps involved in manufacturing Si wafers. 46
2.26 Vaporisation cells inside a high-vacuum chamber cylindrical beakers of Al, Ga, As liquid do-pants onto a GaAs layer. 48

2.27 Cross section of MBE-grown crystal with layers of GaAs(dark) and AlGaAs (light) [3]. 49

3.1 Design methodology. 59
3.2 VCSEL development flowchart. 61
3.3 VCSEL development flowchart continuation. 62
3.4 Simulated seven quantum well structure. 65
3.5 P-doped and n-doped regions sand witching an InGaAsP seven quantum well active region. 66
3.6 Figure showing light intensity distribution in the Vcsel structure. . . 67

4.1 Emitted power vs Anode Current. 70
4.2 Emitted power vs Anode voltage. 70
4.3 Anode voltage vs Anode current. 71
4.4 Optical wavelength vs anode voltage for 30:28 and 45:43 vcsel structures. 72
4.5 Emitted power against optical wavelength for 30:28 and 45:43 structures. 73
4.6 Absorption for 30:28 and 45:43 vcsel structure. 74
4.7 Reflectivity for 30:28 and 45:43 structures. 75
4.8 Wavelength transmission for 30:28 and 45:43 structures. 75
4.9 Optical wavelength vs anode voltage for 30:28 mirror ratio. 76
4.10 Optical wavelength vs anode voltage for 45:43 mirror ratio. 77
4.11 Emitted power vs optical wavelength for 30:28 mirror ratio. 78
4.12 Emitted power vs optical wavelength for 45:43 mirror ratio. 78
4.13 Absorption vs optical wavelength for 30:28 mirror ratio. 79
4.14 Absorption vs optical wavelength for 45:43 mirror ratio. 80
4.15 Reflectivity vs optical wavelength for 30:28 mirror ratio. 81
4.16 Reflectivity vs optical wavelength for 45:43 mirror ratio. 81
4.17 Transmission vs optical wavelength for 30:28 mirror ratio. 82
4.18 Transmission vs optical wavelength for 45:43 mirror ratio. 82
4.19 Emitted power vs anode current for 30:28 mirror ratio. 83
4.20 Emitted power vs anode current for 45:43 mirror ratio. 84
4.21 Emitted power vs anode voltage for 30:28 mirror ratio. 84
4.22 Emitted power vs anode voltage for 45:43 mirror ratio. 85
4.23 Anode voltage vs anode current for 30:28 mirror ratio. 86
4.24 Anode voltage vs anode current for 45:43 mirror ratio. 86

List of Tables

2.1 Periodic table showing semiconductors occurrence. 40
2.2 Elemental and compound semiconductors [2]. 40
2.3 Semiconductor Material Properties. S-C is the semiconductor, B-S-T is band structure type (i is indirect and d is direct), C-S is crystal structure (Z is zinc ans W is wurtzite), Eg is the energy band gap, a is the Angstrom, ϵ_r is the dielectric constant of the material, D is the density and M-P is the melting point [2]. 41
2.4 Reflectivity VS. Cavity length. 45
2.5 Results comparisons. 51
2.6 Table of literature showing methods and results by other researchers. 54
2.7 Materials and methods for VCSELs used in data communication. . . 57

3.1 Table showing parameters used for the 30:28 mirror rating for 1-12 QWs. 63
3.2 Table showing parameters used for the 45:43 mirror rating for 1-12 QWs. 64

List of Abbreviations

LED	**L**ight **E**mitting **D**iode
LASER	**L**ight **A**mplification by **S**timulated **E**mission of **R**adiation
MASER	**M**icrowave **A**mplification by **S**timulated **E**mission of **R**adiation
DNA	**D**eoxyribo-nucleic **A**cid
LAN	**L**ocal **A**rea **N**etwork
HDTV	**H**igh- **D**efinition **T**elevision
3D	**T**hree **D**imensional
VCSEL	**V**ertical **C**avity **S**urface **E**mitting **L**aser
DBR	**D**istributed **B**ragg **R**eflector
2D	**T**wo **D**imensional
Ga	**G**allium
As	Arsinide
Al	**A**luminum
In	**I**ndium
P	**P**hosphorus
N	**N**itrogen
Zn	**Z**inc
Cd	**C**admium
B	**B**oron
C	**C**arbon
H	**H**ydrogen
Ca	**C**alcium
F	**F**luorine
O	**O**xygen
Si	**S**ilicon
Ge	**G**ermanium
Se	**S**elenium
Te	**T**ellurium
SRH	**S**hockley **R**ead **H**all
CW	**C**ontinuous **W**ave
SSL	**S**olid **S**tate **L**aser
FEL	**F**ree **E**lectron **L**aser
LL	**L**iquid **L**aser
GL	**G**as **L**aser
QW	**Q**uantum **W**ell
MQW	**M**ultiple **Q**uantum **W**ell
DH	**D**ouble **H**etero
TM	**T**ransverse **M**agnetic
TE	**T**ransverse **E**lectric
SEM	**S**canning **E**lectron **M**icroscope

TEM	**T**ransmission **E**lectron **M**icroscope
CBE	**C**hemical **B**eam **E**pitaxy
LPE	**L**iquid **B**eam **E**pitaxy
CVD	**C**hemical **V**apor **D**eposition
MBE	**M**olecular **B**eam **E**pitaxy
VPE	**V**apor **P**hase **E**pitaxy
OMVPE	**O**rgano-metallic **V**apor **P**hase **E**pitaxy
MOVPE	**M**etal-organic **V**apor **P**hase **E**pitaxy
MOCVD	**M**etal-organic **C**hemical **V**apor **D**eposition
TMI	**T**ransmission **E**lectron **M**icroscope
TMG	**T**ransmission **E**lectron **M**icroscope
PLFHWM	**T**ransmission **E**lectron **M**icroscope
EDFA	**E**rbium **D**OPED **F**ibre **A**mplifier
ER	**T**ransmission **E**lectron **M**icroscope
BW	**B**and **W**idth
WDM-PON	**W**avelength **D**ivision **M**ultiplexing **P**assive **O**ptical **N**etwork
PIC	**P**eripheral **I**nterphase **C**ontroller
N/S	**N**ot **S**tated
L-I	**L**ight-power **C**urrent
I-V	**C**urrent **V**oltage
W	**W**urtzite
C-S	**C**rystal **S**tructure
M-P	**M**elting **P**oint
D	**D**ensity

Physical Constants

Speed of light	c	$= 3.0 \times 10^{8}\,\mathrm{m/s}$
Boltzmann constant	k_B	$= 1.38 \times 10^{-23}\,\mathrm{J/K}$
Planck constant	h	$= 4.14 \times 10^{-15}\,\mathrm{eVs}$
Reduced Planck constant	$\hbar$	$= 6.58 \times 10^{-16}\,\mathrm{eVs}$
Charge of an electron	q_e	$= 1.602\,176\,62 \times 10^{-19}\,\mathrm{C}$
Rest electron mass	m_o	$= 0.511 \times 10^{6}\,\mathrm{eV/C^2}$
Permittivity-free spce	ε_o	$= 8.85 \times 10^{-14}\,\mathrm{F/cm}$
Thermal voltage-0300 K	k_BT/q	$= 0.0259\,\mathrm{V}$

List of Symbols

I	Signal Intensity	dB
α	Attentuantion coefficient	m^{-1}
E	Energy of electron	eV
K	Electron momentum	kgm/s
V_a	Applied voltage	V
v	frequency	Hz
P_E	Radiometry power efficiency	W
λ	Wavelength	m
A_e	Einstein coefficient for spontaneous emission	/s
B_{12}	Einstein coefficient for stimulated absorption	Srm^2/J s
B_{21}	Einstein coefficient for stimulated emission	Srm^2/J s
B	Einstein coefficient	Srm^2/J s
G_g	round-trip power gain	-
n_{abs}	absorption rate	/m^3 s
n_{sp}	Spontaneous emission rate	/m^3 s
n_{st}	Stimulated emission rate	/m^3 s
N_O	Population of excited state	/m^3
q_{abs}	Energy absorption rate	W
q_{st}	Energy rate of stimulated emission	W
R_{abs}	Number of stimulated absorptions per unit time	/s
V_e	Potential energy of electron	J
x	Electron position in X-direction	m
β	Small-signal gain coefficient	/m
β_{th}	Small-signal gain coefficient	/m
χ	Electric susceptibility	-
ψ	Wave function of electron	-
S_{IJ}	Probability of nonradiative decay between levels i and j	/s
W_{ij}	Probability of thermally excited atom between levels i and j	/s
W_{pc}	Critical pumping rate	/s
W_{pt}	Threshold pumping rate	/s
W_s	Probability of induced transition caused by laser action	/s
τ_{ij}	Lifetime for transition from level i to level j	s
C_b	Conduction band	-
e^-	Electron	-
E_c	Energy level in conduction band	J
E_g	Energy of forbidden gap	J
E_v	Energy level in valence band	J
F_c	Energy of Fermi level in conduction band	J
F_n	Fermi level for p-type semiconductor	J

F_p	Fermi level for p-type semiconductor	J
F_v	Energy Fermi level in valence band	J
P_c	Probability of occupation of conduction band	-
P_v	probability of occupation of valence band	-
V_b	Valence band	-

This work is dedicated to my family, friends and mostly to my lovely mother, Tshenolo Moatlhodi.

Chapter 1

Introduction

Optical communication involves the transmission of data from one point to another, usually over long distances using light [1, 2]. Fibre optics is the confined ray of light by a method called total internal reflection over long rods of fibre made of either plastic or glass [3]. The foundation of optical sources gave a sensible setting for the transmission of information at a high data rate [4]. Fibre optic links in recent times are utilised for sending voice, pictures and other information at a speed closer to that of light [5]. The limitations on the transmission of light through the atmosphere (for instance cloudiness, fog, absorption and rain) forced the inclusion of light emitting diodes (LED) and light amplification by stimulated emission of radiation (laser) [6, 7]. LEDs have been a reliable optic source dominating the optical transmitter/receiver market over the years, but semiconductor lasers took over [8]. The laser is a device that emits an intense beam of monochromatic light (same wavelength) and coherently (same phase and direction) through an optical amplification process based on the stimulated emission of electromagnetic radiation [9]. The present day optical communication systems use semiconductor lasers that transmit light through optical fibres [10]. These systems are extensively used for applications ranging from large telecommunications backbone structures to Ethernet systems, broadband distributions and general data network [11]. Since the light wave is used for transmission, all the good properties of light wave are available with these communications [12].

Charles H. Townes is the first individual who exploited the process of stimulated emission as an amplifier by considering and making the principal Maser [13, 14]. The Maser was invented in 1951 by Charles H. Townes, who was a professor at Columbia University in New York City in 1952 [15]. The means that drove from the Maser to the laser owed a ton to his working relationship with one of his research partners at Columbia, Arthur Leonard Schawlow, a Canadian physicist who was focusing on the utilisation of microwave spectroscopy to organic science [16]. Regardless of the fact that Schawlow did not work on the Maser, he looked out for it

through his association with Townes, with whom he wrote a book about microwave spectroscopy [17, 18]. Afterward, at Bell Telephone Laboratories in Murray Hill, N.J., Schawlow had begun to think about creating infrared light with concentrated light emission in mid 1957 [2, 6, 19]. At the time, Townes was an expert on Bell Lab and occasionally consulted with Schawlow. It was at one of their social occasions that the two first talked about how to develop infrared or even visible light laser. Schawlow picked to energise the particles of potassium fume, since potassium was the primary substance that he knew it's first and second lines of range in the visible range [20]. The choice of emission mode showed to be a hindrance since it included designing the resonator cavity with the objective that it would only the accommodate the desired frequency [21] . The first laser developed was a Ruby laser used in 1960 by Theodore H. Maiman at Hughes Research Laboratories for the treatment of eye and skin infections under the direction of hypothetical work of by Charles H. Townes and Leonard Schawlow [22].

Lasers are used in optical disk drivers, laser printers, standardised tag scanners, DNA sequencing instruments, fibre optic communication systems, free space optical communication, laser medical procedures, skin treatments, cutting, welding materials, laser lighting shows for entertainment, military, law enforcement gadgets used for making targets and assessing degree and speed [23, 24, 25]. In recent years, lasers are used for vehicle headlamps by using the blue and phosphor laser to transmit directional white light[26]. The performance of a laser is still being improved by considering the general properties of lasers that are specific to a certain application and thus way changing the structure and material used [15]. This is because different lasers produce laser effects at wavelengths in different regions of the electromagnetic spectrum [6].

1.1 Background of optical communication

Corning gorilla glass specialists Donald Keck, Peter Schultz and Robert Maurer developed Optical Wave direct Fibres or fibre optic wire patent number 3,711,262 which is more efficient than copper wire at transferring data multiple times since data transmitted by a periodical arrangement of light waves can easily be decoded at a station kilometres away [27]. Specialised fibre optic materials and the techniques they developed paved the way for fibre optics commercialisation. From a significant long distance telephone utility to the web and clinical gadgets like endoscopes, fibre optics are currently a significant piece to present day life [28].
In 1854, Tyndall John showed that light could be led through a bent stream of water,

thereby demonstrating the bending of light signals [29].
In 1980, Alexander Graham Bell developed his Photo telephone which sent a voice signal through the emission of light. After focusing light rays with a mirror, Alexander talked into a system that made the mirror to vibrate. Vibrating beams were detected at the receiver and decoded back into voice in a similar way a telephone did with the electrical signals [30]. However, different things like a cloudy day could easily interrupt the transmissions and affect the operation of the phone, which led Bell to stop any further research into this development [31]. In the same year William Wheeler developed an arrangement of light pipes that were fixed with a highly reflective coating that illuminated homes with the light of an electric round lamp in the basement and coordinated the light around the home with the pipes[32].
The medical group lead by Roth and Reuss utilised twisted glass rods that were bent to light up the cavities of the human body [33].
Engineer Henry Saint-Rene developed a system of bent glass rod to control light pictures for early television in 1895 [34].
In the 1920s Clarence W. Hansell and John Logie Baird approved the patent for the use of transparent rods arrays to transmit television pictures and exact copies of printed materials [35].
In 1930 Heinrich Lamm used a bunch of optical strands to transmit a picture. Lamm's objective was to concentrate on parts of the body that were not easily accessible. During his lab experiments, he announced the transmission of the image of a light bulb. The image was of low quality, but his work on documenting a patent was denied due to Hansell's British patent [36].
In 1954 Harold H. Hopkins a British researcher and Abraham Van Heel a Dutch researcher wrote papers about imaging packs. Hopkins gave an account of imaging bundles of unclad fibre strands while Van Heel covered straightforward bundles of clad fibres. He gave a report of the uncovered fibre having a transparent cladding with a lower refractive index. This shielded the reflective surface of the fibre from outside contortion and significantly decreased impedance between the fibres. At that point, the best deterrent to a suitable utilization of fibre optics was in accomplishing the lowest signal light loss [37].
In 1961 Elias Snitzer of American Optical distributed a hypothetical portrayal of a single-mode fibre, a fibre with a centre core that was so narrow that it could transmit light with a single mode of wave control. Snitzer's thought was good for instruments used in medical fields to look inside the human, yet the fibre had a light loss of one decibel for each meter. Communication transmission devices were expected to function over any longer distances and required a loss of light of close to ten or 20 decibels (an estimated light value) per kilo meter or less [38].

In 1964 a basic but critical and hypothetical detail was distinguished by Dr. C.K. Kao for long-range communication systems. The detail was 10 or 20 decibels of light loss per kilo meter, which set up standards. Kao additionally outlined the requirement for a purer type of glass to help decrease light losses [39].
In 1970, a group of specialists started exploring different avenues regarding fused silica, a material fit for outrageous purity with a low refractive index and a high melting point. The group had tackled the issues introduced by Dr. Kao.
In 1975, the United States government chose to connect the PCs at the NORAD headquarters at Cheyenne Mountain utilising fibre optics to decrease interference [40].
In 1977, the principal optical phone communication system was introduced about 1.5 miles under midtown Chicago. Each optical fibre transmitted what is comparable to 672 voice channels. Before the end of the century, more than 80% of the world's long distance traffic was transmitted over 25 million kilo meters of the optical fibre link. Maurer, Keck, and Schultz-planned links have been introduced around the world [41].

1.2 Problem statement

There has been a massive growth in both the telecommunications and data communications traffic due to change in human needs and wants in the telecommunications industry. The new generation technology is judged on how much, how fast and over what distances information can be conveyed. The disadvantages of commonly used fibre optic transmitters (LED's) are low efficiency, limited output power, incoherent light giving limitations in the development of fibre optic communication systems that covers a wider range of areas and at higher speeds. The presentation of new services, for example high definition TV (HDTV) and grid computing comes with an increase in bandwidth demands. Grid computing gives on-request access to both local and remote computational assets for storage and visualisation and enables the effective and profitable utilisation of expensive resources to simulate scientific, engineering and commercial applications. Three-dimensional (3D) motion pictures which are currently presented in cinemas, will soon be developed for home amusement. Despite the fact that radio innovation are still in use, optical communication networks have become the most important technology for high-speed transmission of information, which would be inconceivable on a large scale using radio waves.

1.3 Overall research aim

The aim of the proposed subject is to study, simulate and analyse the performance characteristics of a VCSEL used in optical communication systems.

1.3.1 Research objectives

The objectives of this research are as follows:

1. To determine characteristics of light wave and mobile telecommunications that influence device selection.
2. To simulate a semiconductor laser with a low loss window emission wavelength for optical fibre applications.
3. To evaluate the simulated VCSEL structure and compare the performance with the existing ones.
4. To obtain static and dynamic plots and analyse the output power of the designed laser.

1.4 Justification of study

Among the various kinds of opto electronic devices, semiconductor lasers are currently the least researched and financed but they are rapidly gaining recognition because of the following factors: adaptability, efficiency and high performance. Semiconductor lasers have been broadly created resulting in a great potential of developing laser devices at other wavelength. This development should include a few gatherings, covering a few disciplines and expertise from Chemistry to Material science and assembling of the required components (couplers, filters, mirrors). Despite developing a device that will benefit our economy and society, laser researchers need to be aware of the needs of laser end users and be involved with all end users, from manufacturing industries, to Physicians and environmental researchers.

1.5 Chapter summary

The variation of the reflectivity of the mirrors and the quantum analysis are the key features for the realisation of a semiconductor laser in this research. A major reduction in threshold current was achieved by introducing a quantum well structure in the active region of surface emitting lasers [5]. This new development of the active

region and improvements in Distributed Bragg Reflectors (DBRs) led to the demonstration of a few devices with milli-ampere thresholds. In addition, the emission of the device permits the use of any kind LED packaging. The current should be confined in the lateral direction for effective device operation [42]. This can be achieved by using an oxidation layer around the active region to electrically insulate photons from other regions, forcing current to flow through the centre of the device [21].

1.6 Research questions

The following research questions will be applied:

1. What are the first used fibre optical transmitters?
2. What is the most recent development of fibre optical transmitters ?
3. What are the different types of material composition used for fibre transmitters?
4. What are the optical fibre low loss transmission windows?
5. What are the most recent laser structures used in optical fibre communication systems?
6. What are the parameters that are studied in laser manufacturing?
7. What are the developments on the most recent laser structures used in optical structures?
8. What are the limitations in recent studied laser application?

Chapter 2

Literature review

The literature begins with the review of fibre optic communication systems and their components, the properties of all optical sources and it also covers a discussion of the ideal laser. It also includes all of the basis for laser operation. The literature will then help identify all the gaps in this research. There is more focus on light emitting materials and the methods of layer deposition used in laser fabrication. As the research focus is semi-supervised learning, the semi-supervised section will include contributions as well.

2.1 Fibre optic system

Fibre optic communication systems are used extensively for applications ranging from major media communications backbone structures to Ethernet systems, broadband distributions and general networking [2]. Since the light wave is used for transmissions, all of the great characteristics of the light wave are available with these communication systems. This study covers a discussion of all the potential ways to improve data speed and it also includes a discussion of a various fibre optic transmitters [2, 6]. The optical signals transmitted from a source to a detector can be improved if an optical fibre (usually drawn from a boule of glass to a measurement of around 25 μm) is placed between the light source and a detector [2, 7]. A fibre optic cable is a light pipe wave guide for optical frequencies without the need for ideal alignment between the source and detector. All fibre optic communication systems comprises of a transmitter (light source), fibre optic link and a receiver(detector) [2, 11]. However, depending on the magnitude of the losses in the fibre, repeater stations may be required. In this case numerous detectors and laser sources are required in a fibre optic structure [43, 44, 45]. Therefore, the development of semiconductor devices, including proper binary, ternary and qua ternary mixture for both the emitters and detectors are essential for the successful implementation of such optical communication systems [2].

2.1.1 Optical fibre basis

A standard optical fibre cable structure is shown in figure 2.1. Fibre comprises of three distinct regions: the core, the cladding and the buffer coating layer [46]. The signal travels through the core region of the optical fibre cable. The signal is constricted mainly to the core by total internal reflection. The index of refraction of the core (n_2) is usually bigger than that of the cladding (n_1). The speed of light decreases with increasing index of refraction [47]. As a result, the light wave is completely reflected when it travels through the fibre core, which establishes a confinement. Most cables are made of glass or plastic and the most important properties when choosing the material for making optical fibre cables are the capability to be drawn into long cables, flexibility and differences in index re-fractions that are used to characterise the core and cladding. These differences in index of refraction can be modified by adding impurities to change the indexes [48]. Usually silica is the most commonly used material when compared to other materials like fluorine. There are three principal transmission bands as shown in figure 2.2. Currently the lasers in optical communications operate at or around 850 nanometers (nm) which is the first low loss window. The 1310 nm is called the second loss window and the 1550 nm represents the third and fourth windows [49]. Lower attenuation can be achieved by operating at longer wavelengths. In the early opto electronic frameworks for fibre optics, it was generally advantageous to use the built up GaAs/AlGaAs systems to design LEDs and lasers which operated at around 0.9 μm. Although the detectors were competent, the attenuation was more prominent than with the longer wavelengths [50]. This resulted in current systems operating at around the 1.3 - 1.55 μm. This wavelength enables the development of lasers using InGaAs or InGaAsP and lattice matched with InP as a substrate.

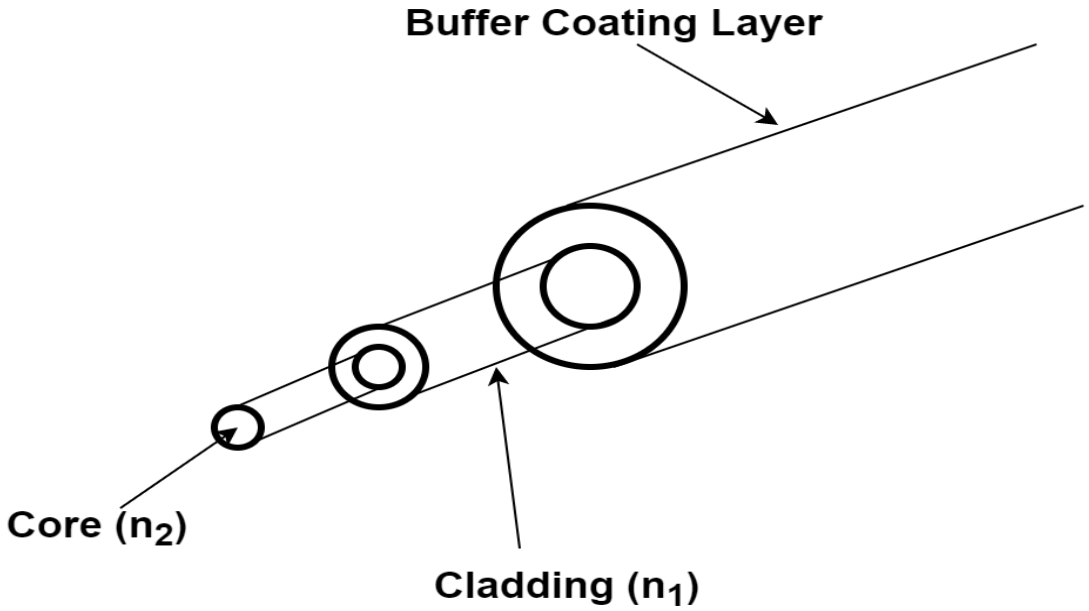


FIGURE 2.1: Optical fibre cable typical sketch [1].

Parameters affecting fibre performance

- **Attenuation**
  The decrease in the signal optical power as it moves between different points is called attenuation [51]. Power losses caused by absorption and dispersion are commonly expressed in decibels (dB) and can be identified by the attenuation coefficient. The losses are usually in (dB/km) for a given length or per unit length of fibre at a specified transmission wavelength. It is not the same for all wavelengths, so it is important to carefully choose a signal wavelength [2]. The signal intensity at a distance x along the fibre is related to the initial signal intensity by :

$$\mathbf{I}(x) = \mathbf{I}_0 e^{-\alpha x} \tag{2.1}$$

  where
  $\mathbf{I}(x)$ is Signal intensity at distance x
  $\mathbf{I}_0$ is the Initial Signal intensity
  α is the attenuation coefficient
  x is the Distance at which Signal intensity is measured

  Figure 2.2 shows the three windows of activity. These compares wavelength with regions where attenuation is low and grouped in their bands.

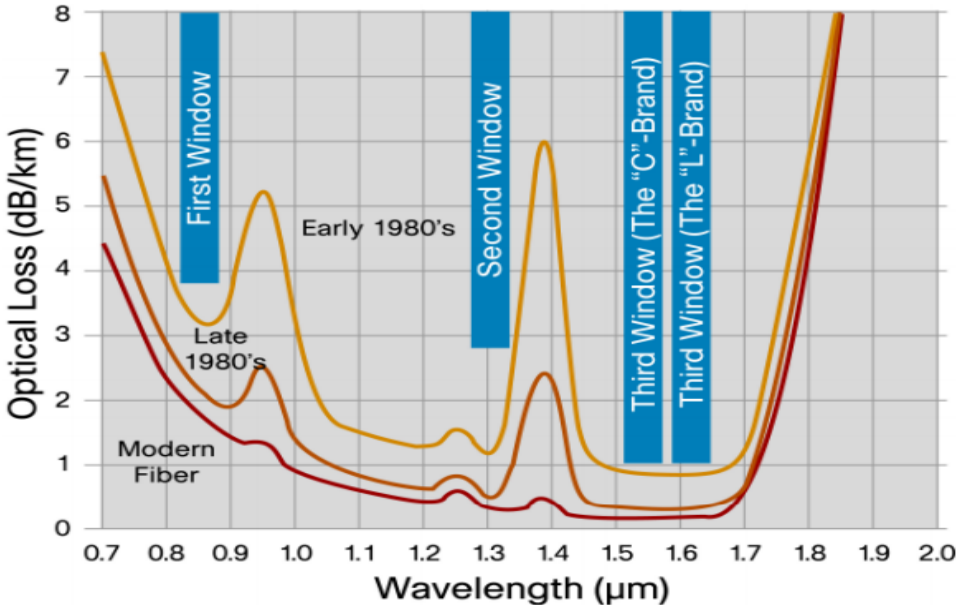


FIGURE 2.2: Attenuation V.S wavelength for a fused silica optical fibre [2].

- **Pulse dispersion**
  Pulse dispersion is inversely proportional to the bandwidth, which simply means the data carrying capacity of a fibre is limited, as a result of pulse spreading [19]. Pulse spreading is caused by chromatic scattering in single-mode fibre links due to different colours of light propagating at different speeds, causing a transmitted pulse to spread as it moves through the fibre [2]. Chromatic scattering is less articulated at the 1.3 μm window as shown in figure 2.2 [52]. Another reason for this effect is that different modes propagate at different path lengths which can be reduced by degrading the core refractive index so that some modes can be refocused along these lines, thereby reducing the path lengths [53]. So likewise, pulse spreading in multi mode fibres is caused by modal scattering when the geometry of a multi mode fibre core is looked into. These are defined by taking into consideration various techniques used so that the laser outputs are independent at the fibre interface and propagate simultaneously down the fibre [7]. The propagation of the data pulses as they move down the fibre should be examined when selecting operating wavelength. Since the wavelength is dependent on the refractive index, this causes pulse dispersion leading to different frequencies travelling through the fibre at slightly different speeds [54, 55, 56, 57]. These modes propagate with slight delays compared to each other causing the pulse to spread as it moves through the fibre [6]. At a point where pulse spreads too far, the signals at

the receiving end of the system cannot be easily distinguished because they overlap [2]. Figure 2.3 shows pulse spreading caused by dispersion.

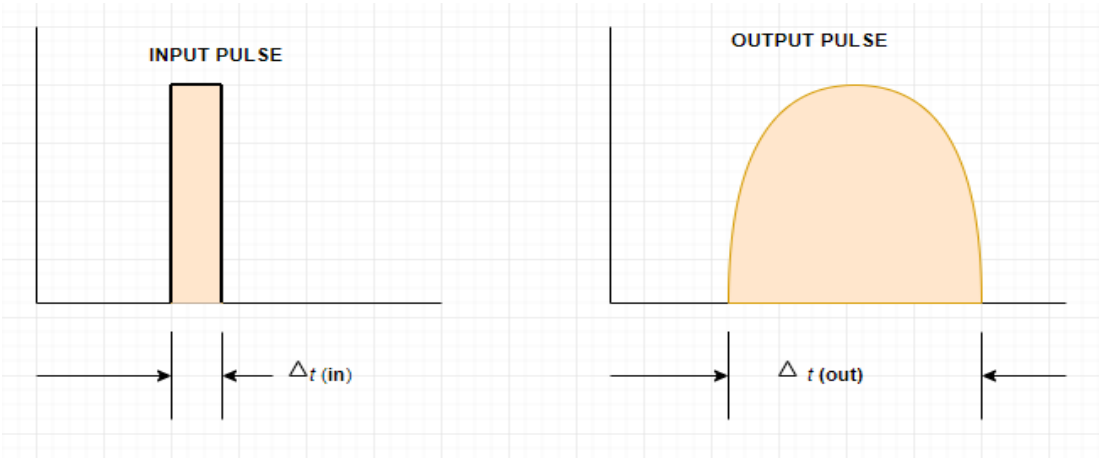


FIGURE 2.3: Pulse Spreading Caused by Dispersion.

2.2 Fibre optic cables merits

The transmission systems that use fibre optical links offer more benefits than other transmission media such as copper cables since they are normally smaller or modest in width, light in weight and have greater advantages in terms of flexibility [49]. They also offer a large amount of capacity normally in terahertz, which allows future changes or improvements to the communication system [58, 59]. These links have low transmission losses and scattering losses and offer more security. In addition, they have a high cross-talk immunity and good isolation [37]. For the reasons mentioned above, these are the most commonly used cables for data transmission.

2.3 Typical optical fibre communication system

The distance that a signal can travel can be limited by attenuation [49]. For this reason, signal amplification, re-transmission and restoration should be carried out regularly for longer transmissions [60]. In numerous systems that were used in the early years, the signal was converted to electrical signals, electronically re-shaped and finally re-converted over into light signals. This was achieved by using a repeater. Using a repeater is advantageous because distortions and any noise can easily be eliminated [61]. It distinguishes a signal, digitally extracts its contents, re-constructs it and forwards it to the receiver without distortion or noise interference. Repeaters are placed along network systems to ensure accurate data delivery

without distortions. There must be some electro-optic conversion in all repeaters since there is no fully optical repeater. Therefore, every time a signal is changed, another repeater is required which will make the network more complicated and costly [62]. Amplifiers can be installed in networks, but this results noise interference and distortions. However, they are valuable in networks where such noise and distortions are minimal. Figure 2.4 shows an example of a fibre optical frame with input information defined by 0s and 1s that are sent as electro magnetic waves. The transmitter circuit distinguishes 1s as high frequency waves and 0s as low frequency waves. The data entered into the channel is converted into forms that can be transmitted by pulse of light through the fibre optic links. Then they go through circuitry and repeaters until they reach the receiver, where there are decoded and sent to the end users [37].

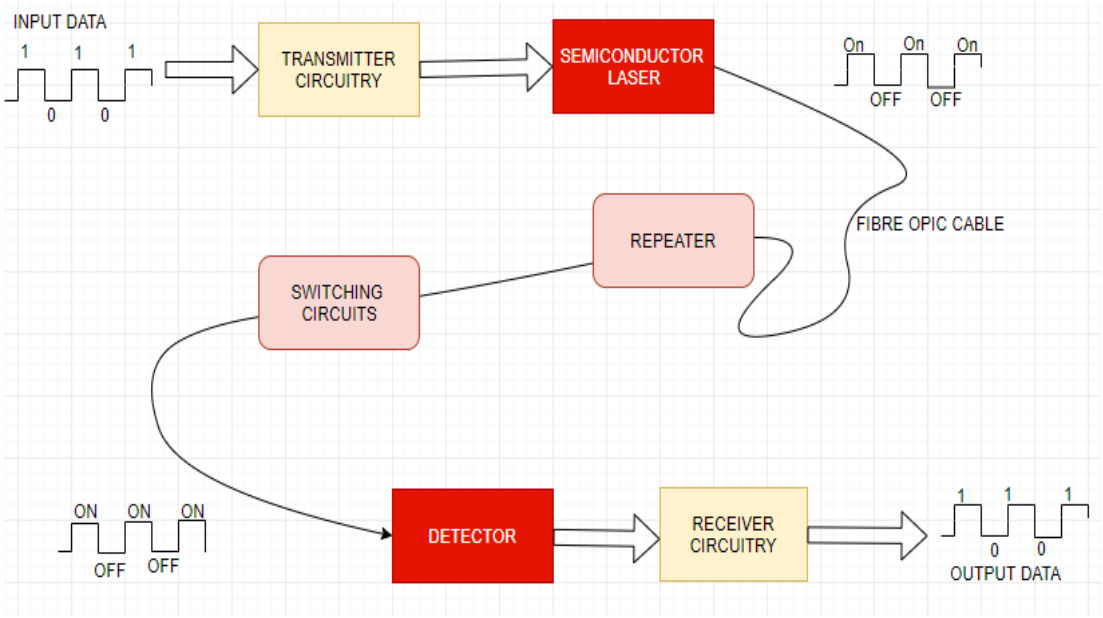


FIGURE 2.4: Schematic of a fibre communication system showing amplifiers and repeaters [2].

Types of optical fibre cables

The first fibre optic models still in use are fused single-mode (approximately 5μm) and multi-mode fibre (generally 25μm) (step or graded indexed) [6]. The differences in fibre types results in a variety of wavelengths, range, quantity of different channels or frequencies at which the light is sent or received, the distance and speed at which these signals can travel without amplification, restoration or enhancement [7, 63]. The three optical fibre types are briefly explained below.

1. Step-index Single-mode: It is realised so that the centre core is so narrow that only one light wave can be supported for transmission, which means that only one mode can be spread [63].

2. Step-index multi-mode: This is designed so that the centre is large enough to allow numerous light waves with different wavelengths to pass through [49]. The index of the centre core is in some ways more pronounced than that of the cladding. It generally has uniform refractive indexes in the centre. In addition, it has a crisscross or zigzag pattern for way of light spread [37]

3. Graded-index multi-mode: It works like the step index multi-mode, yet the only difference is that the index of the centre core changes slowly away from the axes. The refractive index of the centre core is not uniform in this particular design [49]. It has a helical pattern for way of light spread and generally has a lower attenuation and gives a higher transmission capacity than the step-index designs [64].

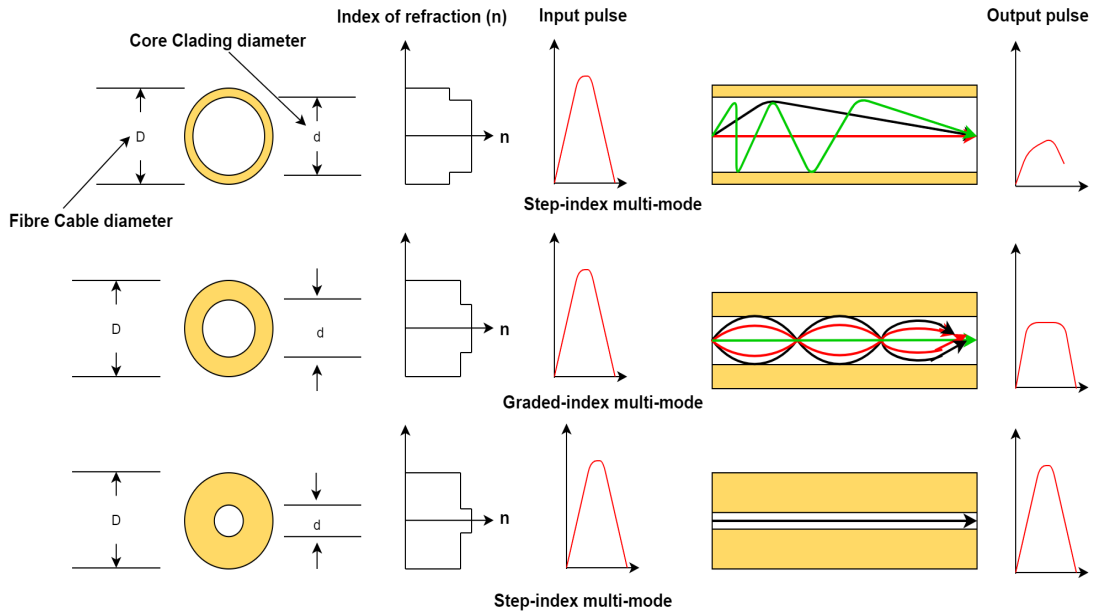


FIGURE 2.5: Fibre types [2].

2.4 Types of optical sources

The choice of light source is determined by the designer's requirements with regard to the light output power and the frequency of the light pulses [65].Light emitters are the front-end parts of a light wave communication frame and light-emitting diodes

or either lasers have been advantageously used in optical frames when the signals are fed into the fibre links. The two types of optical sources examined in the coming sections.

2.4.1 Light Emitting Diode (LED)

LEDs are a forward biased p-n junction diodes that make up the majority of commercialised optical semiconductor products [66]. Electrons and holes are infused into the depletion region. Under the forward bias, in the frequency of carrier concentration within the depletion region exceeds the equilibrium concentration, hence there is a radiative carrier recombination . The forward biasing subsequently prompts the injection of the minority carriers, followed by radiative recombination that is accompanied by light emanation [5]. A couple of perspectives in understanding LEDs with radiative recombination predominance include the use of high-purity direct band material with their substrate (a look into the band structure of the material normally GaP and GaAs are normaly used). Another aspect is to design in such a way that the transmitted light can escape from the designed structure. The energy of an electron when its free is communicated as follows:

$$E = \frac{\hbar^2 k^2}{2m} \tag{2.2}$$

energy of an electron and a hole in a crystal structure are expressed as follows:

$$T = \frac{\hbar^2 k^2}{2m_e^*} \tag{2.3}$$

$$T = \frac{\hbar^2 k^2}{2m_h^*} \tag{2.4}$$

where E is the energy expression, $\hbar$ is the planc's constant k is the momentum and m is the mass with e and h representing electrons and holes.
The material that the LED is made of should have a direct band gap, which means that the holes and electrons involved in the transition have the same momentum (k) near the conduction and valence bands. On the other hand, an indirect band material has a difference in the momentum of the holes and electrons. The energy v.s k-vector relationship for the conduction and valence bands as well as the direct and indirect gap material sketches are shown in the figures 2.6 and 2.7 [5].

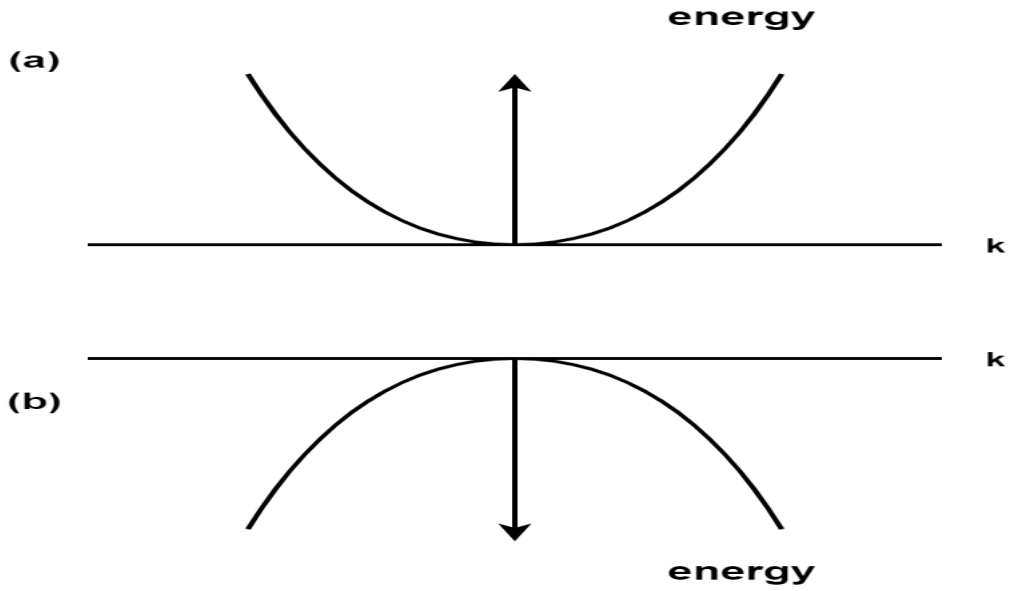


FIGURE 2.6: energy v.s K relationship for (a) conduction band and (b) valence band with parabolic curves and E (k) centred about = 0

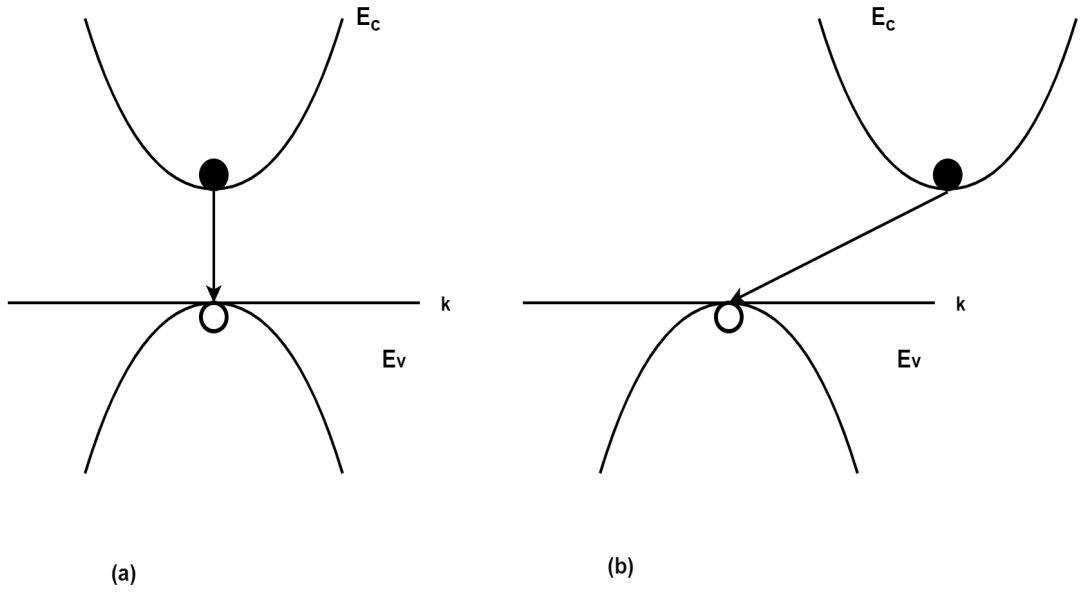


FIGURE 2.7: (a) direct band gap semiconductor showing electron-hole recombination sketch. (b) indirect band gap electron-hole semiconductor sketch.

Some material compositions with direct band gap emissions are the ternary-$In_{1-x}Ga_xN$ emitted in the blue portions. Impurities can be added to the GaP to make it direct and emit in the green portions. Orange and yellow can be obtained by

inserting impurities into the indirect compositions of GaAsP. A 40% direct band gap phosphorus $GaAs_{1-x}P_x$ emits in the red portions and other colours can be achieved using the qua-ternary AlGaInP compound. LEDs have great advantage over incandescent and fluorescent lighting devices in terms of efficiency, life span, durability, reliability and its luminous performance. Luminous performance refers to the optical yield (a measure of how efficient the performance, given as the ratio of the total luminous flux to the input power in watts) of the device. The lumen is the unit used to measure photometric flux-the science of visible light and its perception by the human eye. The luminous performance is given by the product of the eye sensitivity function called the CIE curve, and the radiometric power efficiency (total power radiated in watts) and it can be defined as the ratio of the output power to the input power [5].

$$P_E = [(photon/s)x(energy/photon)]/[(current)x(appliedvoltage)] \tag{2.5}$$

$$P_E = \eta_{ext}\frac{E}{V_a} \tag{2.6}$$

where η is the external quantum efficiency defined as the ratio of the number of photons emitted from the device per incident injected electron, E is the energy of the emitted photon and V_a is the applied voltage.

$$\eta_{ext} = \eta_{int}C_{ex} \tag{2.7}$$

where η_{int} is the internal quantum efficiency defined as the number of photons produced for every injected electron and C_{ex} is the extraction efficiency defined as the fraction of generated photons that escape from the device packaged. Internal quantum efficiency can be affected by traps and impurities that cause non radiative re-combinations leading to low internal quantum efficiencies. Non radiative re-combinations events are Shockley-Read-Hall (SRH), thermal band to band recombination and Auger re-combinations [5].

2.4.2 Types of LEDs

The main types of LEDs are the surface and edge emitting lasers. Surface emitting structures are designed such that the bottom edge reflects the light towards the top surface to enhance the output intensity. Edge emitters are illuminated from the side of the device and have a relative direct radiation. Figure 2.8 shows the sketches of the two types of LEDs, surface and edge emitting LEDs [5].

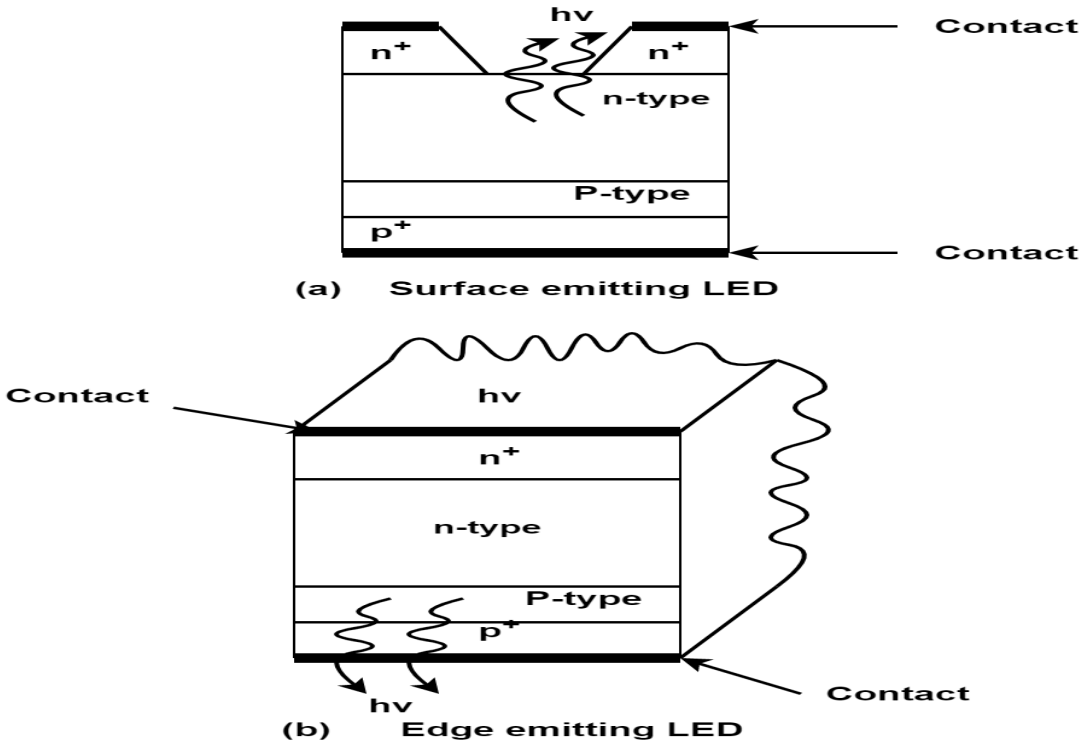


FIGURE 2.8: Types of LEDs

2.4.3 Laser v.s LED

The narrow spectral line width is one of the advantages of lasers (about 1 nm or less). This is very useful in applications where multiple emissions with different peak activation wavelengths are required [67]. In addition, due to their low divergence, laser beams have a very high fibre coupling efficiency, which allows simple and direct light manipulation through mirrors or lenses [68].On the other hand, LEDs have a relatively wider spectral line width with a broad emission pattern (a few tens of nm) and a pronounced beam divergence, which generally makes it difficult to achieve good LED-to-fibre coupling as required in order to deliver high light output powers. Some disadvantages of lasers are high costs, with yellow lasers being the most expensive, stable and they have a long warming time. These disadvantages cause problems in applications that require high speed modulations, particularly diode pumped solid state (DPSS) lasers. LEDs do not require complex control electronics, are more cost effective, and can be easily modulated in the millisecond range [69].

2.5 Light Amplification by Stimulated Emission of Radiation (LASER)

LEDs have been a reliable optic source that has dominated the fibre optic transmitter market over the years, but the introduction of semiconductor lasers has changed optical issues and created new fields of fundamental and applied optics [2].The laser is a device that emits a beam of intense monochromatic (same wavelength) and coherent (same phase and direction) light through an optical amplification process based on the stimulated emanation of electromagnetic radiation [53, 19].Different lasers emit light in the infrared and deep ultraviolet regions that cannot be detected (invisible) by the human eye. Lasers can be divided into classes by observing their structures, the properties of the emitted light wave, molecule characteristics and the light matter interactions. Their structures can be used to divide them into hetero junction and homo junction lasers [70, 19]. If we consider how they emit their output light with time and power as independent, they can be organised into continuous wave and pulsed lasers. The basic properties of light wave include interference, diffraction, reflection, and refraction and particle like properties depend on light dissipating. On the one hand, the coherent and monochromatic emission of lasers differs from other light sources, which makes them interesting to work with and be applied in opto-electronics, particularly in fibre-optic communication. Furthermore, common light waves travel independently and randomly, cancel each other out therefore cover shorter distances [19, 71, 72].

2.5.1 Types of lasers

The different types and structures of lasers are steadily expanding and can be widely grouped by their fabrication methods. The general classifications are:

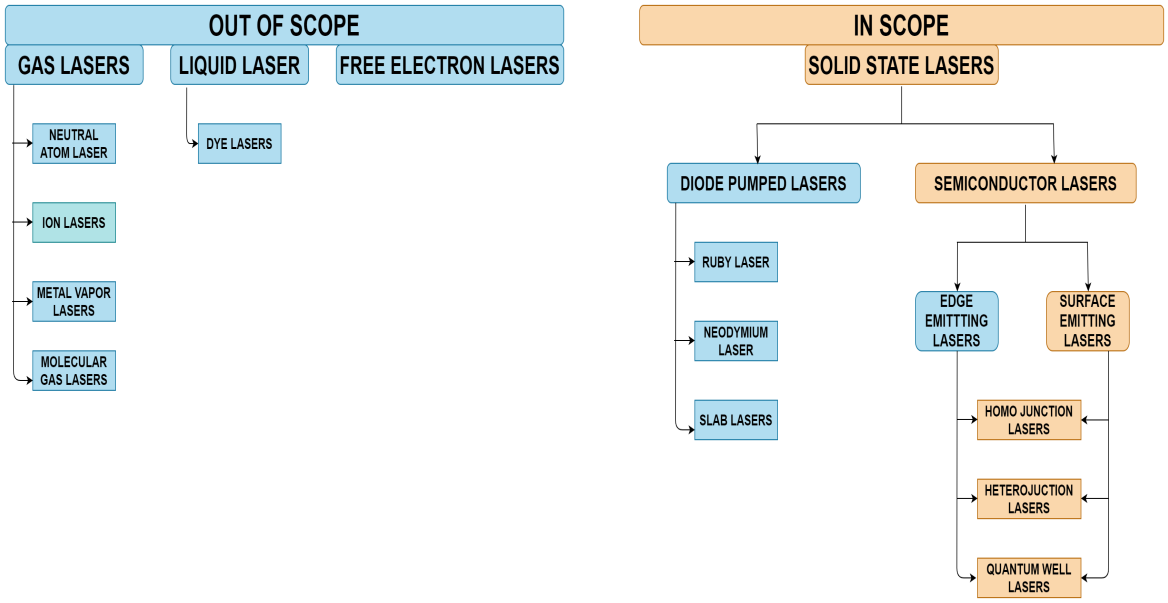


FIGURE 2.9: Classifications of lasers.

2.5.2 Laser applications

Many lighting applications are influenced by the device beam properties. In terms of stimulated emission of radiation, these properties can be adjusted using laser components. The components influencing laser beam properties are: gain medium size, location, segmentation and reflectivity of optical mirrors. The presence of beam path losses within the cavity is another influencing factor. Some of the properties like laser modes are determined by different features [24]. The beam oscillating pattern relates to the laser modes which are wavelike properties of the beam as it moves back and forth through the amplifier and grows at the expense of existing losses. The improvement of the laser modes includes the attempt to fit a precise number of their waves into the optical cavity [23]. Lasers can also be grouped into continuous wave lasers and pulsed wave lasers. This implies that there are lasers that emit a continuous wave beam and those that emit a pulsed beam [24]. Continuous wave laser include gas and optically pumped solid-state lasers, while other lasers fall under pulsed lasers. Continuous wave lasers a have lower power yields (goes between milli-watts to megawatts) than pulsed lasers (with ranges between giga-watts and exa-watts) [2].

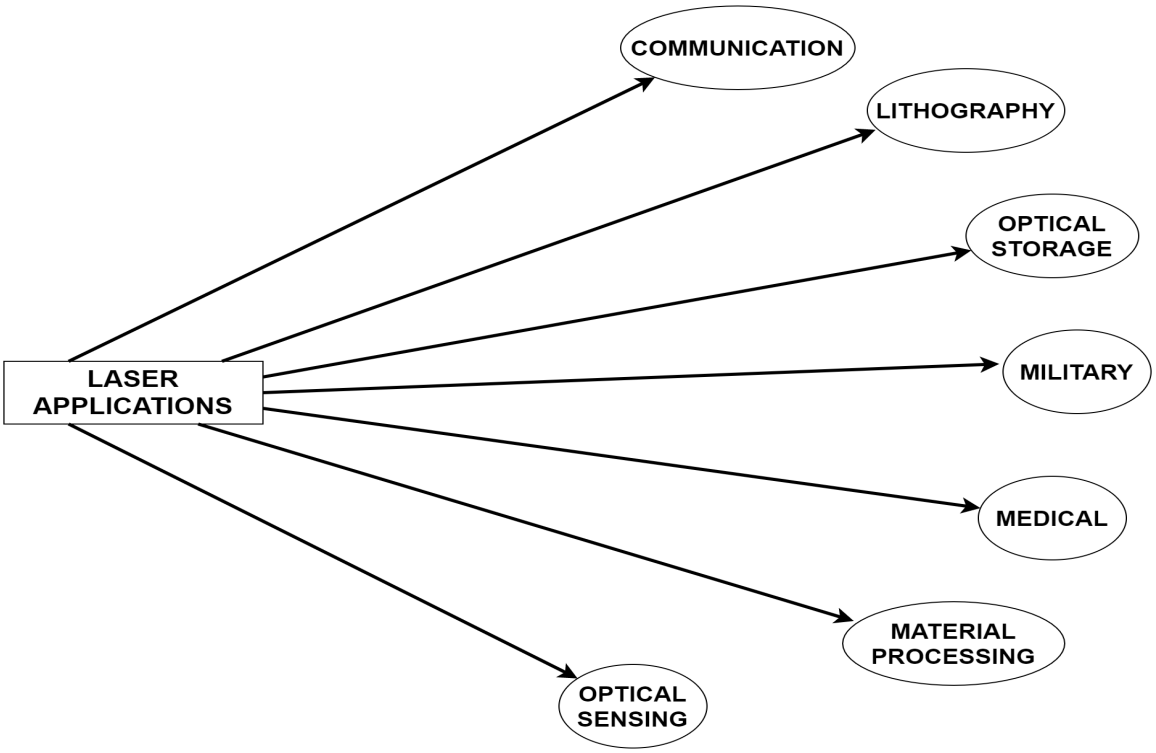


FIGURE 2.10: Laser applications.

2.5.3 Basic laser operation

The basic semiconductor laser operation includes three important building blocks, which are namely; the Gain medium, which is often referred to as the active region, the pump or power supply and an optional feedback. The movement of an electron from an upper energy state to a lower energy state results in the emission of light or energy in the form of a photon. Absorption occurs when the opposite occurs i.e the movement of an electron from a lower energy level to an upper of energy level. Any movement from one energy level to another is associated with a distinct quantum of photon energy of a certain specified frequency or wavelength that can be described by the following equation

$$\Delta E = \frac{h_p C}{\lambda} = h_{12} v \tag{2.8}$$

where the speed of light in (m/s) is represented by C, λ represents the wavelength (m), the transition frequency from one energy level to another in (Hz) is represented by v and ΔE is the difference in energy between one energy state and another energy state of interest [73].

Population distribution.

The relation of populations of electrons at lower level (n_1) and that of upper level (n_2) is given by Boltzmann's law as shown in equation 2.9. The distribution at thermal equilibrium shows that lower levels of energy (E_1) are greatly populated than higher levels of energy (E_2) i.e. $(E_1 > E_2)$.

$$\frac{n_2}{n_1} = e^{-(E_2-E_1)/k_BT} = e^{-h\upsilon_{1_2}/k_BT} \tag{2.9}$$

K_B and T being the Boltzmann's constant in (K/J) and absolute temperature of the system in (K) in that order.

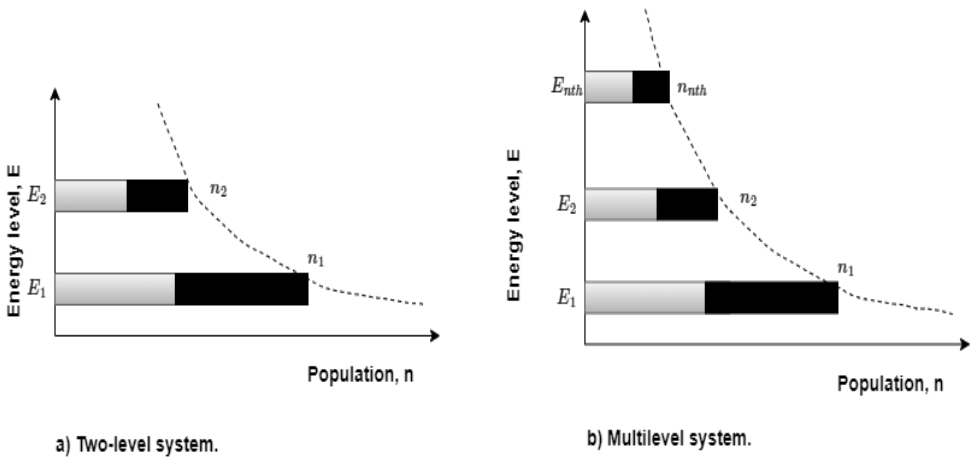


FIGURE 2.11: Boltzmann's law schematic on multilevel systems.

Stimulated absorption.

The quantum theory states that every atom can contain energies in certain distinct states or energy levels [74]. It assumes that electrons have easier existence in the ground state, hence they are found there [19].Electrons absorb external photon energy from sources such as flash lamps and mercury bends, to stimulate and energise electrons to an upper energy level commonly referred to as an excited state [75]. In relation to equation 2.8, electrons absorb external photon energy and migrate to an

upper level with a practically comparable energy as the photon field which struck them and the activity is called Stimulated absorption [2] given by the following equation :

$$n_{abs} = B_{12} n_1 \rho(v_{12}) \tag{2.10}$$

The absorption rate is represented by n_{abs} meaning the number of absorption per unit time and volume, B_{12} is Einstein coefficient for stimulated absorption $(m^3 Hz/Js)$ and $\rho(v_{12})$ is energy density at the frequency v $(J/m^3 Hz)$.

Spontaneous emission.

The process that follows stimulated absorption is spontaneous emission. It is caused by an unstable electron which in its excited state, has a shorter emission life time. If an electron was stable in a high energy state, no spontaneous emission would be witnessed. After a while, an electron in an upper level (excited level) will eventually fall and emits a photon in the process [76]. The higher the fall the higher the energy emitted. This process is called spontaneous emission. The two processes, in particular absorption and spontaneous emission, occurred in a regular conventional light source [2].

$$\Delta E = E_2 - E_1 = h v_{12} \tag{2.11}$$

The degree of emission against the unit volume symbolised by (n_{sp}) is only relative to the population n_2 and independent of radiation energy density only in emissions that are spontaneous.

$$n_{sp} = A_{21} n_2 \tag{2.12}$$

where n_{sp} represents the rate at which spontaneous emission occur and A_{21} represents Einstein coefficient for spontaneous emissions.

Stimulated emission.

Under stimulated emission, the molecule is stimulated to release its photon earlier than it would be with spontaneous emission. This is crucial for laser activity [77]. Electrons in a higher level (E_2) waiting to spontaneously fall to a lower level (E_1) are accompanied by the emission of a independent photon energy, and each having an energy of $(hv_{12}) = E_2 - E_1$. Each of the awaiting electrons can be buried in a field of photon energies independently having the same energy of $(hv_{12}) = E_2 - E_1$ and in phase as illustrated in figure 2.12 [19]. Electrons are activated to fall in energy from

higher energy states to lower ones (E_2 to E_1) adding to photons whose waves are in phase with the existing radiation field. A vast radiation can develop if the process of stimulation of electrons to produce photons can reoccur and continue in a similar manner [78]. The emitted radiation is monochromatic because now each photon has an energy of around $(hv_{12}) = E_2 - E_1$ which is coherent with all photons and in phase thus strengthening the radiation field [2, 53]. Stimulated emission rate (n_{st}) is given by :

$$n_{st} = B_{21} n_2 \rho(v_{12}) \tag{2.13}$$

Where B_{21} is the Einstein coefficient for stimulated emission $(m^3 Hz/Js)$

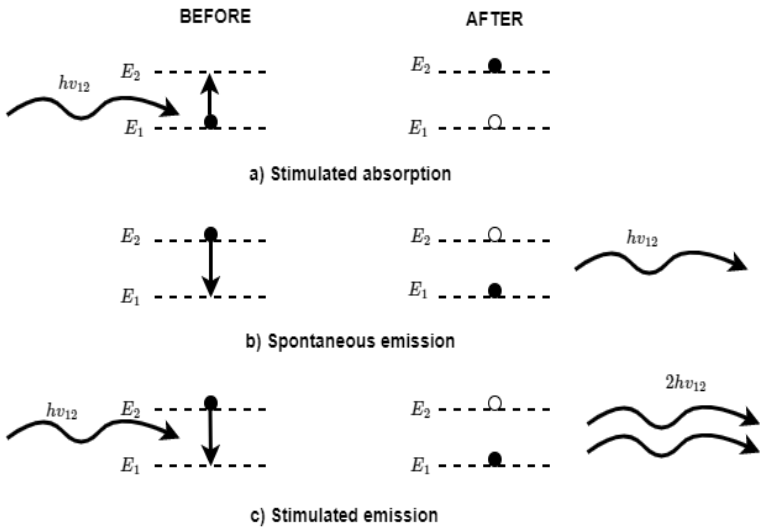


FIGURE 2.12: Illustrations on conditions for laser operation.

2.5.4 Einstein coefficients.

Under thermal equilibrium, upward and downwards transitions must be the same.

$$n_{12} = n_{21} \tag{2.14}$$

giving

$$B_{12} n_1 \rho(v_{12}) = A_{21} n_2 + B_{21} n_2 \rho(v_{12}) \tag{2.15}$$

Substituting equation 2.9 into equation 2.15 and rearranging it, energy density equation is obtained :

$$\rho(v_{12}) = \frac{A_{21}}{B_{12} e^{\frac{hv_{12}}{K_B T}} - B_{21}} \tag{2.16}$$

It can be assumed that B_{12} = B_{21} = B under equilibrium scenarios and a relation between Stimulated and Spontaneous emissions can be summed up by equation 2.17. B_{12} and B_{12} being the likelihood that a Stimulated emission process will take place while A_{21} is the likelihood that a Spontaneous emission process will take place [79].

$$\frac{A_{21}}{B} = (e^{\frac{hv_{12}}{K_B T}} - 1)\rho(v_{12}) = \frac{8\pi h v_{12} v^3}{c^3} \tag{2.17}$$

2.5.5 Life time.

A measure of how of long electrons can remain at an excited energy level is given by a time constant (τ_{sp}). It is generally referred to as the time period (life span) over which a spontaneous emission occurs [80]. It is considered that the likelihood (p) of an electron leaving the higher energy state in the fundamental time interval will be :

$$p = p_t \Delta t \tag{2.18}$$

where p_t represents the likelihood against a unit time that an emission that is spontaneous takes place and (Δt) is the time interval. If there are electrons in that energy state at a time (t), the change in the population of electrons (Δn) in the fundamental time interval (Δt) is given by equation 2.19. A decline in the number of electrons is accounted for by the negative sign.

$$\Delta n = -n p_t \Delta t \tag{2.19}$$

Equation 2.19 is defined by the use of limits to get equation 2.20 :

$$\frac{dn}{dt} = -n p_t \tag{2.20}$$

Integrating equation 2.20 the following is achieved :

$$n = n_0 e^{-} p_t t \tag{2.21}$$

The population of electrons in the higher energy state at a time (t = 0) is given by n_0. The life span of Spontaneous emission will then be given by :

$$\tau_{sp} = \frac{1}{p_t} \tag{2.22}$$

A_{21} being the Spontaneous emission likelihood, it will then be computed as :

$$\tau_{sp} = \frac{1}{p_t} = \frac{1}{A_{21}} \tag{2.23}$$

$$A_{21} = \frac{1}{\tau_{sp}} \tag{2.24}$$

2.5.6 Optical absorption.

The study of how laser beam power can be controlled depending on its distance as it propagates is important in the field of laser opto electronics. Equation 2.10, shows the number of absorptions that are stimulated against a unit time in a medium, and it is represented by (R_{abs}) as shown in equation 2.25. An emitted beam of a specified frequency v moves in a x direction through a volume of medium ($\Delta x \Delta y \Delta z$).

$$R_{abs} = n_{abs} \Delta x \Delta y \Delta z \tag{2.25}$$

Stimulated emission and energy absorption rates are given by (q_{st}) and (q_{abs}) as :

$$q_{abs} = h v_{12} R_{abs} = n_{abs} h v_{12} \Delta x \Delta y \Delta z \tag{2.26}$$

$$q_{st} = n_{st} h v_{12} \Delta x \Delta y \Delta z \tag{2.27}$$

Net energy absorption (q_a) is given by equation 2.28 when considering only the contributions made by Stimulated emissions and Stimulated absorptions.

$$q_a = [n_{abs} - n_{st}] h v_{12} \Delta x \Delta y \Delta z \tag{2.28}$$

Energy flux against a unit time $(q(x))$ is given by :

$$q(x) = I(x) \Delta y \Delta z \tag{2.29}$$

where $I(x)$ is the energy intensity at a distance x. The output Flux out of the medium is given by :

$$q(x + \Delta x) = I(x + \Delta x) \Delta y \Delta z = I(x) \Delta y \Delta z + \frac{dI(x)}{dx} \Delta x \Delta y \Delta z \tag{2.30}$$

with a resultant net flux energy of :

$$q_e = q(x + \Delta x) - q(x) = \frac{dI(x)}{dx} \Delta x \Delta y \Delta z \tag{2.31}$$

With steady state conditions, it is expected that the absorbed energy and the emitted energy should be equivalent in value (magnitude), but with opposite signs. Equation 2.32 can be drawn by looking at equation 2.28 and 2.31.

$$\frac{dI(x)}{dx}\Delta x\Delta y\Delta z = -[n_{abs} - n_{st}]hv_{12}\Delta x\Delta y\Delta z \tag{2.32}$$

Substituting n_{abs} and n_{st} from equation 2.10, 2.13, 2.17 and equation 2.23 computed is equation 2.33 :

$$\frac{dI(x)}{dx} = -\frac{c^3}{8\pi v^2\tau_{sp}}\rho(v_{12})(n_1 - n_2) \tag{2.33}$$

the beam intensity which is the energy against a unit area and time of a light output, can be written as the product of the energy density and propagating speed which is expressed as the energy against a unit volume (energy per unit volume).

$$I = c_m\rho(v_{12}) \tag{2.34}$$

c_m = c/n represents the velocity of a light beam in a medium with n representing the refractive index of that medium. For mono directional propagation equation 2.33 can then be written as :

$$\frac{dI(x)}{dx} = -\alpha I(x) \tag{2.35}$$

where

$$\alpha = \frac{c^2 n}{8\pi v^2\tau_{sp}}(n_1 - n_2) \tag{2.36}$$

integration of equation 2.35, then gives :

$$I(x) = I_0 e^{\alpha x} \tag{2.37}$$

2.5.7 Population inversion.

If $n_1 > n_2$ from equation 2.36 then absorption coefficient (α) in units per unit length becomes positive. Since n_1 is greater than n_2 bounded by thermal equilibrium circumstances, it will cause narrowing of a studied beam as it moves through a particular medium. However if the conditions are reversed and making n_2 greater than n_1, this will make α a negative value and the beam intensity will exponentially increase as it moves through that medium.

$$I(x) = I_0 e^{\beta x} \tag{2.38}$$

$$\beta = \frac{c^2 n}{8\pi v^2 \tau_{sp}}(n_2 - n_1) \tag{2.39}$$

Population inversion is termed by the condition that $n_2 > n_1$ and is the reversal of the normal thermal conditions as stated by the Boltzmann's equation. β being positive represents the small gain coefficient.

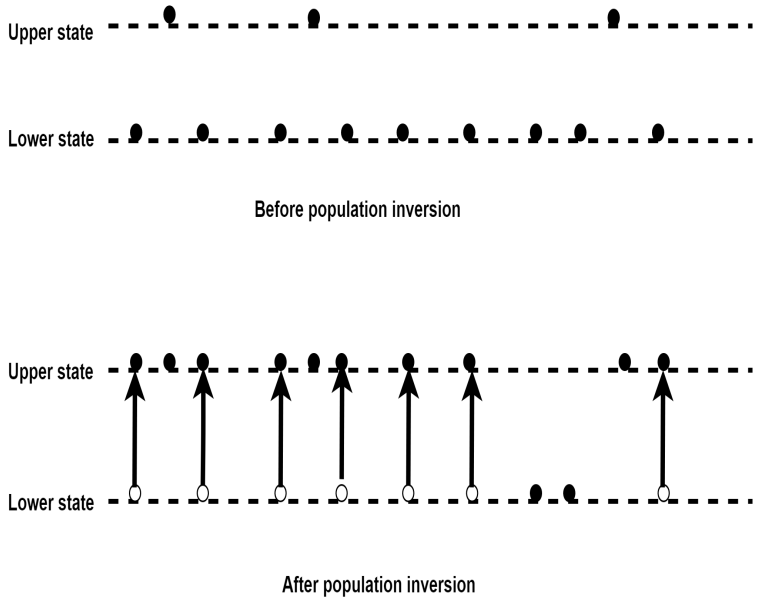


FIGURE 2.13: Population inversion illustration.

2.5.8 Cavity construction.

An optical resonator determines the longitudinal and transverse modes. Longitudinal modes are the resonance frequencies that may be permitted m to build up inside a resonator. The transverse mode is basically the field distributions. Certain discrete frequencies that satisfy the round trip phase equal to multiples of 2π are the only ones allowed in a resonator cavity.

$$k_0 n 2L = q 2\pi \tag{2.40}$$

$$\frac{2\pi}{\lambda_0} v n 2L = q 2\pi \tag{2.41}$$

$$\frac{2\pi}{c} v n 2L = q 2\pi \tag{2.42}$$

$$v_q = q\frac{c}{2nL} \tag{2.43}$$

Where v_q is the resonance frequency, k_0 is the round trip phase, n represents the medium refractive index, L representing the length of the cavity and q being an integer. In a semiconductor laser wave guide and having $n_1 > n_2$ determines the number of modes supported in the cavity (which are usually TE_0 and TM_0). With the correct choice of n_1, n_2 and d, it is possible to control the number of modes by using the V parameter.

$$V = \frac{2\pi d}{\lambda}\sqrt{n_1^2 - n_2^2} \tag{2.44}$$

$V < \pi$ is equal to 1 mode oscillating and $\pi < V < 2\pi$ gives 2 modes oscillating in a resonator cavity. Where n_1 represents the active region refractive index, n_2 is the refractive index of the cladding (usually spacer) and d represents the active region thickness.

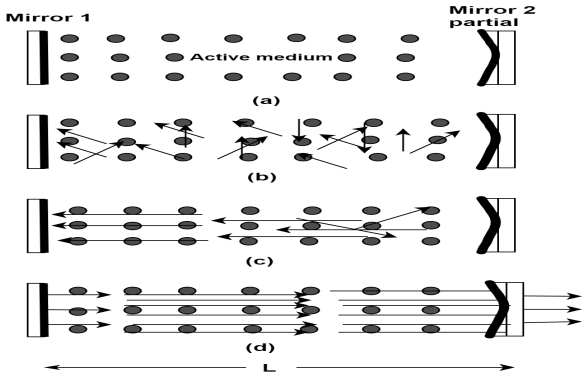


FIGURE 2.14: Cavity construction.

2.5.9 Threshold gain.

In order for the laser oscillations to be reformed and maintained in the active region, a threshold gain should first be achieved. When the threshold gain is reached, the loss of the device should at least be equivalent to the gain (β_{th}) when designing the system [81]. The losses were not taken into account in equation 2.36 and 2.39 as they showed that α and β have the same values, which in the real laser production does not apply [82]. An element ($e^{\beta L}$) amplifies the beam power which then is attenuated by another element ($e^{-\alpha L}$).

$$I = I_0 e^{(\beta - \alpha)L} \tag{2.45}$$

The active region medium is represented by L, I_0 is the initial beam power (intensity).Reflection losses from the mirrors further reduce the beam intensity. For example, a reflection from the first mirror (mirror 1) has its own losses. Another transition through a medium accompanied by a reflection from the second mirror

(mirror 2) makes a whole complete passage through a cavity resonator and creates one resulting beam intensity.

$$I = I_0 R_1 e^{(\beta-\alpha)} L \tag{2.46}$$

Where R_1 is mirror 1 and R_2 is mirror 2.

$$I = I_0 G_g = I_0 R_1 R_2 e^{2(\beta-\alpha)L} \tag{2.47}$$

where G_g is the full cycle (round-trip) power gain [83]. Oscillations can only be sustained if the beam energy intensity does not decline after each round-trip passage

$$I \geq I_0 \tag{2.48}$$

$$G_g = R_1 R_2 e^2(\beta - \alpha) \geq 1 \tag{2.49}$$

With steady state scenarios I = I_0 and the small signal threshold gain is expressed by:

$$\beta_{th} = \alpha = \frac{1}{2L} ln(\frac{1}{R_1 R_2}) \tag{2.50}$$

$(\frac{1}{R_1 R_2})$ of equation 2.50 reflects losses due to constructive output coupling [84]. Taking into consideration, the threshold condition and substituting equation 2.36 resulting in :

$$n_2 - n_1 = -\frac{8\pi v^2 \tau_(sp)}{c^2 n}(\beta_{th} - \frac{1}{2L} ln \frac{1}{R_1 R_2}) \tag{2.51}$$

Population inversion is bound to obtain a specific threshold or critical value shown by equation 2.51.

2.6 Rate equations

2.6.1 Two level system.

Boltzmann's law in general form :

$$\frac{n_j}{n_i} = e^{-\frac{\Delta E_{ij}}{K_B T}} \tag{2.52}$$

In equilibrium the number of electrons in the lower energy state is greater than those in the upper energy state ($n_1 > n_2$) but n_2 increases with increasing temperature [85]. At low temperatures ($k_B T << \Delta E$) no electrons exist in the upper energy level ($n_1 > n_2$). As $k_B T >> \Delta E$, n_2 increases to a closer value to n_1 ($n_1 = n_2$), but it can never exceed the population in n_1 unless non equilibrium conditions such as population inversion are introduced [86]. n_i is the population of electrons against a unit volume in the lower energy state, n_j is the number of electrons against that particular unit volume in upper energy level and ΔE_{ij} represents the energy difference between the two energy states. For a level 2 system the rate that n_2 changes is derived from equation 2.10, 2.12and 2.13 thereby giving :

$$\frac{dn_2}{dt} = n_1 B_{12}\rho(v_{12}) - n_2 B_{21}\rho(v_{12}) - A_{12}n_2 \tag{2.53}$$

0r from equation 2.23 and 2.24.

$$\frac{dn_2}{dt} = (n_1 - n_2)B_{12}\rho(v_{12}) - \frac{n_2}{\tau_{sp}} \tag{2.54}$$

The first expression ($n_1 B_{12}\rho(v_{12})$) from equation 2.53 is the rate of increase of population of electrons in the upper energy level (n_2) from excitation from lower energy level (E_1). The second expression ($n_2 B_{21}\rho(v_{12})$) is the rate at which losses occur due to stimulated emissions from upper (E_2) to lower energy level. The last expression ($A_{12}n_2$) is the rate at which losses occur now due to spontaneous emissions. It is then got

$$n_1 + n_2 = n \tag{2.55}$$

$$\Delta n = n_1 - n_2 \tag{2.56}$$

$$n_1 = \frac{1}{2}(n + \Delta n) \tag{2.57}$$

$$n_2 = \frac{1}{2}(n + \Delta n) \tag{2.58}$$

Equation 2.53 will then be :

$$\frac{d}{dt}(\Delta n) = \frac{n}{\tau_{sp}} - \Delta n[2B_{12}\rho(v_{12}) + \frac{1}{\tau_{sp}}] \tag{2.59}$$

Under steady state conditions, the degree at which of population of electrons changes with time is zero $d(\Delta n)/\mathrm{dt}$

$$\Delta n = \frac{n}{1 + 2\tau_{sp} B_{12} \rho(v_{12})} \tag{2.60}$$

Equation 2.60 shows that the rate of electron population change (Δn) decreases as energy density ($\rho(v_{12})$) goes up. Energy density relies on the population of electrons in the resonator cavity mode and as absorptions rises up, $\tau_{sp} B_{12} \rho(v_{12}) \rightarrow \infty$ as $\Delta n \rightarrow 0$.

$$n_1 = n_2 = \frac{n}{2} \tag{2.61}$$

Population inversion is difficult to achieve in a system with two transition levels because absorption ceases when electrons are pumped to a point where the number of electrons in the lower energy state equals the number in the higher energy state.

2.6.2 Three level system.

With a population against a unit volume identified by n_1, n_2, n_3, electrons are pumped from E_1 to E_3 followed by a fast decline to E_2 and radiative shift that ends in a lasing activity happening within E_2 and E_1 transitions. Equation 2.62 gives the rate at which the number of electrons in E_3 change.

$$\frac{dn_3}{dt} = W_p n_1 + W_{13} n_1 + W_{23} n_2 - W_p n_3 - W_{31} n_3 - W_{32} n_3 \tag{2.62}$$

or

$$\frac{dn_3}{dt} = (W_p + W_{13}) n_1 + W_{23} n_2 - (W_p + W_{32} + W_{31}) n_3 \tag{2.63}$$

The likelihood against a unit time of actuated shifts brought about by the energising rays in the frequency range (v_{13}) is commonly known as the pumping rate represented by $W_p = B_{13} e(v)$. $e(v)$ represents the energy density of the pumping beam and W_{ij} represents the likelihood against a unit time of the electron being thermally energised between level i and j [87]. Spontaneous emissions are then given by the following equation.

$$W_{ij} = A_{ij} + S_{ij} \tag{2.64}$$

where A_{ij} denotes part of Einstein coefficients linked with spontaneous emissions where $S_i j$ arises from non radiative decay activity for instance transferring of energy to nearby electrons in vibrational, kinetic or other energy forms.
($W_p n_1$) from equation 2.62 denotes the rate at which electrons increase at E_3 as a

result of pumping, ($W_{13}n_1$) is the rate at which electrons increase as a result of thermal excitation, ($W_{23}n_2$) results from thermal excitation from E_2 to E_3 and ($W_p n_3$) is a result of losses from E_3 to E_1 and to E_2 respectively, due to thermal excitation [85]. If an assumption that $K_B T << \Delta\ E_{ij}$ is made, then from equation 2.52 it is concluded that:

$$W_{ij} << W_{ji} \tag{2.65}$$

i represents the lower energy state and j represents the higher energy state or simplified as $W_{12} << W_{21}$. Equation 2.63 then becomes :

$$\frac{dn_3}{dt} = W_p(n_1 - n_3) - (W_{32} + W_{31})n_3 \tag{2.66}$$

like wise for n_2 the following is witnessed

$$\frac{dn_2}{dt} = W_s n_1 + W_{12}n_1 - W_s n_2 - W_{21}n_2 - W_{23}n_2 + W_{32}n_3 \tag{2.67}$$

$$\frac{dn_2}{dt} = W_s(n_1 - n_2) - W_{21}n_2 + W_{32}n_3 \tag{2.68}$$

$W_s = B_{12}e(v)$ is the likelihood with a unit time of forced shifts of electrons produced by the lasing activity in a frequency range v_{12}

$$\frac{dn_1}{dt} = -W_p n_1 - W_s n_1 - W_{12}n_1 - W_{13}n_1 + W_s n_2 + W_{21}n_2 + W_p n_3 + W_{31}n_3 \tag{2.69}$$

which then becomes :

$$\frac{dn_1}{dt} = -W_p(n_3 - n_1) + W_s(n_2 - n_1) + W_{21}n_2 + W_{31}n_3 \tag{2.70}$$

n will then represent the total population of electrons in the system which can be represented by the following :

$$n = n_1 + n_2 + n_3 \tag{2.71}$$

Equation 2.66, 2.68 and 2.6 makes up the rate equations for three level laser designs and they represent a laser behaviour that is time-dependent and specific for that design. A reflection on steady state conditions that pumping rate is stable and $\mathrm{d}n_i/dt = 0$ is made. Hence the whole left hand side of these equations are nullified (fixed at zero) giving :

$$n_1 = (\frac{W_p + W_{31} + W_{32}}{2W_p + W_{31} + W_{32}})(n - n_2) \tag{2.72}$$

$$n_2 = [\frac{W_s}{W_s + W_{21}} + \frac{W_p W_{32}}{(W_s + W_{21})(W_p + W_{31} + W_{32})}]n_1 \tag{2.73}$$

from the above equations the following equation was deduced :

$$\frac{n_2 - n_1}{n} = \frac{W_p(W_{32} - W_{21}) - W_{21}(W_{31}) + W_{32}}{W_s(3W_p + 2W_{31} + 2W_{32}) + W_p(2W_{21} + W_{32}) + W_{21}(W_{31} + W_{32})} \tag{2.74}$$

When population inversion occurs in a steady state manner with a desirable stated pumping rate W_p, equation 2.74 is used because it represents the continuous wave (CW) mode that produces population inversion stability. Taking into account the above cases, the losses exactly equal to the gain, which is a product of both the stimulated and spontaneous emissions. The population inversion can be obtained for three level systems ($n_2 > n_1$) if $W_{32} > W_{21}$ is fulfilled, which can be seen in equation 2.74.
In other words, a critical level of the population inversion should also be attained. An estimation can be made by following equation 2.24 and 2.64, as shown below:

$$W_{ij} \propto \frac{1}{\tau_{ij}} \tag{2.75}$$

The life span for a change from level i to level j is represented by τ_{ij}. It is believed that the life span for a change from E_3 to E_2 should be shorter than that for a change from E_2 to E_1 in order for population inversion to be achieved in a three energy level design. Other conditions required for the efficiency of the system is that E_2 becomes a meta stable with a rapid drop from E_3 to E_2. E_3 is basically a vacuum as the population inversion continues between E_2 and E_1. The energy level three E_3 is not necessarily a laser level, but a broad band level that permits optical sources with broad bandwidths to be used as pump sources for set ups. The population inversion depends on the degree of pumping W_p. A threshold pumping rate W_{pc} is vital to ensure that the population of E_2 is almost equal to the population of E_1. This can be obtained by making $n_2 = n_1$ from equation 2.74 which gives :

$$W_{pc} = \frac{W_{21}(W_{31} + W_{32})}{W_{32} - W_{21}} \tag{2.76}$$

Threshold pumping rate W_{pt} is key in maintaining laser oscillating waves which can be attained by realising a critical population inversion using equation 2.51 and merging it with equation 2.74.

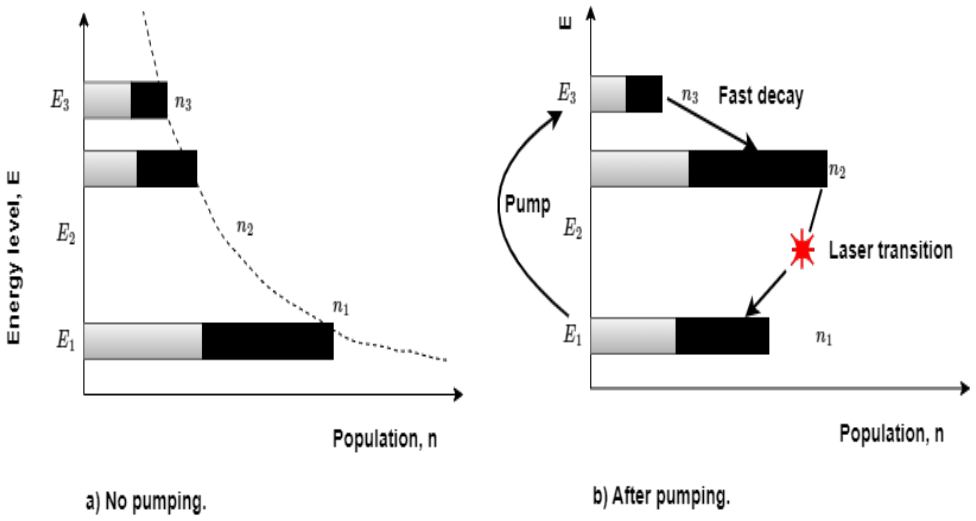


FIGURE 2.15: Three level system.

2.6.3 Four level system.

There are four energy levels that are considered which are $E_0, E_1, E_2, and E_3$. Deduced below are the rate equations commonly used for four level systems :

$$\frac{dn_3}{dt} = W_p(n_0 - n_3) - (W_{32}n_1 + W_{31} + W_{30})n_3 \tag{2.77}$$

or

$$\frac{dn_3}{dt} = W_p(n_0 - n_3) - W_3 n_3 \tag{2.78}$$

$W_3 = W_{32}n_1 + W_{31} + W_{30}$ in this case and energising of electrons from lower to upper has been ignored. The first expression indicates effective rate of excitation of electrons from the lowest energy state to the highest energy level whilst the second expression represents the fall of electrons from highest to lowest. The rate of change of E_2 is then given by :

$$\frac{dn_2}{dt} = W_s(n_1 - n_2) - W_{20}n_2 - W_{21}n_2 + W_{32}n_3 \tag{2.79}$$

0r

$$\frac{dn_2}{dt} = W_s(n_1 - n_2) - W_2 n_2 + W_{32}n_3 \tag{2.80}$$

where $W_2 = W_{20} + W_{21}$, giving :

$$\frac{dn_1}{dt} = W_s(n_2 - n_1) - W_{10}n_1 - W_{21}n_2 + W_{31}n_3 \tag{2.81}$$

and

$$\frac{dn_0}{dt} = W_p(n_3 - n_0) + W_{10}n_1 + W_{20}n_2 + W_{30}n_3 \tag{2.82}$$

finally having

$$n = n_0 + n_1 + n_2 + n_3 = constant \tag{2.83}$$

A Four level system is realised in a way that $W_{32} >> (W_{31}$ or $W_{30})$, similarly $W_{21} >> W_{20}$. Then under steady state cases population difference between n_1 and n_2 from equation 2.78 and equation 2.83 is attained as :

$$\frac{n_2 - n_1}{n} = \frac{(W_{10} - W_{21})W_{32}}{W_{32}(W_{10} + W_{21}) + W_3W_{31} + \frac{2W_p+W_3}{W_p}W_2W_{10} + W_s(2W_{32} + [\frac{2W_p+W_3}{W_p}]W_{10})} \tag{2.84}$$

It is clear from equation 2.84 that n_2>n_1 can be obtained if

$$W_{10} > W_{21} \tag{2.85}$$

For a four level system under steady state, the life span from E_1 to E_0 must be shorter than life span from $E_2 to E_1$. $W_{32} >> W_{21}$ and $W_{10} >> W_{21}$ and making equation 2.84 to become :

$$\frac{n_2 - n_1}{n} = \frac{W_{10}W_{32}}{W_{32}W_{10} + W_3W_{31} + \frac{2W_p+W_3}{W_p}W_2W_{10} + W_s(2W_{32} + [\frac{2W_p+W_3}{W_p}]W_{10})} \tag{2.86}$$

At minimal pumping power, the population inversion for a four energy level set up is obtained much simpler than that of a three-energy level set up since it is independent of the pumping power rate. The population inversion depends on the rate at which electrons are pumped from a lower energy state to the highest state (pumping rate). E_3 is not a laser level in four level design and has a broadband (wide bandwidth transmissions of data) with $E_{01} >> K_BT$. As soon as the population inversion for the CW operation is achieved, it remains in a stable state, no matter how the pumping rate exceeds it, because the gain must be equivalent to the system losses and must also be consistent (stable).

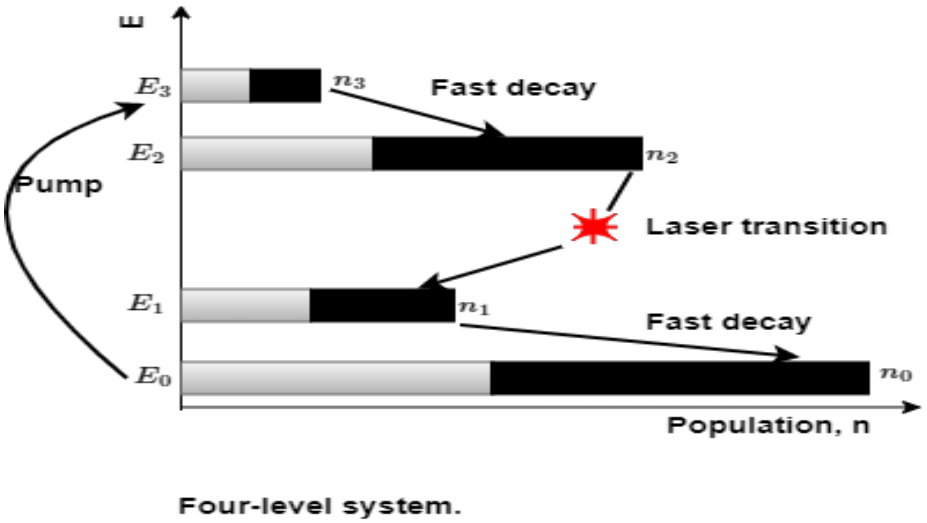


FIGURE 2.16: Four level system.

2.7 Semiconductor laser structures

A semiconductor laser is a p-n junction that is forward biased made of materials with a direct energy band gap [88].The first lasers were the p-n homo junction lasers. The homo junction structures have high current densities since both the carrier and optical confinement within the active region are minimal. Carriers injected by forward bias into the active region may simply pass through without recombination or diffuse to the outside and do not contribute to the lasing [89].In addition, the optical fields leak into the surrounding inactive layers bordering the gain medium. Both effects increase in threshold current density for lasing and lower laser efficiency. The use of different semiconductor materials, which are combined after the lattice matching can improve and produce hetero junction structures [90].Hetero junction lasers operating at room temperature are more efficient with lower losses and offer design flexibility (different compositions of alloy fractions can be used). In addition, hetero junction offers a better carrier and an optical confinement, that is, the carriers injected will be narrowed to a thinner region so population inversion could build up with lower threshold currents. Double hetero (DH) junction structures helps in more confinement of carriers injected into the active region. The changes at junctions in the refractive index help to further limit the light waves generated, thereby reducing the total current required to drive the device. The discontinuities in the conduction and valence band energy of the two structures acts greatly act to confine injected carriers within the narrow gap of the active region resulting in the trapping of holes and electrons in the active region. The disadvantage of this arrangement is that both the optical wave guide and the carrier confinement depend on a similar

hetero junction. Quantum wells offer an alternative to DH structures, as the energy of the emitted photon can be made substantially higher than that of the band gap. With a good choice of the well width, the energy of the emitted photon can be justified by allowing lasing at different wavelengths using the same material. A single QW is similar in design to a DH, except for a narrow gap close to the de Broglie's wavelength. Only certain discrete energy states are available in a well (allowed energy levels of the system). When radiation is absorbed or emitted, the electron jumps from one state to another and can only occupy a permissible quantum state. The narrower the well, the higher the quantum state energy. Multiple QWs improve the capturing probability of injected carriers.

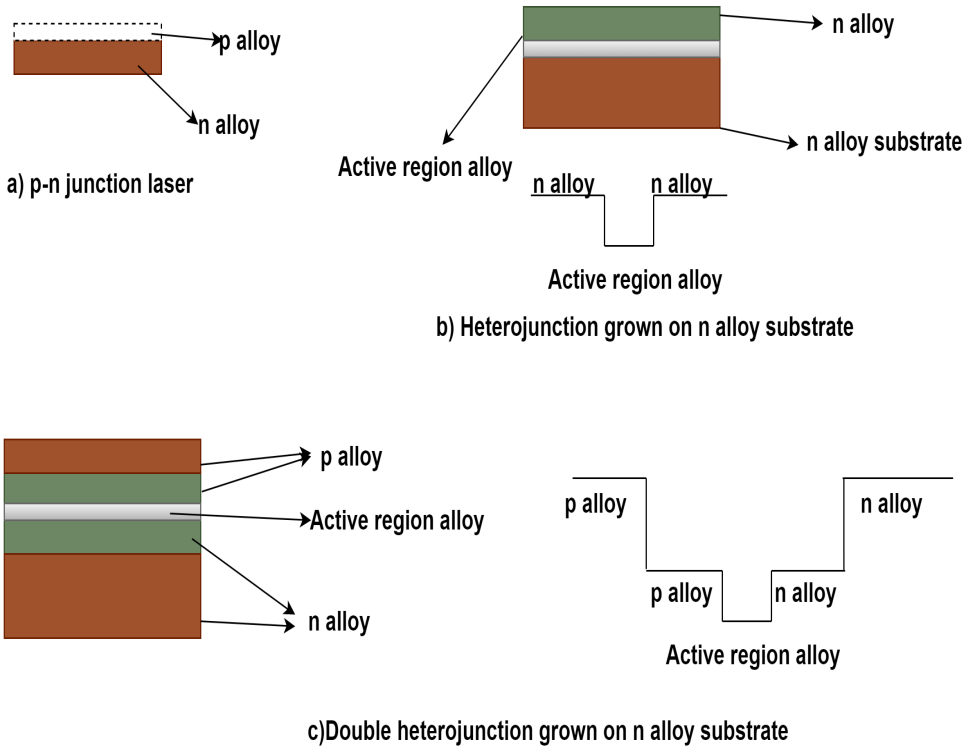


FIGURE 2.17: Junction laser structures.

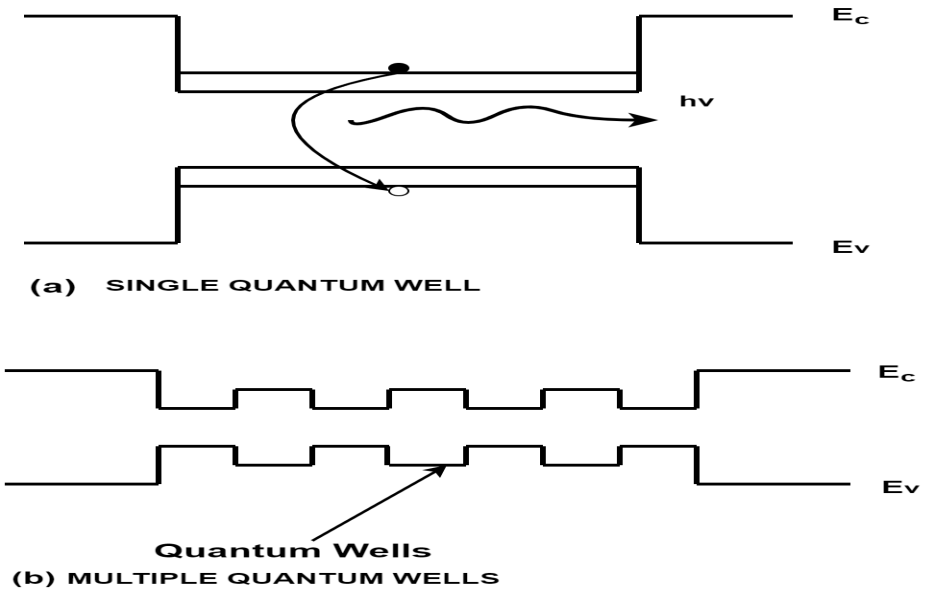


FIGURE 2.18: Quantum Well laser structures (a) showing a single quantum (b) Multiple Quantum Wells.

2.7.1 Carrier Distribution of Structures.

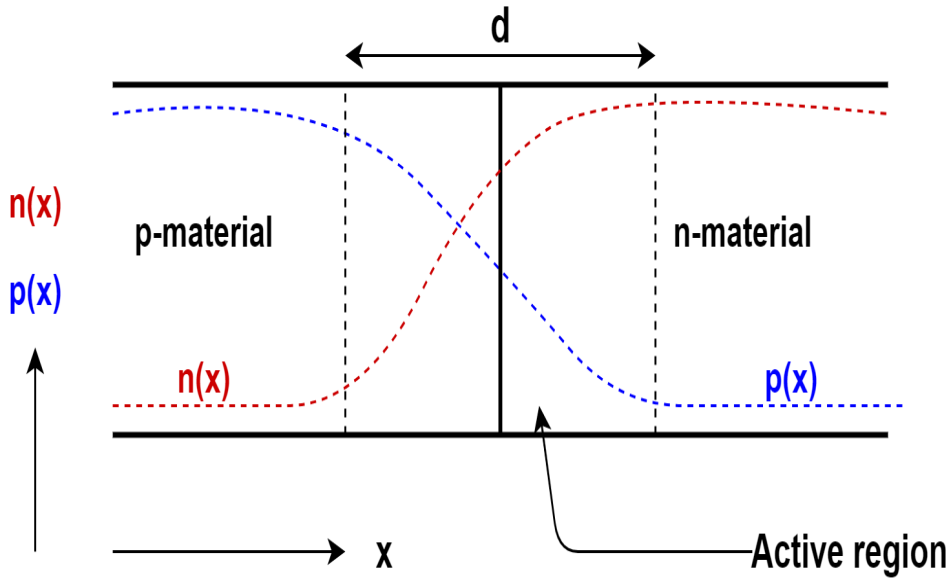


FIGURE 2.19: Carrier distribution across a homo junction.

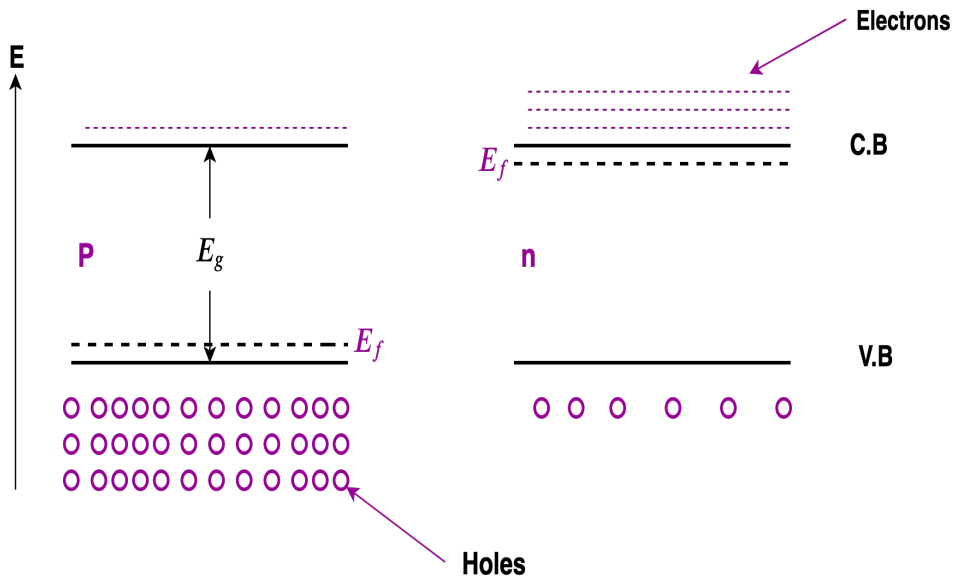


FIGURE 2.20: Homo junction before contact.

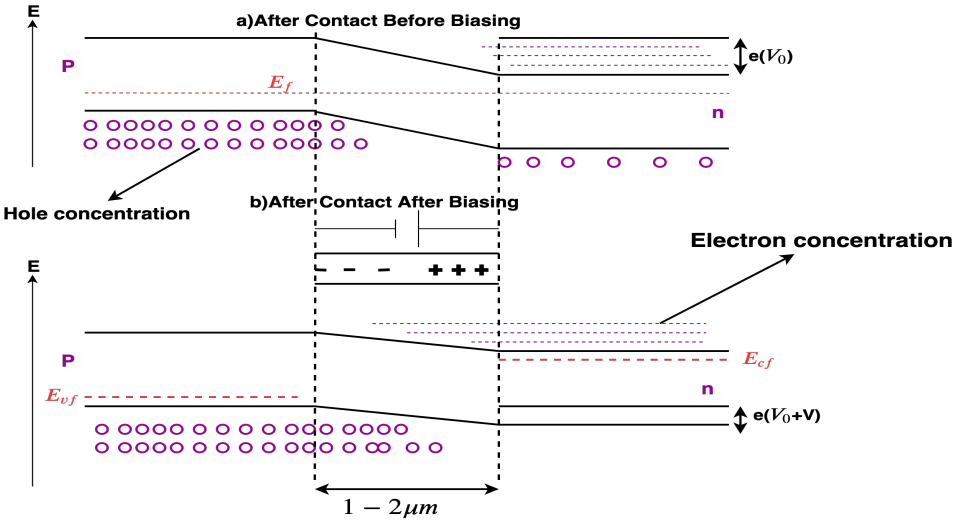


FIGURE 2.21: Homo junction after contact, before and after biasing.

2.8 Materials For VCSEL realisation

The elimination, selection, and differentiation of some materials from others to make them suitable for semi-conductor lasers is based on conditions that they can easily form p-n junctions and that they are efficient light emitters. Semiconductors formed from materials with an indirect band gaps have proven to be ineffective light emitters for laser applications [91].Examples of good light emitting structures are the Binary group III-V alloys, which make the growth of their ternary and quaternary structures useful for other light applications [2]. Tables 2 and 3 show the material

compounds and their properties. The light emission from the infrared and visible portion of the electromagnetic spectrum by light emitting devices is made possible by a wide range and variety in the band gap [92].

TABLE 2.1: Periodic table showing semiconductors occurrence.

Group two elements (II)	**Group three elements (III)**	**Group four elements (IV)**	**Group five elements (V)**	**Group six elements (VI)**
	B	C	N	
	Al	Si	P	S
Zn	Ga	Ge	As	Se
Cd	In		Sb	Te

TABLE 2.2: Elemental and compound semiconductors [2].

Elemental	**IV compound**	**Binary III-V compounds**	**Binary II-VI compounds**
Si	SiC	AlP	ZnS
Ge	SiGe	AlAs	ZnSe
		AlSb	ZnTe
		GaN	CdS
		GaP	CdSe
		GaAs	CdTe
		GaSb	
		InP	
		InAs	
		InSb	

TABLE 2.3: Semiconductor Material Properties. S-C is the semiconductor, B-S-T is band structure type (i is indirect and d is direct), C-S is crystal structure (Z is zinc ans W is wurtzite), Eg is the energy band gap, a is the Angstrom, ϵ_r is the dielectric constant of the material, D is the density and M-P is the melting point [2].

S-C	**B-S-T**	**C-S**	**Eg [eV]**	**a[Å]**	ϵ_r	**D** [g/cm^3]	**M-P** [°C]
AlP	i	Z	2.45	5.46	9.8	2.40	200
InSb	d	Z	0.18	6.48	17.7	5.78	525
GaSb	d	Z	0.70	6.09	15.7	5.61	712
InAs	d	Z	0.36	6.06	14.6	5.67	943
InP	d	Z	1.35	5.87	12.4	4.79	1070
AlSb	i	Z	1.60	6.14	11.0	4.26	1080
GaAs	d	Z	1.43	5.65	13.2	5.31	1238
GaP	i	Z	2.26	5.45	11.1	4.13	1467
AlAs	i	Z	2.16	5.66	10.9	3.60	1740
GaN	d	Z,W	3.40	4.50	12.2	6.10	2530

2.8.1 Light emitting materials and choice of material

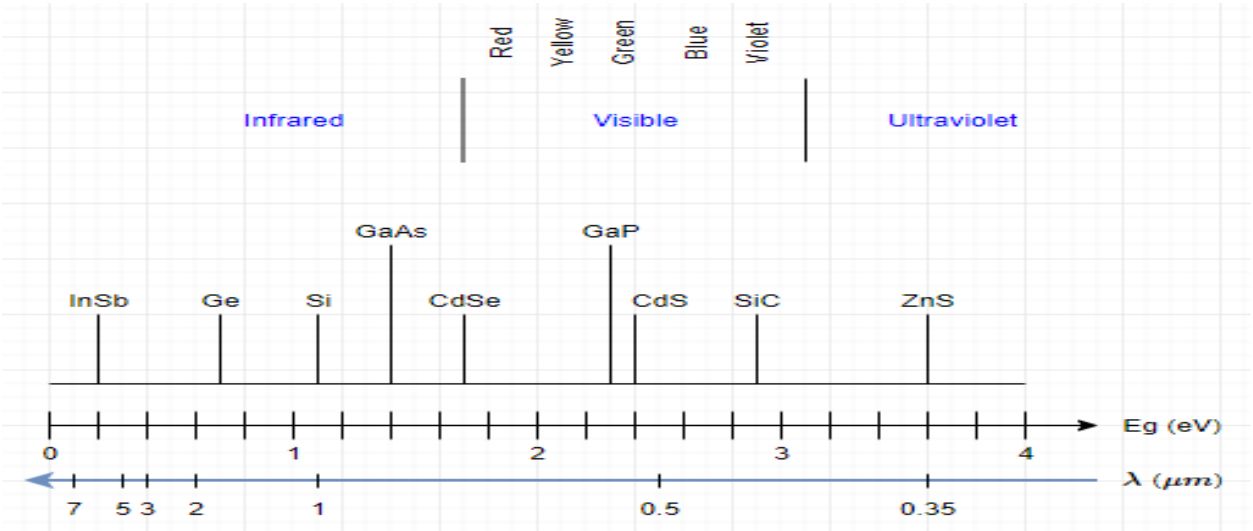


FIGURE 2.22: Band Gaps of some semiconductors.

Laser structures are made up of various materials that emit light that converges to frame intersections that will follow the procedures for lasing. The recombination of the electron holes must be direct, without the need for trapping, for the device to emit light [93]. Doping the material n or p-type to make a p-n junction would be simplified if the E-H recombination is direct. These intersections are made possible

by the lattice matching that can be achieved through epitaxial growth. Indirect band gap semiconductors are not sufficient light producers. Group II-VI compounds are sufficient producers, but their junctions are difficult to make. A sound instance of a suitable material structure for lasers used in fibre optic devices is InP, GaAs and mixed alloys of these compounds such as InGaAsP/InP. The AlGaAs band gap can be changed by selecting the composition of the group III sub lattice, which allows the development of barriers and bounding layers. The quaternary combination in InGaAsP is versatile in laser diodes production and enables wavelength selection and adaptability in lattice matching. By choosing the right composition, lasers can be produced in the infrared range of 1.33-1.55 μ m which is required for fibre optics [3]. Since four compounds can be changed in picking the combination structure, InGaAsP allows the simultaneous choice of energy gap (emission wavelength). Different wavelength ranges are required for laser yield in various applications[19]. Figure 2.22shows a band gap of binary compound semiconductors with a wide range in band gap. By using ternary and quaternary compounds, the quantity of attainable energies can be extended. A decent model is the alloy arrangement of GaAsP as in figure 2.23.As level of P expands, the level of As decreases, and the resulting direct band gap shifts from the direct 1.43-eV gap of GaAs(infrared) to the indirect 2.26-eV gap of GaP(GREEN). For red Displays, the most notable compound structure is x=0.4. For GaAsP with P concentrations more than 45 percent, the band gap is due to the indirect X minimum, as shown in figure 2.23, which suggests an indirect band gap without radiation recombination [2, 19].

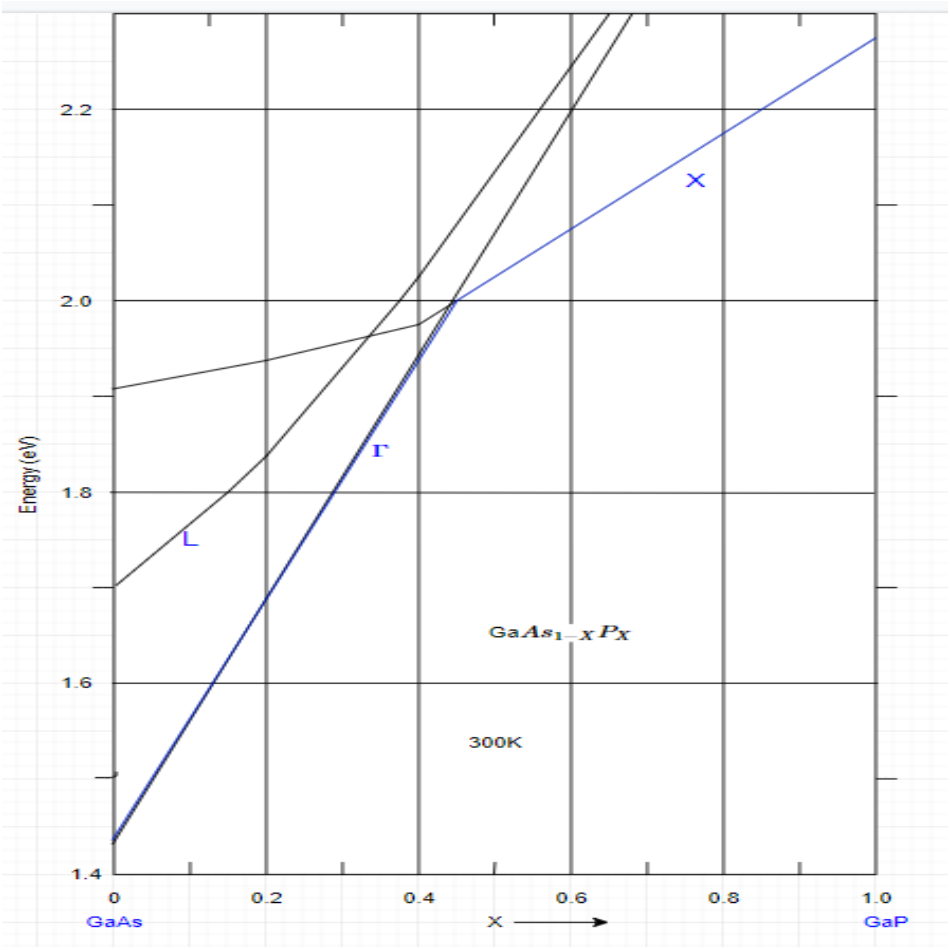


FIGURE 2.23: Conduction band energies of GaAsP.

2.8.2 VCSEL structure.

At the fabrication stage the substrate is deposited by epitaxy. The DBRs form a vertical resonator with the bottom first bragg stack having $(R_2 \approx 100)$ and made of periods of alternating high and low refractive index. An optional oxidation isolation layer can be deposited, usually SiO_2 is used to block the carriers (confining current) and make light to be generated in the central of the active region while guiding the intensity of the optical field within the surface emitting laser [94]. Oxide layers enhance power conversion efficiencies, help to lower the optical losses and the threshold current. An active region with a set of one or more QWs can be deposited and its thickness can only be up to less than 10 μm using this method. The use of QWs over a bulky active region is desirable because a greater optical field is achieved from the electrons confined by barriers of the well, resulting in quantum well effect, which is commonly referred to as electron in a well method. The higher the number of QWs,the better the useful output power for a telecommunication application [95]. The active region is sandwiched between high band gap materials. It

acts as a cavity and in this structure the light builds in the vertical direction. Follows the top DBR stack $(90 \leq R_1 \leq 100)$.

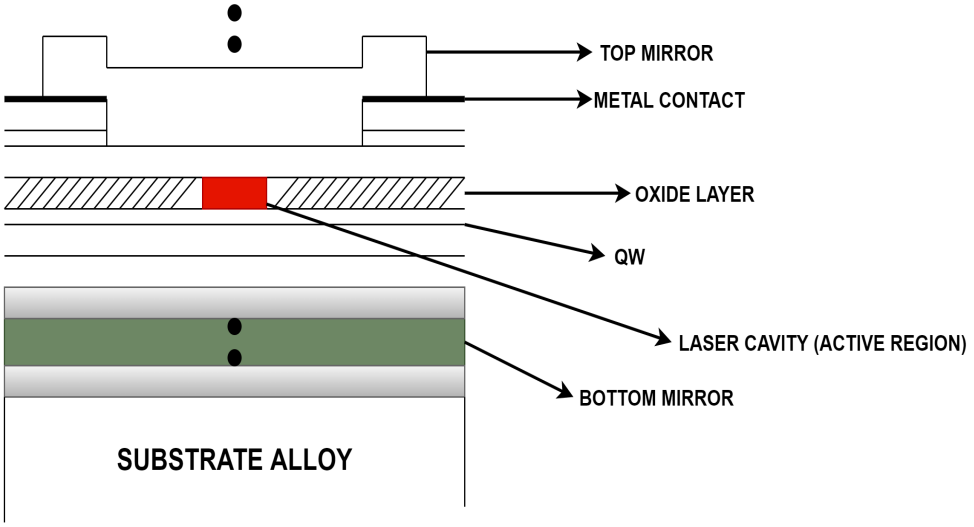


FIGURE 2.24: Typical VCSEL structure.

2.8.3 Dynamics of the Structure.

The thickness of each layer in the bragg stacks is given by :

$$t = \frac{\lambda_0}{4n} \tag{2.87}$$

where
λ_0 = operating wavelength
n = refractive index
t = thickness of each layer

The period$(\bigwedge)$ is then given by thickness of layer with low refractive index (t_1) plus layer thickness of a material with a high refractive index (t_2).

$$\bigwedge = t_1 + t_2 \tag{2.88}$$

With VCSELs a large number of lasers can be grown on a chip all emitting up wards. With Gain profiles for VCSELs for different values of current, scattering diffraction losses (α_s) and losses due to mirrors (α_m) can be found and related to resonance loss (α_r) and gain (γ) by :

$$\alpha_r = \gamma = \alpha_s + \alpha_m \tag{2.89}$$

A relation between mirror losses, cavity length (l) and reflectivity (R) of the two mirrors can then be made :

$$\alpha_m = \frac{1}{2l} ln(\frac{1}{R_1 R_2}) \tag{2.90}$$

Knowing all the losses and the reflectivity of the two mirrors, the length of the cavity can be calculated and with assumptions that ($R_1 \approx R_2 = R$) then equation 2.17 becomes :

$$\alpha_m = \frac{1}{2l} ln(\frac{1}{R}) \tag{2.91}$$

Arbitrary values are used for the purposes of showing the relationship between Reflectivity of the mirrors and the cavity length.

TABLE 2.4: Reflectivity VS. Cavity length.

REFLECTIVITY [R]	LENGTH OF CAVITY l [μm]
0.32	285
0.90	10
0.99	2.5
0.998	0.2

This shows that for a small length of gain medium, the reflectivity must be high. As the length of the cavity (l) is reduced, then mirror losses α_m increases, unless the reflectivity (R) is increased to minimise the loss. When the reflectivity of the mirrors is small, the length of the gain medium should be longer for amplification, and compensate for the mirror losses. With VCSELs, it is impossible to have longer gain mediums, so the reflectivity should be higher. The Reflectivity formula can then be:

$$R = [\frac{1 - [\frac{n_L}{n_H}]^{2N}}{1 + [\frac{n_L}{n_H}]^{2N}}]^2 \tag{2.92}$$

where :
N = Number of periods
n_L = Material layer with a lower refractive index
n_H = Material layer with a higher refractive index

From equation 2.92, it shows that the higher the number of periods the higher the reflectivity.

- Top Layer: Electrical contact for current injection.
- Top Mirror: It is a partially reflective mirror ($99 < R < 100\%$). Layers are made of Distributed Bragg Reflectors (DBRs).
- Oxide Layers : Constructs a light emitting win down so that light beam can be optimised in a circular beam. It confines light.
- Laser Cavity: This is the active region where lazing happens.
- Quantum Well: Explicitly the phenomenon results from electrons and holes being confined into a well that approaches towards a basic quantum estimation called exciton Bohr radius . This will effect in change of electronic and optical properties of the material being tested to the designer's preferences (Quantum confinement). This is where generated photons can bounce back and forth between the top and bottom DBR mirrors.
- Bottom Mirror: It is a highly reflective mirror (R close to 100% reflectivity).

2.9 Growth Techniques

The success of semiconductor devices i.e. their developments and improvements made on materials has be led by the use of Wafers. Pure Silicon crystals as an example has been a massive influence on the advancements of semiconductor devices and the development process of a wafer is presented below.

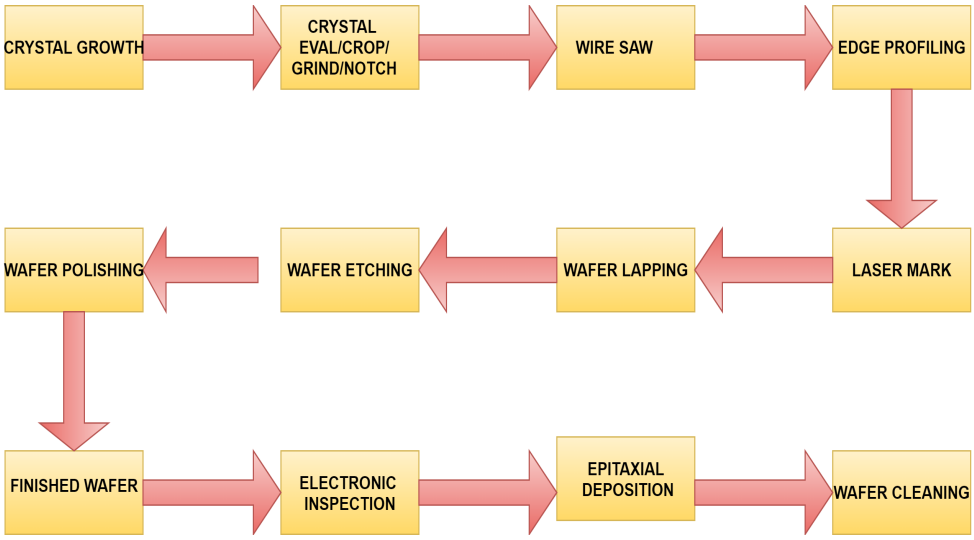


FIGURE 2.25: Steps involved in manufacturing Si wafers.

Liquid phase epitaxy (LPE), Chemical vapour deposition (CVD) and Molecular beam epitaxy (MBE) make available suitable atoms to a surface of a growing layer.

Some vital conditions should be considered, such as maintaining the arrangement (orientation) of crystal structure and the substrate. Orientation can be achieved by using a crystal thin layer on a wafer that has the same lattice structure as the wafer. The crystal layer can be composed of the same material or a different material from that of the wafer. A natural match between the epitaxial layers and the substrate is attained when both have the same materials. For example, a Ga layer grown on a Ga substrate will have a natural lattice match. However, a Hetero epitaxy may be desirable, but there must be a match in the lattice structure and the lattice constant between the various epitaxial layers. AlAs and GaAs have the same lattice constants and AlGaAs and the entire compositional range from AlAs to GaAs have similar lattice constants. Therefore, the composition of x in the compound $Al_xGa_{1-X}As$can be varied and matched on GaAs. For example, an AlGaAs alloy can be grown on a GaAs substrate, and Ge substrates can be used to grow GaAs epitaxial layers all because of higher probabilities of slight insignificant mismatches in their sub lattices.

2.9.1 Lattice matching.

In order to broaden the range of quaternary alloys such as InGaAsP, the sub lattices compositions or the alloys of group three (III) and four (V) can be changed according to the desires of the designer to form lattice epitaxial matching layers [96]. This is an added advantage in the selection of a specific band gap whilst giving a convenience for lattice-matching to binary compounds such as InP and GaAs [40].]. Assuming that the lattice constants of ternary compounds change directly with the composition of x,hen a GaAsP's lattice constant can be found in between that of GaP and GaAs, if $In_xGa_{1-X}As_yP_{1-y}$ has an x composition approximately 0.53 and can grow on substrates containing InP with a material composition dependent energy band gap of 0.75 - 1.35 eV. This means that $In_xGa_{1-X}As_yP_{1-y}$ can be directly grown in InP without tempering with the lattice constant during the growth process.

Vapour Phase Epitaxy (VPE)

A controlled process where a chemical vapour normally compromising of Silicon (Si) can be used for deposition of epitaxial layers:

$$\underset{\text{silicon tetra chloride}}{SiCl_4\downarrow} + \underset{\text{hydrogen gas}}{2\,H_2\downarrow} \rightleftharpoons \underset{\text{Silicon}}{Si\downarrow} + \underset{\text{anhydrous HCl}}{4\,HCl\downarrow}$$

At a reaction temperature of approximately 1150-1250 °C, the Anhydrous (HCl) remains gaseous and does not interfere with the crystal development process [40]. For etching instead of deposition, the process can be reversed. Pyrolysis, a process

shown below is practicable at a lower temperature of about (500-1000 °C) :

$$\underset{\text{Silane}}{SiH_4}\downarrow \rightarrow \underset{\text{Silicon}}{Si}\downarrow + \underset{\text{Hydrogen gas}}{2\,H_2}\downarrow$$

Reactions that take place at lower temperatures minimise the movement of impurities from the substrate to the epitaxial layers. The VPE method is vital in Light emitting structures. For example, VCSELs, since they utilise it to grow thin Si layers. Other practicable methods are organo-metallic vapour-phase epitaxy (OMVPE) or metal-organic vapour-phase epitaxy (MOVPE) [97]. Top quality epitaxial layer growth GaAs can be achieved by the following process which happens at approximately 700°C:

$$\underset{\text{trimethylgallium}}{(CH_3)_3Ga}\downarrow + \underset{\text{arsine}}{AsH_3}\downarrow \rightarrow \underset{\text{Gallium arsinide}}{GaAs}\downarrow + 3\,\underset{\text{methane}}{CH_4}\downarrow$$

Molecular Beam Epitaxy (MBE)

In this method, substrates are confined in high vacuums in which atomic or molecular beams of the heated constituents breakthrough the substrate surface [40]. If, for example, the AlGaAs layers are to be grown on the substrates, then all three material components, namely; . Al, Ga and As will be heated in isolated cylindrical beakers. The atomic beams of these components are released into the vacuum and directed onto the surfaces of the substrates, where their striking rates can be controlled. Doping from GaAs to AlGaAs can be achieved by adjusting cylindrical blinds (shutters) if the growth rates are slow. Gas source MBE or gaseous chemicals (chemical Beam Epitaxy (CBE)) combines the merits of VPE and MBE [98].

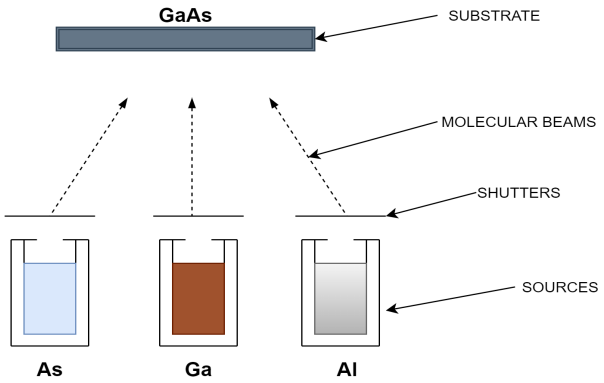


FIGURE 2.26: Vaporisation cells inside a high-vacuum chamber cylindrical beakers of Al, Ga, As liquid do-pants onto a GaAs layer.

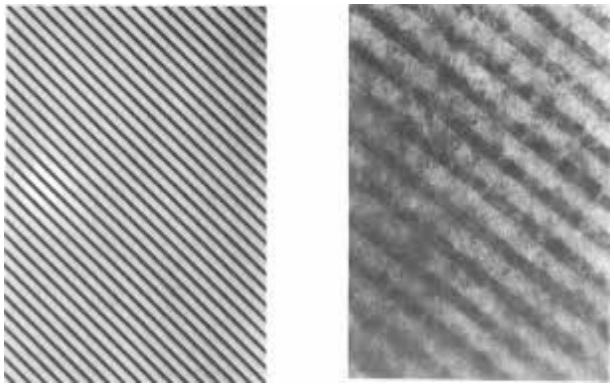


FIGURE 2.27: Cross section of MBE-grown crystal with layers of GaAs(dark) and AlGaAs (light) [3].

2.10 State of art of VCSELs

Various research groups have added to the success of lasers until the introduction of surface emission, which included the practise of conductor distributed bragg reflectors (DBRs) as mirrors [99, 100]. This was followed by exercise of surface emission [101, 102, 103, 104], putting into practise the quantum well (QW) theory [105, 106, 107, 108, 109] and oxide aperture operation [110, 58, 59, 111] then followed. Melngailis is the first to report a laser with an output normal to the surface of a wafer [112, 113]. Prof. Emeritus K. Iga then reported the first VCSEL in 1977 from Tokyo Institute of Technology [114, 115]. In 1979 and 1987 the first laser with low threshold operation and micro cavity were witnessed [115, 116, 103]. VCSELs for long wavelengths have been demonstrated by the use of various recommended materials consisting of highly strained Quantum wells of GaInAs/GaAs [117, 118, 119, 120, 121, 122], GaAlInAs/InP QW [123, 124, 125, 126, 127, 128, 129, 130, 131, 132], GaInNAs, GaAsSb QW [133, 134, 135, 92, 136, 137, 138, 139, 140, 141, 142, 143] and GaInAs quantum dots [144]. Better modulation speed performances with GaInAs VCSEL having the highest modulation speed were shown [145, 146, 147]. Molecular beam epitaxy (inherent beam flux gradient) was used to realise the first multiple wavelength two dimensional (2-D) VCSEL array [148]. MOCVD was then introduced to realise a VCSEL array by epitaxially growing AlGaAs and GaAs on GaAs nonplanar substrates [149]. A few reports from 1995 to 2000 on devices with multiple emission wavelengths in the range of 850-980 nm were introduced [150, 151, 152]. Various research groups have been involved in VCSEL applications from 1980 to the present day [153, 154].

2.11 Related research results

[97] recorded theoretical and experimental results of $In_xGa_{1-x}As_yP_{1-y}/In_zGa_{1-z}As$ QWs for laser structures in the 1.3 μ m and 1.55 μ m ranges as they are applied in Optic communications systems. Their wafers were developed by a low pressure OMVPE process. Their method for finding the operating wavelength of the structure involved the use of Schrodinger equation which was solved by single partial model. The Van de Walle model solid theory was used to determine the band offset and energy band gap at the hetero interface [155]. Energy band gap (E_g), energy band differences for two materials A and B (ΔE_c^{AB}, ΔE_v^{AB}), averaged valence band energy (E_{vav}) and other used parameters were gotten from [155] and [156] with suitable growing conditions found in [157]. Epitaxial layers were grown on InP substrate that was S-doped (100) oriented. The results presented showed $In_{0.53} - Ga_{0.47}As$ with a lattice mismatch of about 1000pm. The epitaxial layer thickness was recorded to be 1% of the designed thickness which was measured by TEM and SEM. The Photo luminescence was used to get the emission wavelength. To determine the degree of strain for an InGaAs strained QW, Linear interpolation was used. The GaAs's and InAs lattice constants were linked with the rate at which materials grow, the TMI w.r.t TMG incorporating efficiency. InP/$In_{0.53}Ga_{0.47}As$ QWs recorded an offset conduction band of about 256meV (42.56% of band gap difference (dEc%)). The $In_xGa_{1-x}As_yP_{1-y}/In_{0.53}Ga_{0.47}As$ has a declining dEc% with a reducing band gap of $In_xGa1 - x - As_yP1 - y$. Model-solid theory theorises a decreasing dEc% with a rising composition of arsenic compound with a decreasing rate is 25.4y%. Their results showed that the strain increased the dE% by 1.3S. The wafers showed an eminent match at room temperature for InGaAsP/$In_{0.53}Ga0.47As$ unstrained QW. A 5% difference from measured data concludes that there is a valence band mixing and a down shift for valence band.

[158] explored and studied total group V flow, pause time to InP layer and growth temperature of Strained and unstrained InGaAsP. MOCVD Axitron 2600 reactor was used to get PL emission of 1.1-1.6 μ m for InGaAsP. Samples were grown on n-type undoped (100) InP substrate. super lattices of InGaAsP/InP with 20 periods were matched and grown on InP with a 1.28 μ m of wavelength. To tighten PL FHWM and bettering the surface morphology (reduction in defect density and texture), the phosphine flow i.e. V:III ratio was increased during the growth process. Results showed that in the time of deposition, shorter pauses are most preferred to longer pauses during as their sub lattices are much narrower. Super lattice PL emission is again made narrow by high phosphine (PH_3) composition or flows. For strain and

PL analysis, higher phosphine PH_3 flows, short pauses, lesser periods and strained super lattices of InGaAsP/InP were applied. All the mentioned conditions were chosen so that the 75 well with InP barriers had an emission of approximately 1.55 μ m. It then can be concluded that performance of a MQW can be degraded by a bad or undesirable interface between layers (transitional layers). This undesirable condition can be caused by any king of pausing on any kind of hydrides that will lead to X-ray losses or multiplication of emission peaks.

[159] compared two material compositions i.e. InGaAsP and InGaAs at 1480 μ m. The materials studied are used to realise device structures as pumping sources for EDFA optical boost signal. In the study, power equations were derived and for carrier and photon density correlations rate equation were. The study had parameters that varied throughout the experiment and those that were fixed as per composition for the two materials. Results showed that the output power in the active region was affected by intrinsic carrier concentration and operation voltage of which were listed as fixed parameters. The Frequency and volume for active region are the most significant parameters for both the two materials (InGaAs and InGaAsP). The following results for Injection current Vs Voltage, carrier density, photon density and power for the two material compositions were recorded.

TABLE 2.5: Results comparisons.

At 1 volt	**InGaAs at 1480 μm**	**InGaAsP at 1480 μm**
Injection Current [mA]	18.714	50.275
Threshold Current [mA]	11.759	21.217
Photon Density $[Cm^{-3}]$	$3.79.10^{16}$	$8.5038.10^{16}$
Carrier Density $[Cm^{-3}]$	$2.166.10^{15}$	$2.104.10^{15}$
Output Power [mW]	30.401	126.661
Slope Efficiency [mW/mA]	4.371	4.359

Electro reflectance (ER) estimations were used to control the band gap energy of qua ternary alloy InGaAsP that was lattice matched to InP. It was found that the band gap energy (Eg) of the InP lattice matched alloy In1-xGaxAsyP1-y can

be illustrated and written as a function of the As composition of y as Eg=1.35-0.738centerdoty+0.138centerdoty2 at room temperature. The band gap energy is not same as the peak energy of the photo luminescence spectrum which commonly utilised as a measure of the band gap energy [91].

[21] Rahim devised a 1550 nm air post VCSEL and compared its I-v characteristics simulation results with previous work. A six QW with each well = 5.5nm and $In_{0.76}Ga_{0.24}As_{0.82}P_{0.18}$ as material used in the active region was grown between top $GaAs/Al_{0.33}Ga_{0.67}As$ and bottom GaAs/AlAs distributed bragg stacks with reflection factors of 3.38 and 3.05 and 3.38 and 2.89 respectively. They used empirical data for modelling [160] and realised a structure with a diameter of air post of 4 μm with a circular diameter of 12 μm. In [161] it showed etching of only part of the top mirror and in his work etching depth was continued down to top of lower spacer layer. The substrate in which the structure was grown onto was GaAs. At a bias current of 9mA, their structure showed low optical losses, 6.4mW power and a 0.6mA of threshold current. The blocking of flow of current in the active region and upper spacer caused the series resistance of the structure to increase at high voltages as illustrated by their results. Poisson and continuity equations solvable by Helmholtz and photon rate equations were used as their basis for simulations and they adapted a method called effective frequency model.

[162] Made a study on effects of scaling up VCSELs for optical interconnects. They showed how demands can be met and the effects that came with trying to meet the optical application demands usually caused by growth of communication technology. Maximum bandwidth for future VCSELs based optical interconnects was derived without ignoring the thermal cross talk that came with it. A limit on the number of devices in an array for a wanted BW due to effects of scaling up was discussed. From their calculations they got that VCSELs are scalable from a BW density of 100Gbps/mm^2 to a limit of 15Tbps/mm^2. It highlighted that the system BW could be limited by a few factors like, footprint of the device, number of channels, thermal budget of each device, bit rate per channel and thermal cross talk of VCSELs arrays. It was concluded that energy efficiencies and thermal stability were the two areas to study when scaling up the BW. It was suggested that VCSELs could have optical fan-out and sit on a heat sink made of silicon with a thermal conductivity of about 120W/(Km) to block the sides for heat extraction.

[153] Reviewed recent advances of VCSELs by looking at the wavelength extension and their control. The paper looked at challenges and a potential for new functions of VCSELs for optical communication and signal processing. Their results showed

operations for highly strained QW laser designs at lower threshold current densities with an emission near the 1.2 μm region [163]. They found out that the wavelength photo luminescence (PL) of a GaInAs QW could go over 1.2 μm with no degradation in the quality of the crystal. Inductive plasma coupled etching was used to dry etch the grown samples to make 30 X 30-μm mesas. Highly strained GaInAs QW VCSEL was fabricated on GaAs substrates of either (100) (showing polarisation switching) or (311) B (indicating a large orthogonal suppression polarisation of 30dB) [119]. A higher temperature operation of up to 450K, low threshold below 1mA and a high reliability of $>$ 2000 h were recorded [119].

2.11.1 Methods used by different groups to realise VCSELs used today refer to table 2.6 and 2.7.

Compared to 850 nm devices, those used in the OM3 and 0M4 MMF benefit from a higher temperature insensitivity, low transmission losses, low chromatic dispersions and a higher sensitivity of photo detectors. Compared to unstrained GaAs QWs, InGaAs are used for their higher emission speeds transmitting at 850 nm due to their higher differential gain [185, 186]. InGaAs transmitting at 980 and 1100 nm with a lower transparency carrier density have an advantage as they promise operational results with low threshold currents, reliability with a high modulation bandwidth and better efficiencies Production of VCSEL wafers with larger diameters (usually about 101.6 nm or bigger) can simplified and made reliable by using epitaxial layer designs that are ease to manufacture [187]. Currently more than 90 percent of the MMF links exist with a range of 100 meters [188]. As complexity of data centres increases to meet longer distance coverage (of over 2Km), optical connections at 20-25 Gbps are favourable [189]. With MMF devices, it is hard to meet the desired distances due to modal dispersion. A narrower spectral width is generally a necessity that is found in single mode laser devices. A commonly used, more direct approach is to reduce oxide aperture of laser devices, but they will be more complicated to manufacture. This is because VCSELs, whose oxide apertures are reduced have a higher current density than the Surface-Relief VCSELs.

TABLE 2.6: Table of literature showing methods and results by other researchers.

Paper and wave-length	**Material used**	**Methodology**	**Results and comments**
1.Standard single-mode fibre (WDM-PONs) operating at 1.55 µm [164].	IN ,GA ,AL ,AS ,CA ,F ,ZN ,S , AU.	The laser was developed by atomic beam epitaxy on InP substrate. The active region has 7 QW with the top and bottom mirror having 35 pairs of InGaAlAs and 3.5 pairs of CaF/ZnS.	Output power is 1.5 mW for small aperture and above 0dB for larger aperture at 85 Degrees celcius. Bandwidth and output power is nearly flat for driving currents above 4 mA .Effects of roll over were taken into account and 1550 and 1570 nm wavelength and frequency were measured against current.
2. Wafer-scale fabrication operating at 970 nm [165].	GA, AS, AL, N, SI, IN, O	The semiconductor laser is grown by metal–organic chemical vapor deposition on a low-doped n-type GaAs substrate. The first mirror is epitaxially grown and has n-type GaAs/AlGaAs with eight periods. The second mirror is 36-period p-type GaAs/AlGaAs with Three-quantum-well InGaAs active region.	Threshold current of 25 mA and a slope efficiency of roughly 12 % were found for an aperture size of 28 µm. Performance was increased by reducing heat generation and thermal resistance. Under WAVE the laser output is about 10 mW.
3. High power single mode operating at 1550nm [166].	IN, GA,AS,P, IN	The wafer fusion method was used for etching.The active region made of InGaAsP has six QWs .The top mirror has 30 periods of GaAs/AlGaAs with a reflection factor of 3.38 and 3.05. The bottom mirror has 28 periods of GaAs/AlAs with reflection factor of 3.38 and 2.89.	At room temperature and bias current of 9 mA threhold current is 0.6 mA and output power of 6.4 mW. There was a decrement of 76.52% in threshold current and an increment of 28 % in power from the previous work.

Paper and wave-length	**Material used**	**Methodology**	**Results and comments**
4.High Single-Mode Power Oper-ation operating at 1310 nm [167].	IN, P, AL, GA, AS	It has InP active region and AlGaAs/GaAs distributed Bragg mirrors.Electro-opto thermal simulations based on microscopic physical models have been used to explain the trensverse optical mode switching of the VCSEL as inferred from far-field pattern measurements	At room temperature, the LP_{11} mode turns on at ap-proximately 10 mA, which results in a sudden in-crease of FWHM angle. The current for the higher-order mode turn-on in-creases with temperature. The mode behaviour at different temperatures was analysed.
5. Wafer-scale fabri-cation operating at 980 nm [168].	IN, P, AL, GA, AS, TI, SI, O	The device is grown by solid-source molec-ular beam epitaxy on a semi-insulating (SI) GaAs substrate. 30 pairs of p-doped DBR and 3 pairs of n-doped DBR for wavelength selection.The active region contains two stacks of three 8-mm thick InGaAs/GaAs QW.	Threhold current of 7.5 mA,output power OF 15.0 mW and a side-mode suppression ratio of 39dB. Single mode operation for devices with long active cavity, low output power,higher threshold current and reduced dif-ferential efficiency. Higher threshold currents caused by increasing curvature radius.
6. Con-tinous Wave Opera-tion of all mono-lithic InAlGaAs-InP oper-ating at 1.55 µm [169].	IN, P, AL, GA, AS, ZN, SI,N, AU	The structure was grown on Si-doped InP sub-strate using low-pressure MOCVD.Active region consists of nine 70 angstrom thick InGaAs QW seperated by eight 70-angstrom thick InAl-GaAs barriers. 45 pairs of Si-doped InAlGa-InALAs bottom DBR with reflec-tivity of about 99.83% and 24 pairs of undoped InAlGaAs-InAlAs top DBR with Au layer and reflectivity of 99.90 %.	WAVE L-I and I-V curves for threshold current,voltage and exter-nal quantum efficiency are 1.6 mA,2.3 V and 5.4%. The first transverse mode has a power (20dB) smaller than fundamental lasing mode. The device has high resistance causing heat emission and mismatch between gain peak and cavity resonance. A thin and highly conductive current spreading layer is inserted in between cavity layer.

Paper and wave-length	**Material used**	**Methodology**	**Results and commentss**
7.Single-Mode Operation and Trans-verse -Mode Control operating at 840 nm [170].		The first-order reflection of a diffraction grating used in the grazing incidence configuration is reinjected into the laser cavity by a mirror. The bottom (n) and top (p) mirrors consists of 33.5 and 26 pairs respectively.	A laser forced to emit in any of the two polarization components of the transverse mode has maximum single mode output power of 750 µW correlating to injection current of 2.5 mA and bias current of 1.7 mA.Rotation of the half-wave plate causes threshold reduction of 10%. Single mode emission until I=4 mA matching with 2.7mW output power.The output power of one laser is 1.9 mW with four transverse modes emitting.
8.Direct-Coupled WDM Application operating at 32.9 nm [171].	AL, GA, AS, IN	The quantum well was grown by molecular beam epitaxy. The active region is built of 3 InGaAs-GaAs quantum wells and the device has a 32 period top p-mirror and 19.5 period output n-mirror	Most devices lase at 1.7 mA with bias voltage of 2.4V.Channels 1-6 have same electrical and spectral characteristics when output power is below 5 mW.Channel 4 has 7.3 mW maximum output power,50.3% differential quantum efficiency and 11.8% maximum wall-plug efficiency.Coupling loss is 4.8 dB,maximum available tuning range is 36.7 nm,output power is above 1.0 mW and channels are multilateral-mode with spectral bandwidth of 1.7 nm.
10.Single Trans-verse mode Under High Speed Modu-lation [172].	IN, AL ,GA ,AS,ZN, SE.	The wafer was grown by low-pressure metal organic chemical vapor deposition. The active region has three InGaAs-GaAs QWs sorrounded by AlGaAs spacers. The bottom n-type DBR consists of 36 Pairs of GaAs-AlGaAs , top p-type DBR consists of 18 pairs of GaAs-AlGaAs	The Threshold current is 0.6 mA and output power is 0.9 mW at 4.0 mA. Above 1.0 mA a large OPSR above 25dB is found between prism angles of 90 and 180 degrees.The maximum 3-dB bandwidth was 2.5 GHz at bias current of 0.8 mA.SMSR and OPSR were 35 and 11dB.

TABLE 2.7: Materials and methods for VCSELs used in data communication.

Group	**Material used**	**Method**	**Ref**
IBM (Finisar)	GaAs		[10]
CUT	InGaAs	Double oxide layers were used.	[12]
CUT	N/S	Used a cavity that is half a wavelength and added $Al_{0.96}Ga_{0.04}As$ layers to reduce parasitics and shallow surface etching for tuning the photon lifetime.	[173]
IBM/CUT	N/S	A two-tapped feed process for forward equalisation was used.	[174]
		Four layers with deep oxide for the photon lifetime adjustments, half a wavelength cavity with single oxide apertures at both sides of the bragg reflectors (the n and the p) was deployed [175].	[176]
NCU	Zn	A narrow spectral width with a differential resistance reduction and an oxide relief structure for parasitics reduction was used.	[43]
UCSB	N/S	P-doping optimised profiling in the upper DBRs to lessen losses and resistances. Multiple deep oxide layers for parasitic capacitance reduction and oxide aperture tapered for optical loss reduction was the methodology used.	[177]
TU (Berlin)	N/S	Use of modulation doping and binary DBR for half a wavelength cavity [178].	[179]
TU (Berlin)	N/S	An optical cavity of half a wavelength was used. The structure's photon lifetime was tuned with current spreading layers included.	[180]
TU (Berlin)	N/S	Half a wavelength cavity was used. For strong carrier confinement and optical fields with no deep oxide layers, single aperture was used at both sides of the bragg reflectors of the cavity [181].	[182]
NEC	N/S	Buried type II tunnel junctions were used[183].	[184]
CUT	N/S	Focus was on controlling modes and a surface relief method was used.	[45]

Chapter 3

Methodology

Based on the results discussed, designers can have different VCSEL structures and implementation methods. Therefore, a designer must first identify the application for which the VCSEL must be designed Once the application is identified, the most appropriate emission wavelength and the required output power for that application can then be calculated which will influence material selection, the wavelength against size of the active region, band-gaps energies of the materials used will have a huge impact on whether the designed structure meets the requirements of the designer.

3.1 Research methodology

After a literature survey on VCSELs, a design methodology which has three sections, Design Simulation, Evaluation and Comparison Analysis (see figure 3.1) will be followed for the development of a VCSEL for Fibre Optical communication.

A)DESIGN AND SIMULATION OF A VCSEL
This is the part where the verification and validation of the desired structure is done. It contains mathematical equations that represent the behaviour of the VCSEL. A few light equations relating to VCSEL will be computed. A software called Silvaco (which uses Atlas Language) is used as the core of the project design. It comes with other tools like Dev Edit, Deck build and Athena which are used to develop process and simulation input decks, to edit the structure (creating or modifying existing models) and provide a numerical and physically-based 2D simulations for semiconductor processing. The last part of the methodology is to compare the performance of different design simulation structures under various operating conditions which offers more flexibility in the design of the VCSEL.

B)EVALUATION

A detailed analysis of a final proposed structure is done in this section of the methodology where all the results analysis of the structure's parameters is performed. During the evaluation analysis, experiments and simulations are carried out on various VCSEL structures.

C)COMPARISON ANALYSIS

After observation and recording of the outcomes without manipulation, the similarities and differences between the simulation and experiment results are determined. The similarities and differences of the structures are identified using a collection of data for analysis based on numerical and statistical attributes. Designing comparative studies around a variety of parameters in which individual results are observed and behaviours are recorded.

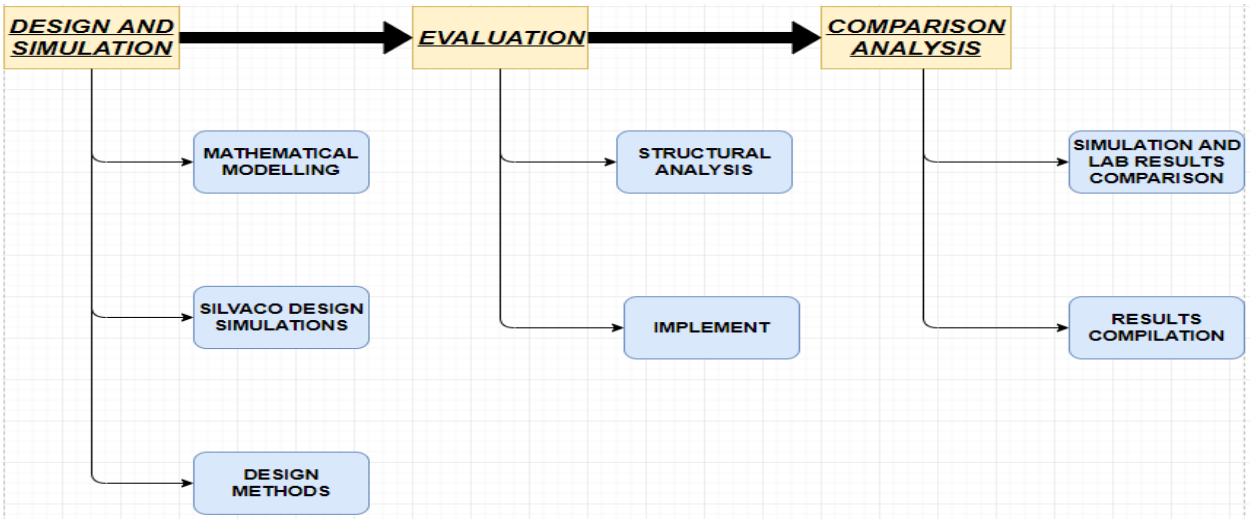


FIGURE 3.1: Design methodology.

3.2 Design methodology

A laser is represented using the Atlas basic language structure found in a product called silvaco that includes regions, mesh, doping distributions, electrodes, and a path that is common to any conventional light applications [190]. The mesh symmetry mirrors are specified in their respective symmetry of the structure and might be important for effectively calculating the light intensity, local optical gain and other internal physical distributions. Mesh spacings are defined to determine heterojunctions in the x and y directions. The Laser structure is made out of regions, and the most significant region is the active region. The material that is used in the active region determines the basic characteristics of the laser. The electrodes (anode and

cathode) must be defined during modelling. The decisive properties of the material are calculated from the synthesis parameters . For example, dielectric constant, energy band gap, densities of the states in the conduction and valence bands. This is done using static conditions. The material statement must include electron and hole lifetimes, optical recombination constants. The electron affinity for the material utilized in the dynamic region has to be characterized to ensure energy band alignment. Laser models are specified according to the initial biasing. As indicated by the hypothesis, no laser action occurs until the diferrence of the semi femi level in the active layer exceeds the material band gap. The purpose if the procedure is to ramp the bias up to some degree, which is not more than the band gap of the active region, and enable the laser model. The next procedure is to characterize the regular mesh for solving the helmhotz equation. It is independent of the triangular mesh utilized for electrical equations [191]. The atlas syntax code is given in appendix A, from which a flow chart Fig. 3.4 and 3.5 was taken.

3.2.1 Flowchart development process

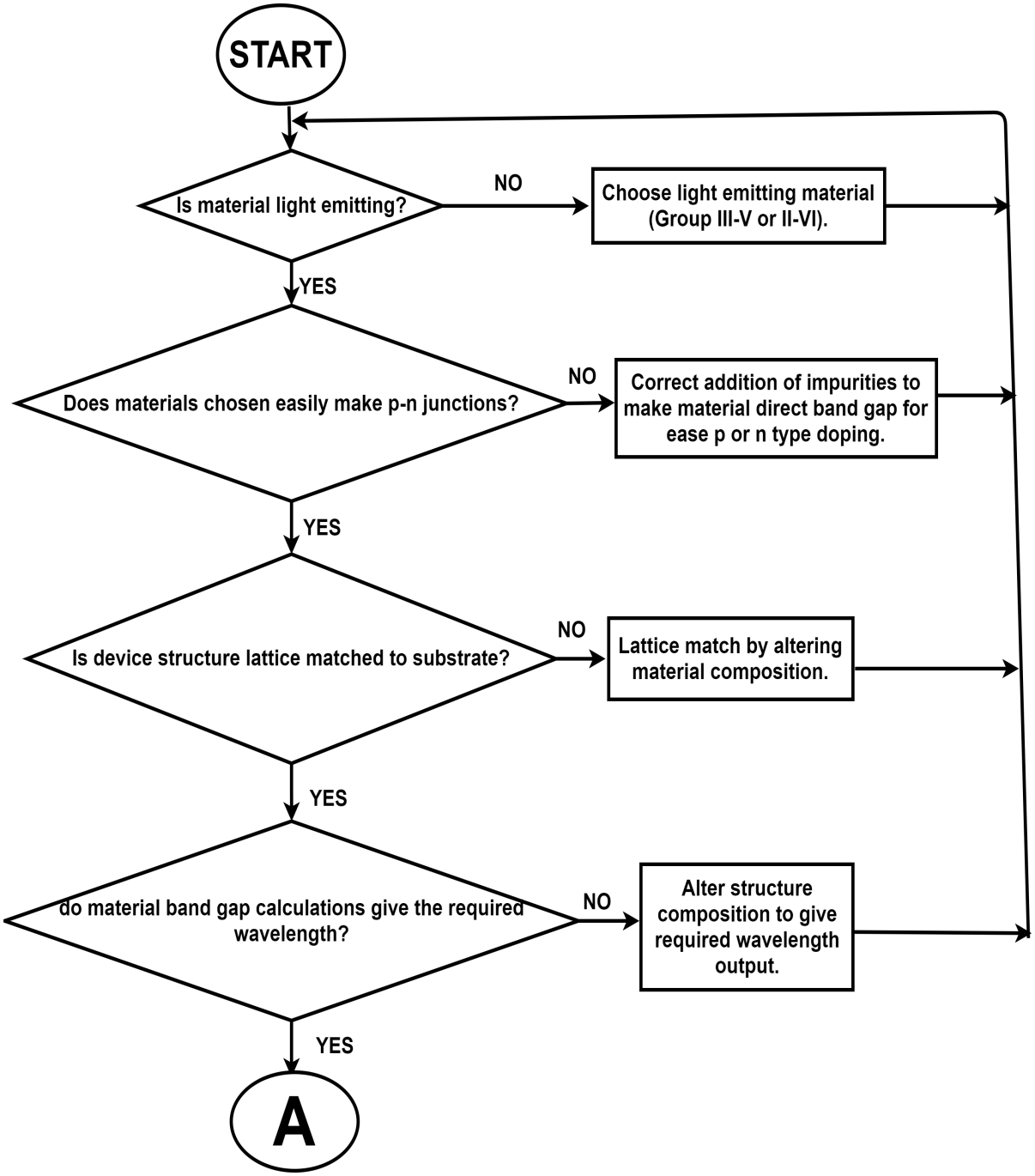


FIGURE 3.2: VCSEL development flowchart.

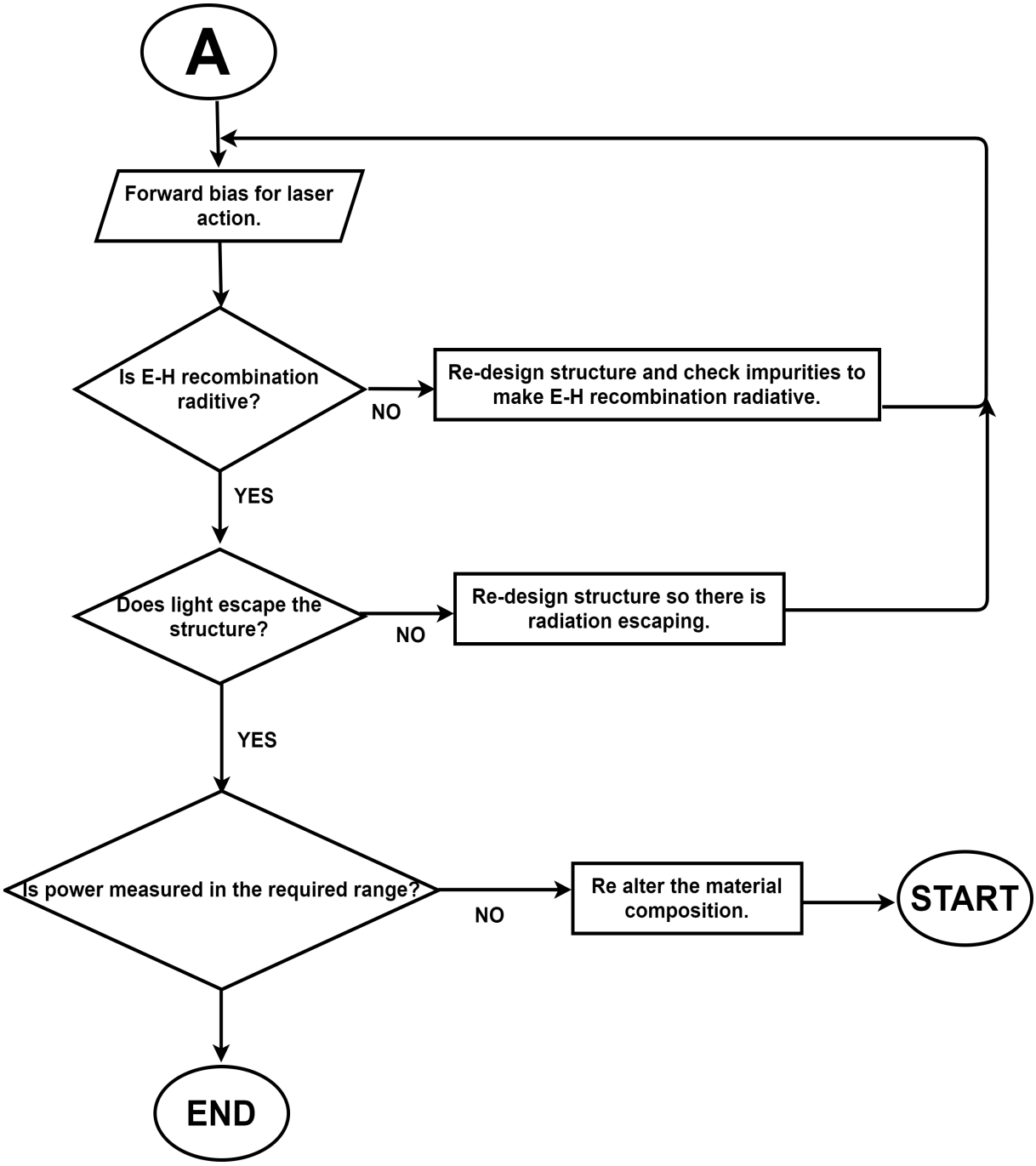


FIGURE 3.3: VCSEL development flowchart continuation.

3.3 Simulation development

The mirror ratings, doping values, energy band gaps and all other parameters shown in the two tables below helped with the structure modelling using the atlas syntax. To create the final VCSEL structure as shown in figure 3.4, simulation parameters in table 3.1 and table 3.2 were used to simulate twenty four VCSEL structures, twelve of which have the same top-to-bottom mirror ratios (i.e the 30:28 and the 45:43). The same materials are used for all the VCSEL structures, as only the I-V characteristics (Power, Voltage and Current) are examined by varying the number of QWs and reflectivity of the two bragg stacks.

TABLE 3.1: Table showing parameters used for the 30:28 mirror rating for 1-12 QWs.

Region	Material	Parameters	Values
Top Substrate	GaAs & GaAs	Thickness Doping	0.01 & 0.02 A-4e19 & 4e17
Top DBR Stack	GaAs & AlGaAs	Thickness Doping Repetition	0.1157 & 0.1273 A-4e17 & 4e17 60
Top Contact region	GaAs & GaAs	Thickness Doping	0.184 & 0.02 A-4e17 & 2e19
Contact for active Region	InP & InP	Thickeness Doping	0.178 & 0.1 A-1e18 & 1e16
Active region material	InGaAsP & InGaAsP	Thickeness x & y comp Repetition	0.008 & 0.0055 0.24 & 0.82 1-12
Contact region	InGaAsP & InP & GaAs	Thickness Doping	0.008 & 0.258 & 0.05 5e18 & 1e18
Bottom DBR stack	GaAs & AlGa	Thickness Doping Repetition	0.1157 & 0.134 D-1e18 & 1e18 56
Bottom Substrate	GaAs	Thickness Doping	0.02 D-5e18

TABLE 3.2: Table showing parameters used for the 45:43 mirror rating for 1-12 QWs.

Region	Material	Parameters	Values
Top Substrate	GaAs & GaAs	Thickness Doping	0.01 & 0.02 A-4e19 & 4e17
Top DBR Stack	GaAs & AlGaAs	Thickness Doping Repetition	0.1157 & 0.1273 A-4e17 & 4e17 90
Top Contact region	GaAs & GaAs	Thickness Doping	0.184 & 0.02 A-4e17 & 2e19
Contact for active Region	InP & InP	Thickeness Doping	0.178 & 0.1 A-1e18 & 1e16
Active region material	InGaAsP & InGaAsP	Thickeness x & y comp Repetition	0.008 & 0.0055 0.24 & 0.82 1-12
Contact region	InGaAsP & InP & GaAs	Thickness Doping	0.008 & 0.258 & 0.05 5e18 & 1e18
Bottom DBR stack	GaAs & AlGa	Thickness Doping Repetition	0.1157 & 0.134 D-1e18 & 1e18 86
Bottom Substrate	GaAs	Thickness Doping	0.02 D-5e18

3.4 Final VCSEL structure

In this simulation the top mirror consists of layers of GaAs/AlGaAs with refractive indexes of 3.299 and 3,099 respectively. The active region consists of layers called QWs of $In_{0.76}Ga_{0.24}As_{0.82}P_{0.18}$ and each well is 5.5 nm with a 8 nm barrier made of the same material composition as the well. The bottom mirror consists of layers of GaAs/AlGa with refractive indexes of 3.299 and 2.912, respectively. Constructive interferences is caused by reflections at the interface between the low and high-indexed layers of the reflective wave around the Bragg wavelength, with the multiple alternating layers acting as mirrors to enhance optical gain. The top and bottom substrates are made of GaAs. The simulated VCSELs structure with the key showing all the material layers differentiated by colour is shown in figure 3.4. It shows an emission by the red arrow, which will be proved by the output power and wavelength, as shown in 4.1 and graph 4.5.

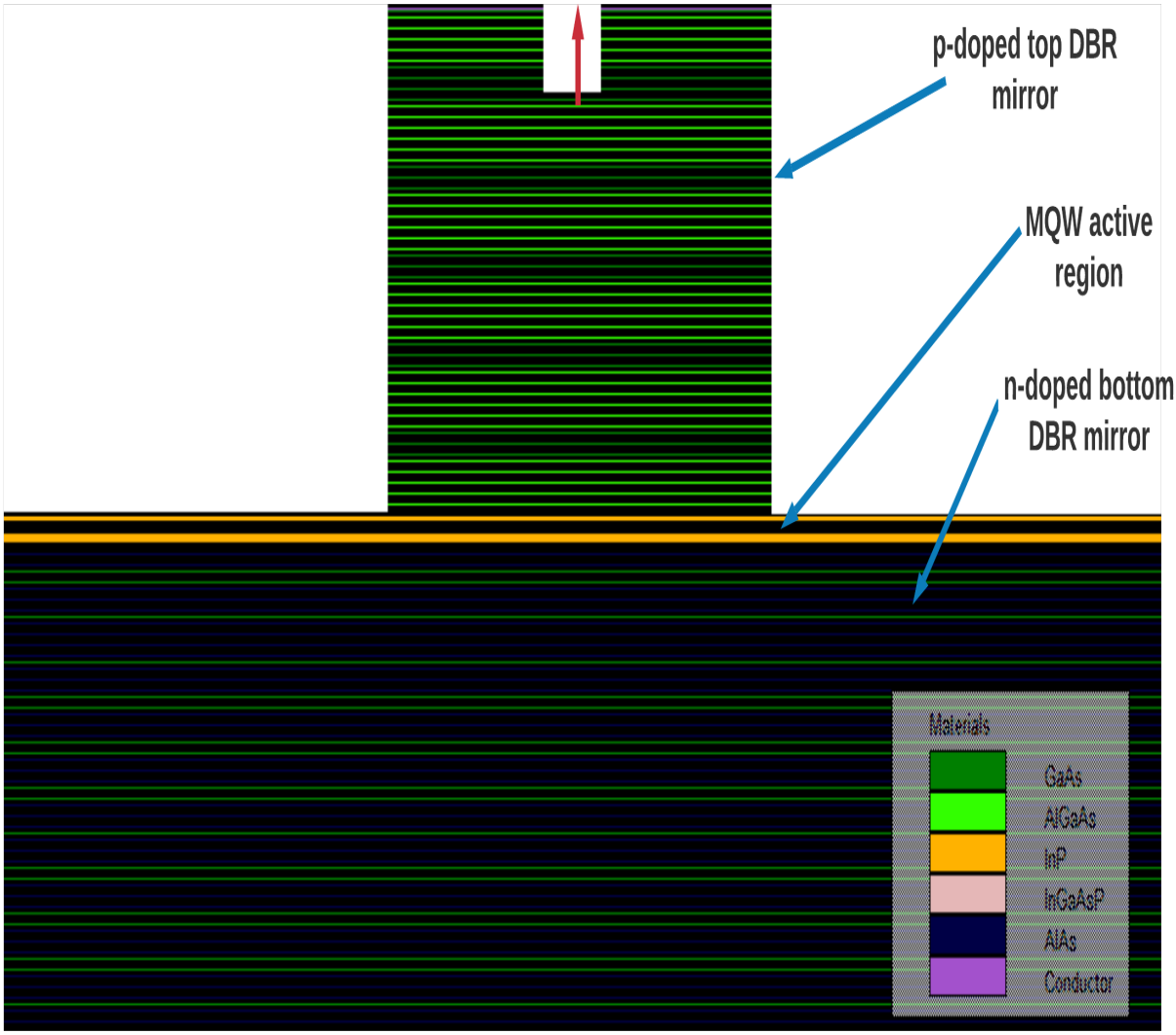


FIGURE 3.4: Simulated seven quantum well structure.

3.4.1 Seven quantum well active region

The seven quantum well structure with the number of Quantum wells visible zoomed is shown in figure 3.5. It shows the p-doped and n-doped spacers sandwiching the In- GaAsP QW region to make the structure a p-n junction device. The p-doped and n-doped spacers give carrier injection for the QWs in between. The GaAs and InP spacers are lattice matched to the QW by their material compositions given in the parameter tables 3.1 and 3.2. The seven quantum wells and eight barriers are made of the same material with the wells having high energy band gaps than the barriers. In the active region, carriers have two states called confined and unconfined states. The confined state means that the injected carriers are confined to the bottom of the wells, and cannot move freely in three dimensions. The carriers in the unconfined

state, referred to as the gateway (G) state can move freely in three dimensions and occupy energy states higher than the carriers at the bottom of the well. Therefore, the gateway state can be seen as an intermediate state for carriers originating from a barrier layer.

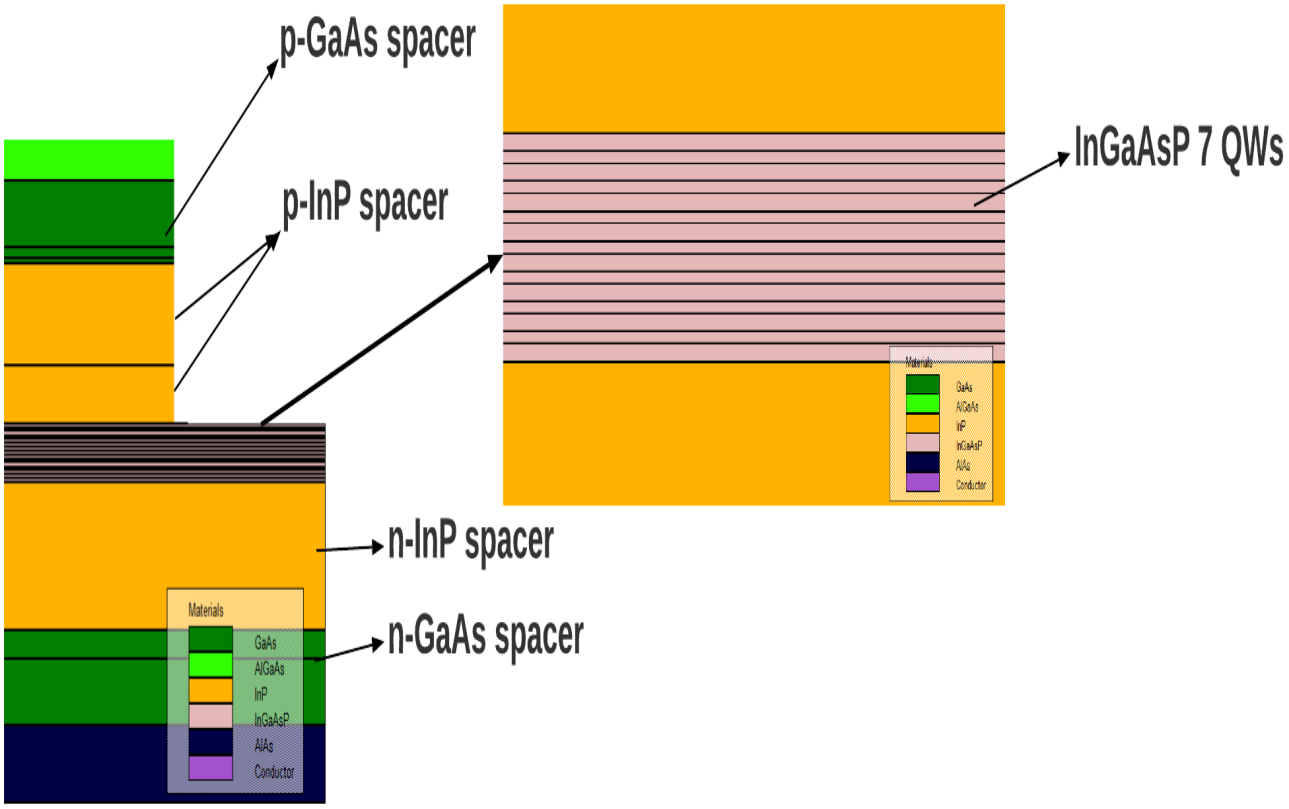


FIGURE 3.5: P-doped and n-doped regions sand witching an InGaAsP seven quantum well active region.

3.4.2 Light distribution over the device structure

The photon and carrier dynamics shown in figure 3.6 determine the overall behaviour of the simulated VCSEL. The injection current is responsible for injecting carriers into the active region. The carriers then diffuse out of the concentration gradient between the n-doped spacer and the p-doped spacer by drifting in accordance to the electric field at the top and bottom contacts. The Carrier movement is between the upper and lower energy bands. Capture is the movement of a carrier to a lower energy band gap and Escape is the movement of a carrier to a high energy band gap region. The process where carriers penetrate through the barrier region is called tunnelling, and it leads to carrier movement between adjacent wells. Photons that are visible through the light intensity key in the figure below are generated through

stimulated emission by electron-hole re-combinations. The photons in this figure shows that they were successfully confined in the active region as it is evident that the highest intensity is in the active region.

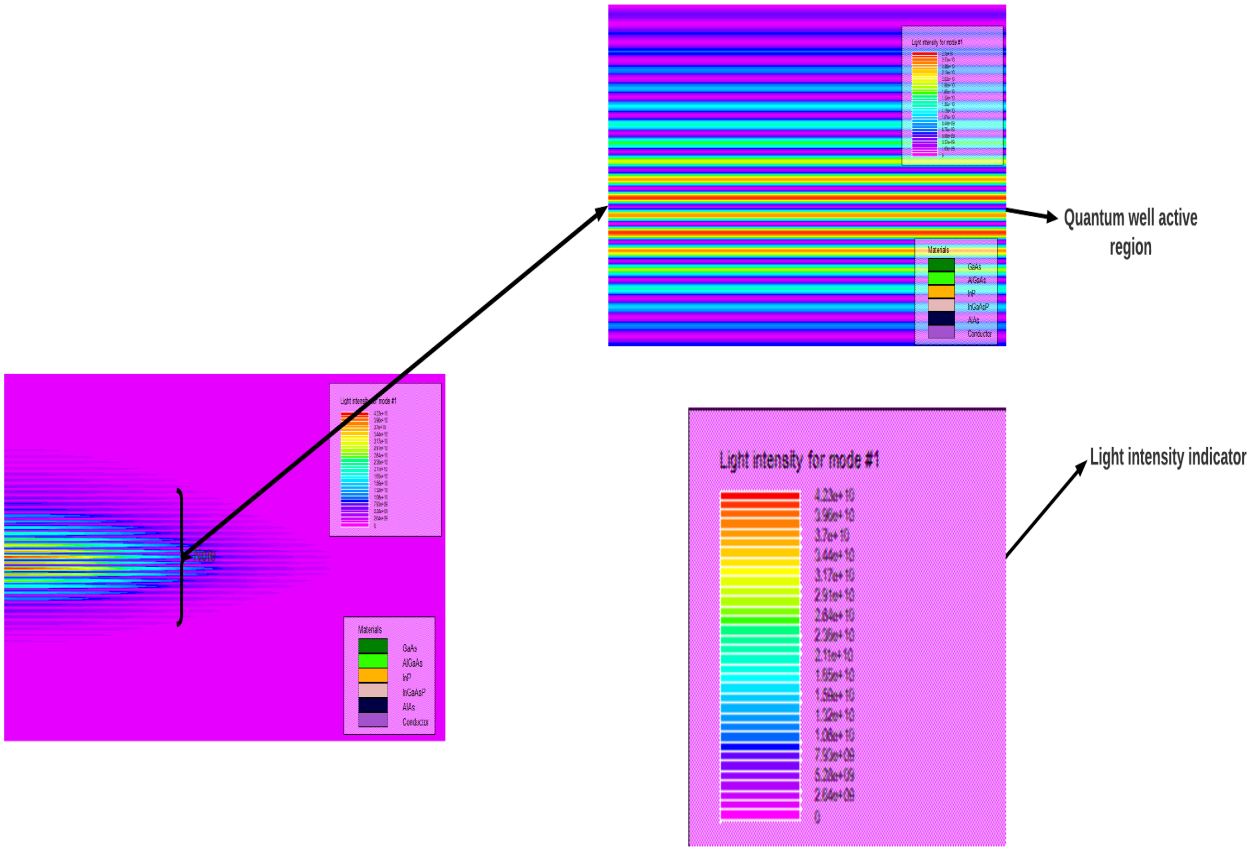


FIGURE 3.6: Figure showing light intensity distribution in the Vcsel structure.

3.4.3 Chapter summary

When modelling laser structures, we should consider electrical and optical communication laser interactions. The light power equation relates to electrical and optical models. Subsequently base of simulation is to solve Poisson and continuity equations for electrons and holes. The basic semiconductor laser equations are solved self-consistently together with Helmholtz and the photon-rate equations. The applied technique for solution of Helmholtz equation depends on improved effective model which demonstrates precision for preliminary problems. Each of the conditions under Poisson and continuity equations that Helmholtz addresses determines the transverse optical field profile, then the photon-rate equation along with the light power equation relates electrical and optical models. This laser has the simplicity of production of the light-emitting diode and the flexibility of the traditional edge-emitting laser for high-speed interconnect applications in communication systems. Its size, manufacture structure and potential simplicity of heterogeneous joining with hardware guarantees a scope of applications that presently cannot be investigated [21].

Chapter 4

Results and Discussions

4.1 Third window emission P-I-V characteristics

The I-V curves are analysed to ultimately select the most efficient structure. Figure 4.1 shows the emitted power versus the anode current of the two seven QW structures with different top to bottom mirror ratios. The 45:43 mirror pair has a threshold current of just under 1mA, and the 30:28 mirror pair has a threshold current that is just above 1mA. This shows that for the two third window structures, the one with a 30:28 top to bottom mirror ratio has a desirable threshold current than the one with 45:43 mirror ratio. In contrast, the 45:30 mirror pair has a better output power than that of 30:28 one. The difference in the emitted power for the two structures is greater than the difference in threshold current, therefore this shows that the 30:28 mirror pair with an out power of 9.5 mW has better performance results than the 45:43 pair with a 7.5mW power. Figure 4.2 compares the two structures based on the warm up voltage. It is ideal for a device to have a lower warm up voltage, but other things like threshold current and power also need to be considered. Although the 45:43 mirror pair has a lower warm up voltage that is close to 1 V, the 30:28 mirror pair with a warm voltage close to 1.25 V still performs better because of their difference in power which is higher than the warm up voltage differences. The differences in the output power, the threshold current and the warm up voltage of the two structure are 2 mW, 0.0007 mA and 0.125 V.

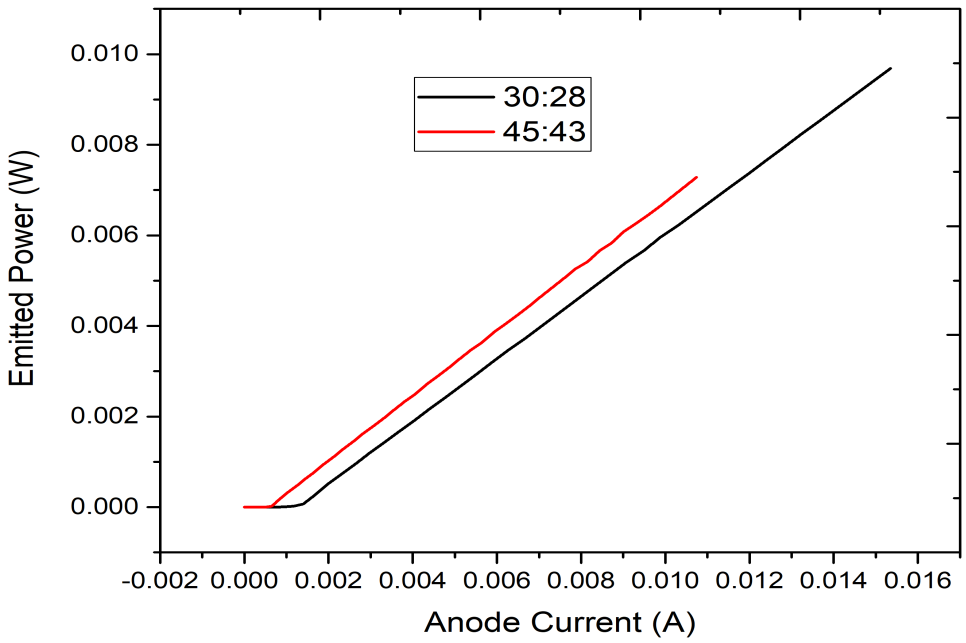


FIGURE 4.1: Emitted power vs Anode Current.

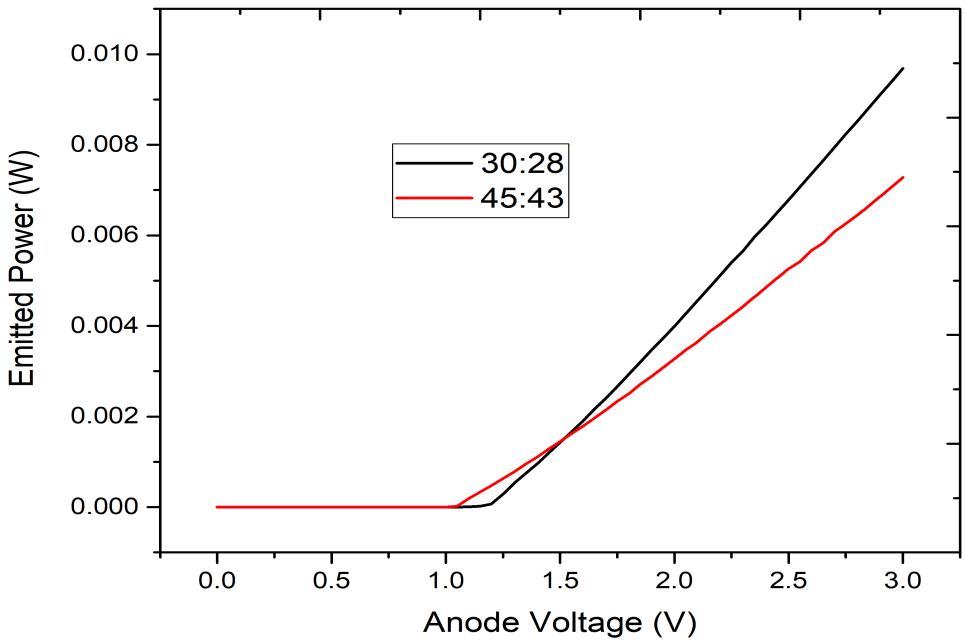


FIGURE 4.2: Emitted power vs Anode voltage.

Figure 4.3 shows anode vs voltage characteristics of the two 7 QW structures. During the 0-1 V interval, there is some current present which does not contribute

to the power-voltage of the device. Therefore, this proves that the simulated device has a nonlinear behaviour which supports the theory that lasers are just an extension of diodes, which are nonlinear devices [192].

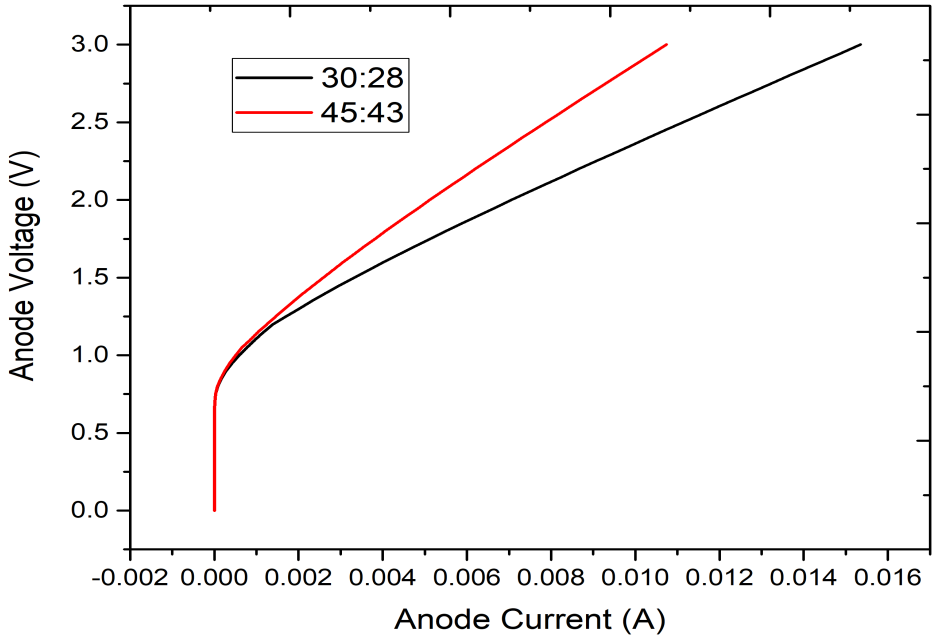


FIGURE 4.3: Anode voltage vs Anode current.

4.2 Optical wavelength emission analysis

After analysing the24 simulated structures; 12 different QWs for the 30:28 mirror ratio, and 12 different QWs for the 45:43 mirror ratio, the structures were reduced to two as it was evident that the 7QW structures emitted at the desired fibre wavelength was near 1550 nm low loss window nm as seen from figures 4.9 to 4.12. From figure 4.4, it can be seen that for the two structures, there is an unstable behaviour between the region 0-1 V, before the device gives a stable optical wavelength. This region can be referred to as the warm up voltage of the device, since the voltage was not enough for the population inversion. An increase in voltage leads to a deviation in the operating wavelength before a stable condition is reached after 1V.

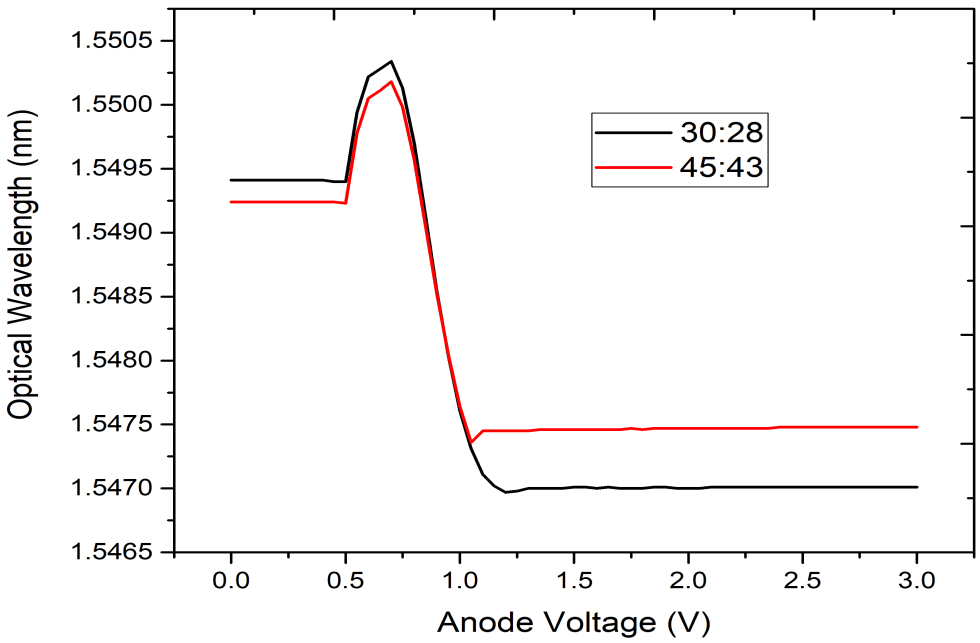


FIGURE 4.4: Optical wavelength vs anode voltage for 30:28 and 45:43 vcsel structures.

Figure 4.5 shows that the structures do not contribute any power at wavelengths that are not supported by the cavity. Only the wavelengths that may be built into the cavity are emitted and it shows by their power ratings. The third window low loss wavelength range of 1520 - 1600 nm has the lowest attenuation that is available on current optical fibre (0.26 dB/km). It can be seen that the power levels for the structure with mirror ratios of 30:28, and 45:43 are zero at other wavelengths and they reach 9.5mW and 7mW at 1.5470 and 1.5475 nm, respectively. An ideal laser should only show power outputs at wavelengths desired by the designer and display a zero.

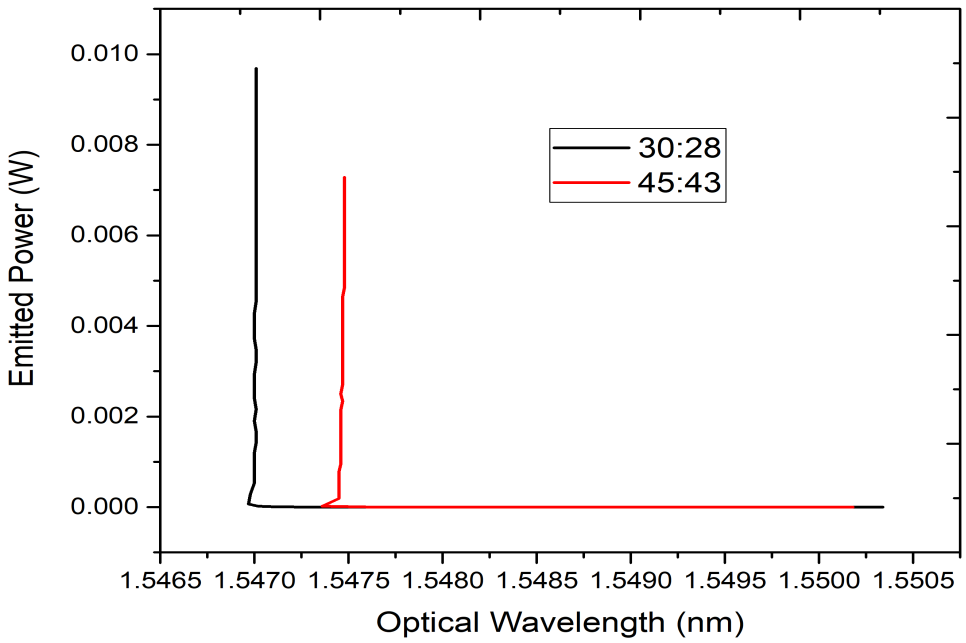


FIGURE 4.5: Emitted power against optical wavelength for 30:28 and 45:43 structures.

Figure 4.6 shows that the seven QW structure with a 30:28 mirror ratio has an absorption value of 0.275, which is much higher than that of the 45:43 mirror ratio. This means that in terms of electrons absorbing external photon energy, the 30:28 ratio structure is more efficient with the same simulation settings. At other wavelengths that no lasers not are not supposed to emit, the electrons absorption rate should be close to zero. When the absorption becomes zero at the desired emission wavelength, then the output power depends only on the voltage input, and the operation of the device will be similar to an LED or a quantum well laser [193].

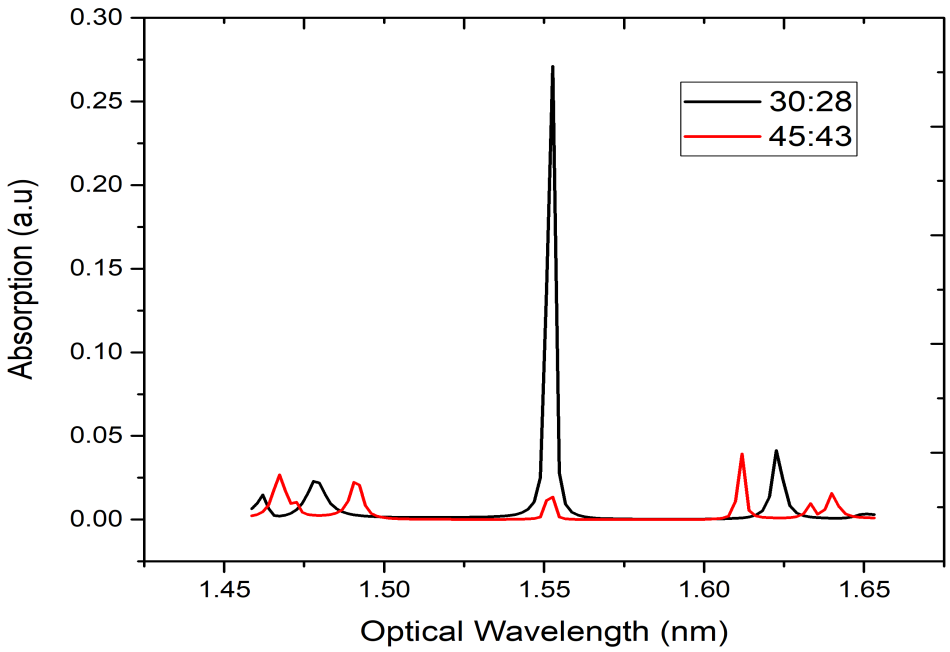


FIGURE 4.6: Absorption for 30:28 and 45:43 vcsel structure.

Figure 4.7 shows that the reflectivity threshold value is close to 100 %, which is represented by 1. Any reflectivity of more than 1 at the desired emission wavelengths causes the photons to be confined to the cavity, and there will be no output. This would mean that the device does not operate like a laser. Figure 4.8 jallows reflectivity and transmission to be inverse, that is,when the transmission is low, the reflectivity is high [194]. For example, the highest reflectivities close to 1, between the ranges 1.50 and 1.55 nm in figure 4.7 show that the lowest transmissions in this range are close to zero, as can be seen in figure 4.8.

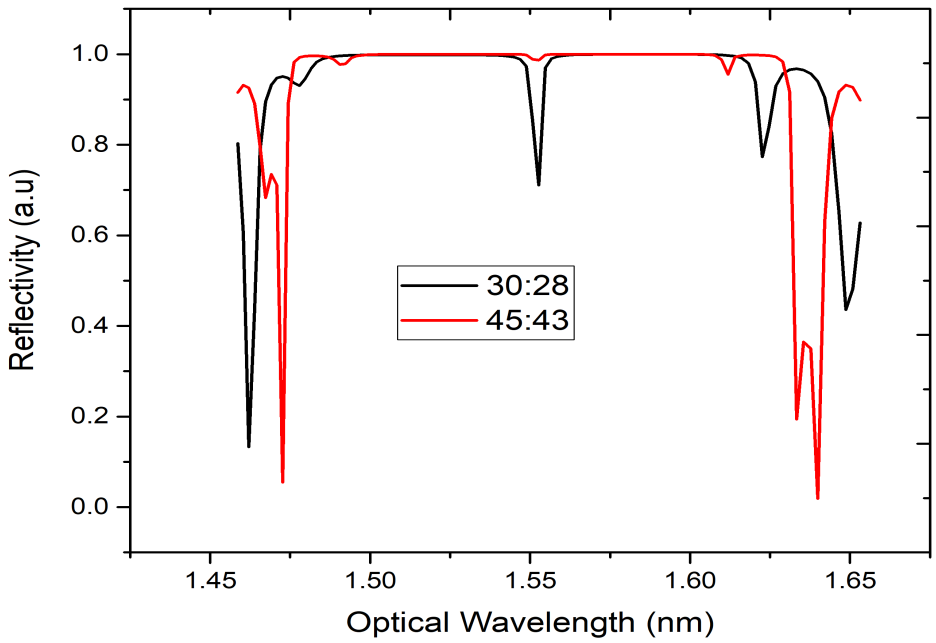


FIGURE 4.7: Reflectivity for 30:28 and 45:43 structures.

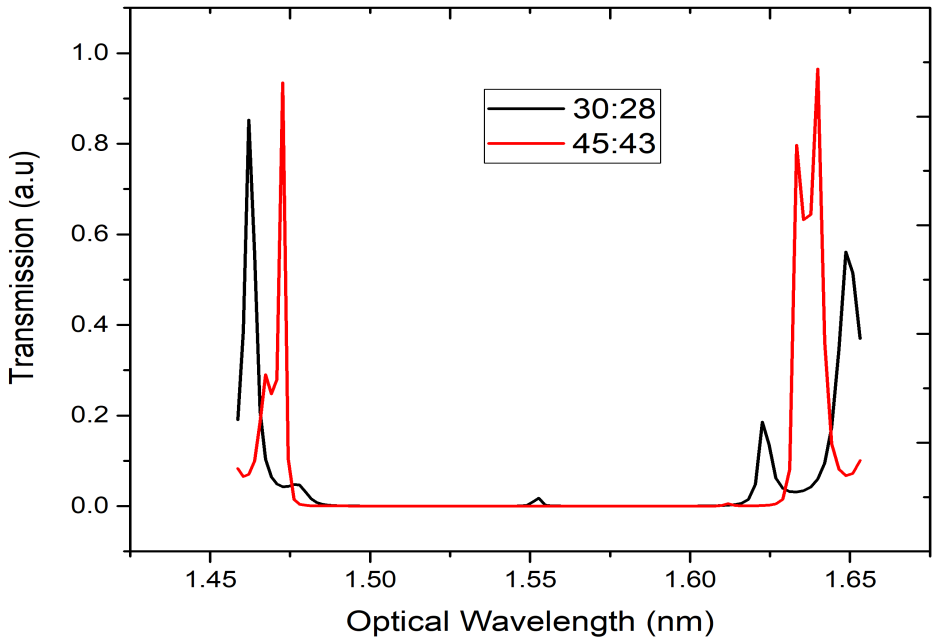


FIGURE 4.8: Wavelength transmission for 30:28 and 45:43 structures.

4.3 1550nm - 1600 nm VCSEL results

Figure 4.9 and 4.10 show a relationship between the optical wavelength and the anode voltage for the 12 different number of wells. This was done for two different mirror ratings to see the impact of mirrors and quantum wells on the required wavelength emission from the third window. It is evident that the mirror stacks did not affect the wavelength as the same number of quantum wells for different mirror ratio emits on the same wavelength. Three of the structures are emitted near the 1550 nm range for the two mirror ratios. Six QW structure are emitted at 1540 nm, seven QW structure are emitted at 1550 nm, and eight QW VCSEL are emitted at 1555 nm for both the 30:28 and 45:43 mirror ratios. A device has a warm-up voltage that does not contribute to any output, hence the deviation between 0-1 V [195, 189, 196, 197, 198].

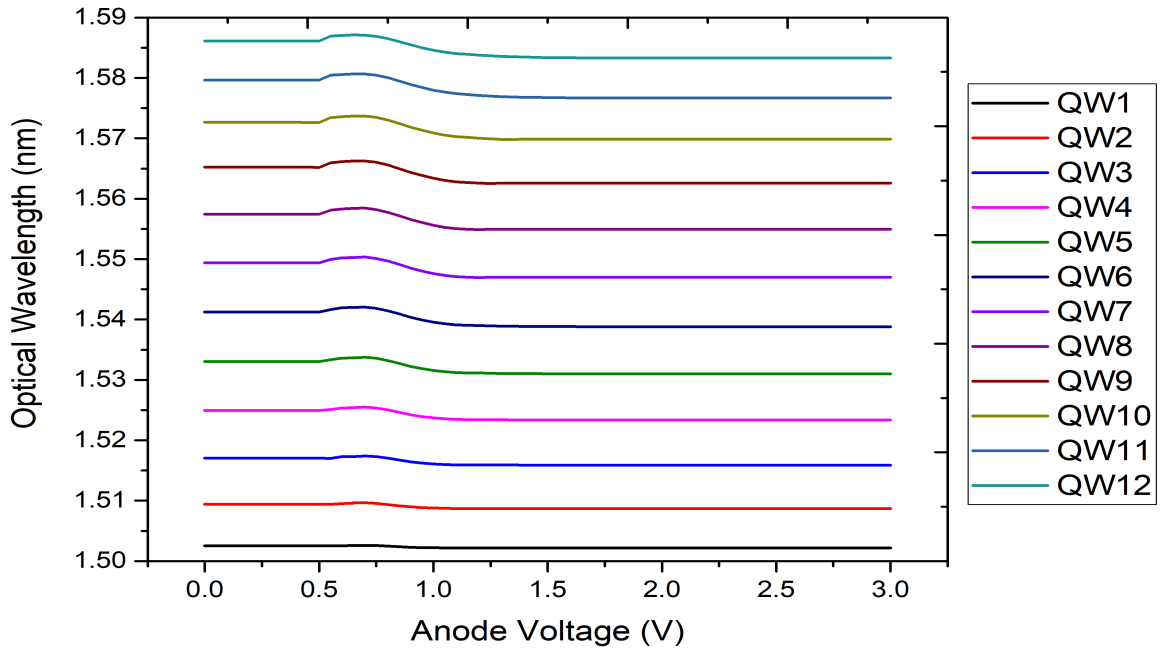


FIGURE 4.9: Optical wavelength vs anode voltage for 30:28 mirror ratio.

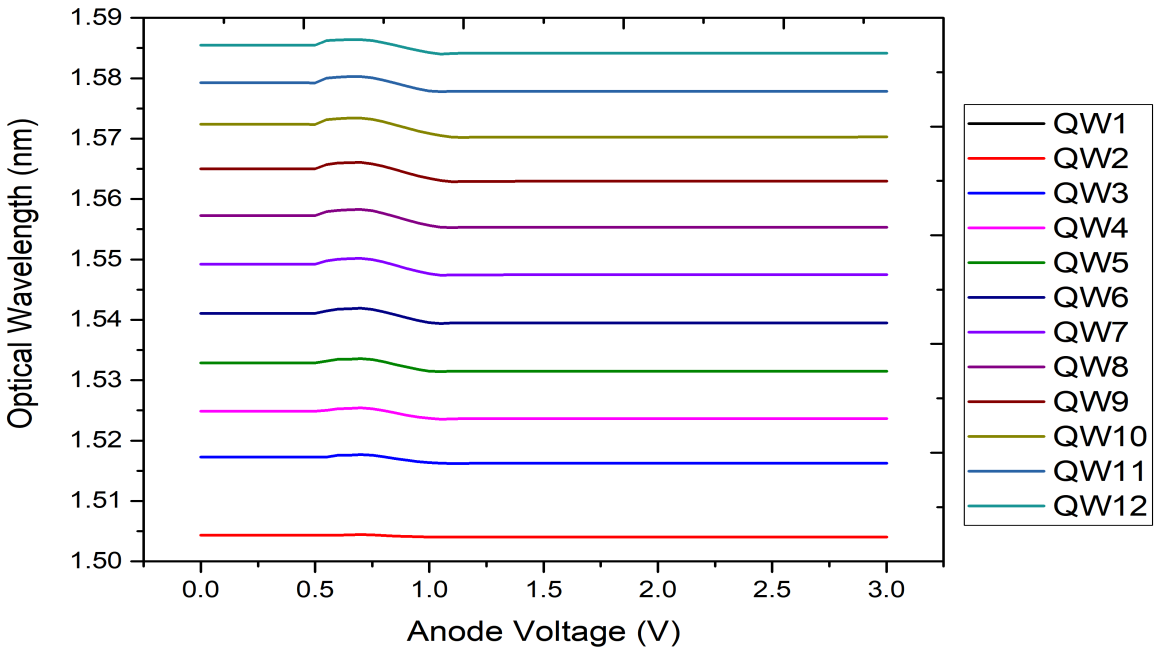


FIGURE 4.10: Optical wavelength vs anode voltage for 45:43 mirror ratio.

4.3.1 Power v.s optical wavelength results

Figure 4.11 and 4.12show the total power emitted by each quantum well against the Optical wavelength for the two mirror ratios. Optical power is important in Optical communication because there are acceptable working power ranges in the fibre and for communication. Therefore, this means that power should be considered because maximising it will benefit communication systems. The device structure should be chosen by taking into account which has a better power, which means better efficiency. This analysis helps determine how changes in the quantum wells and the mirror ratings will affect the emission of a particular source. For 30:28 ratio, only five structures showed power output, and other structures only showed output power after their mirror reflectivities were increased to 45:43, that is, from 95% to 98.5% according to the calculations in section two. This shows the impact of the reflectivity of the mirrors on the cavity length. A structure with a short cavity length requires more mirror reflectivities than a structures with a longer cavity length. This is evident in Figure 4.11 and figure 4.12, as QW 1 to QW 6 only showed power output after their mirror reflectivities were increased. Only structures with more quantum wells will produce output at less reflectivities.

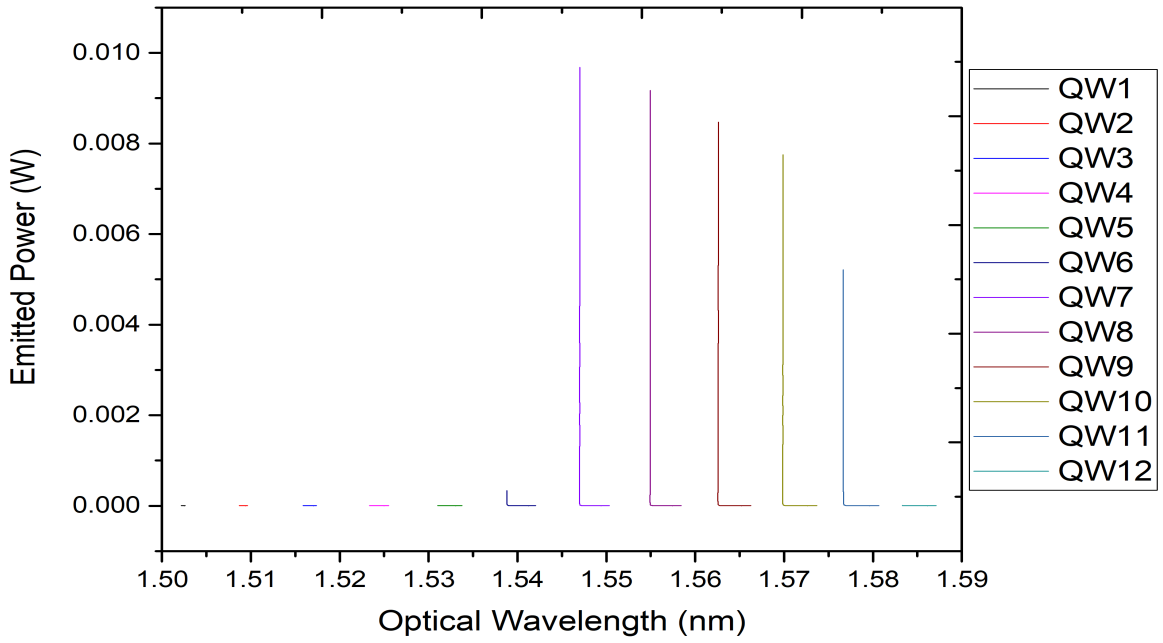


FIGURE 4.11: Emitted power vs optical wavelength for 30:28 mirror ratio.

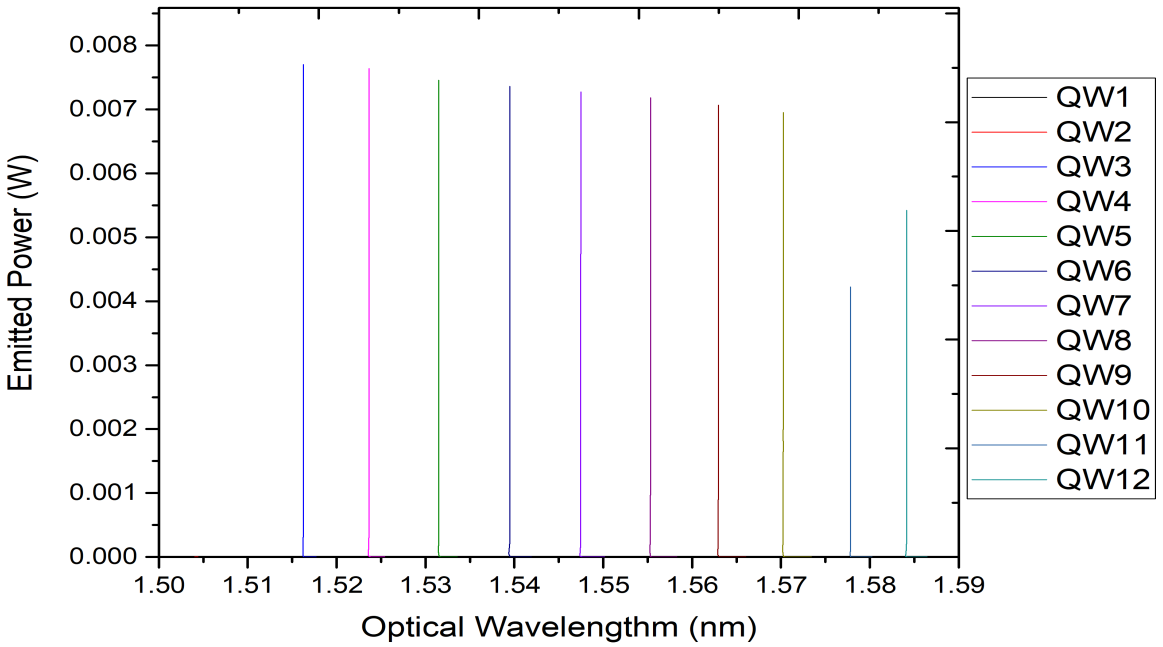


FIGURE 4.12: Emitted power vs optical wavelength for 45:43 mirror ratio.

4.3.2 Absorption v.s optical wavelength results

The absorption of photons is the most important in optic sources operation, as it is responsible for the emitted light output with the required wavelength as per designer's requirements. Figure 4.13 and 4.14 show that absorption, which is a basic operation of a laser, only peaks at operation emission wavelengths. These wavelength peaks show a well-functioning VCSEL structure and are shown by all the 12 simulated QW structures. Only VCSEL structures with seven quantum wells in those settings are ideal for third window optical fibre communication applications because their absorptions pick at the 1550 nm third window wavelength. Therefore, it is critical that the photons in the 7 QW structure are absorbed at the required wavelength of 1550 nm.

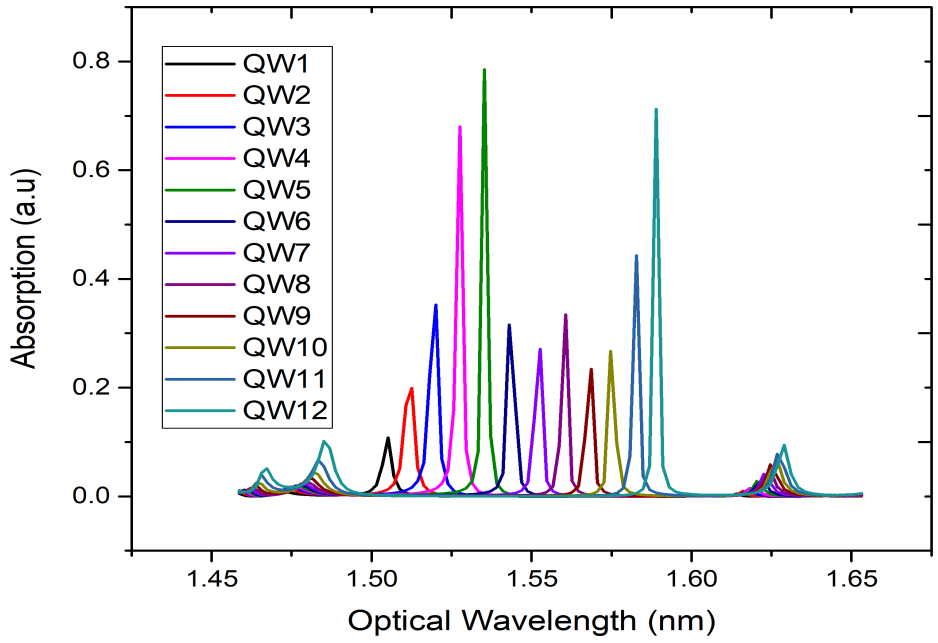


FIGURE 4.13: Absorption vs optical wavelength for 30:28 mirror ratio.

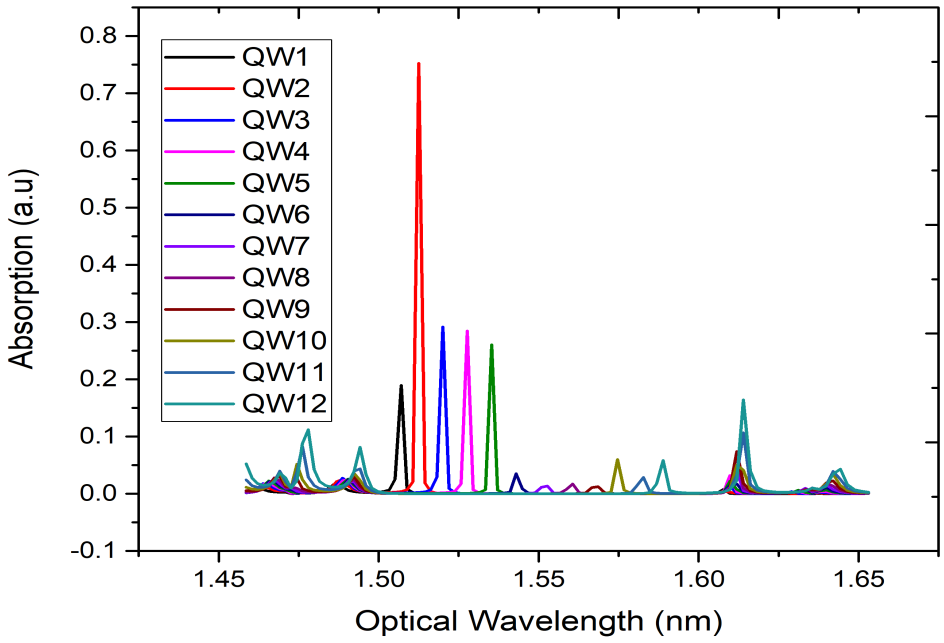


FIGURE 4.14: Absorption vs optical wavelength for 45:43 mirror ratio.

4.3.3 Reflectivity and transmission results

Figure 4.15 and 4.16 show reflectivity versus optical wavelength, while figures 4.17 and 4.18 show the transmission versus Optical Wavelength. It is evident that reflectivity is high at the emission wavelengths, which is an inverse of low transmission as seen from figures 4.17 and 4.18. When reflectivity is high at emission wavelengths during lasing, then it means the transmission of the same device should be low. This is to ensure that the operations do not cancel each other out and produce non-radiative emissions that are incompatible with the laser cavity.

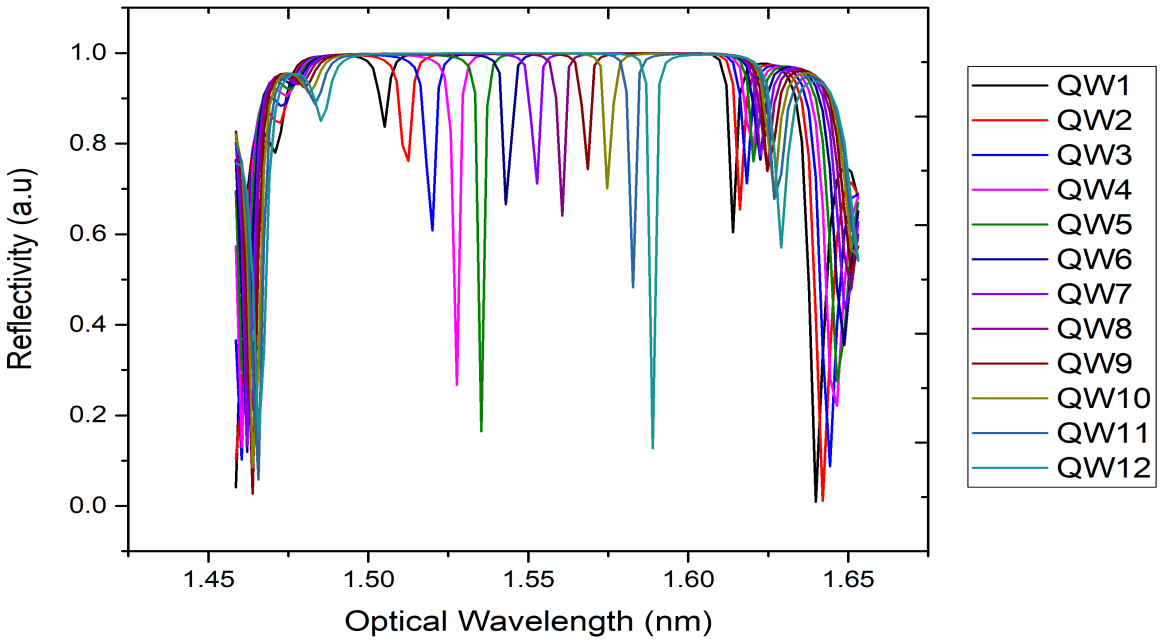


FIGURE 4.15: Reflectivity vs optical wavelength for 30:28 mirror ratio.

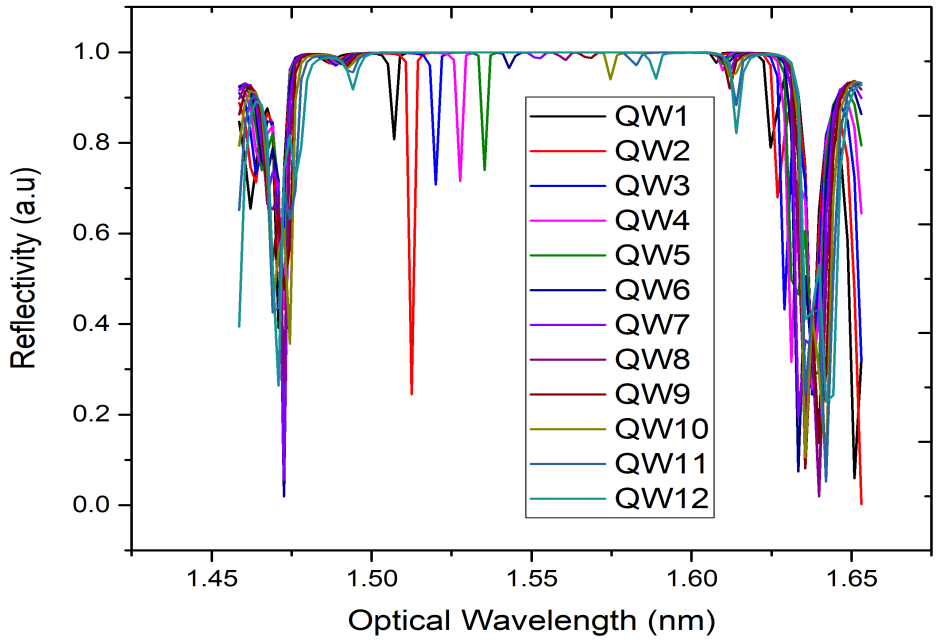


FIGURE 4.16: Reflectivity vs optical wavelength for 45:43 mirror ratio.

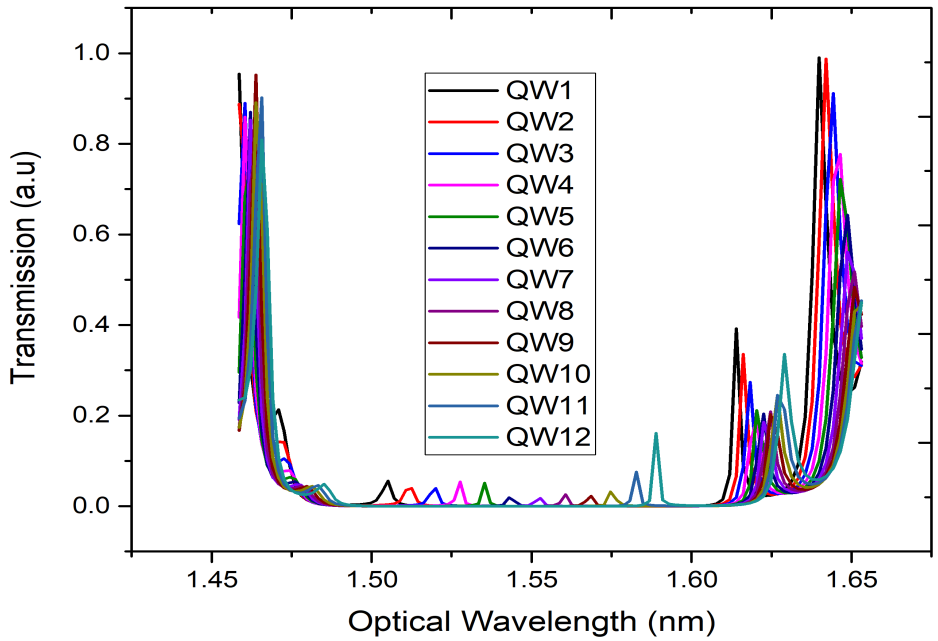


FIGURE 4.17: Transmission vs optical wavelength for 30:28 mirror ratio.

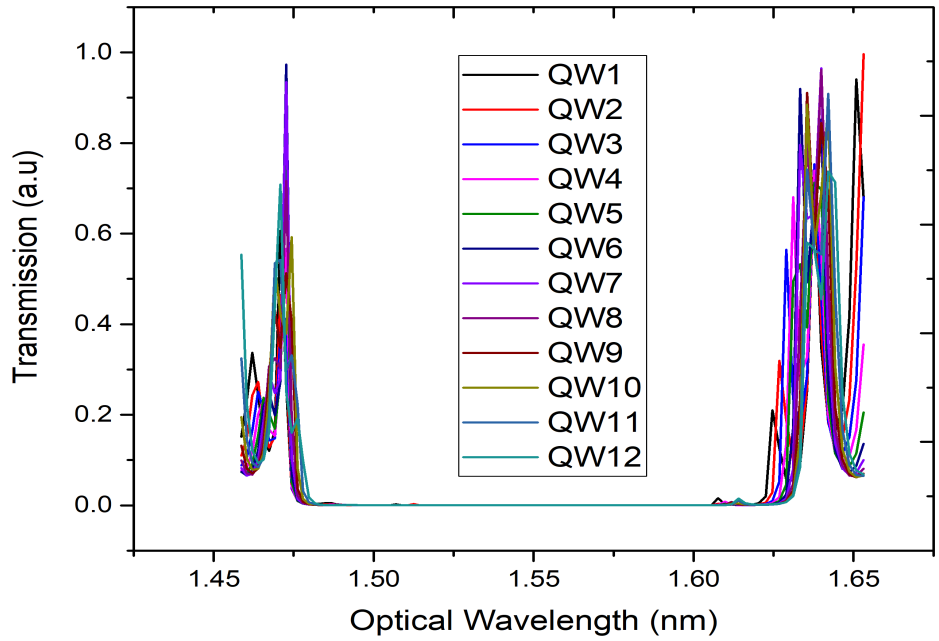


FIGURE 4.18: Transmission vs optical wavelength for 45:43 mirror ratio.

4.3.4 P-I-V characteristics for the 1500 nm - 1600 nm wavelength emission

Power vs Current and Voltage were plotted and analysed as I-V characteristics of the simulated structure. The emitted power, threshold current and warm voltages are analysed when choosing the best structure for VCSEL as the optical source for fibre optical communication systems. A device should have sufficient power, and lower threshold values for it to be considered efficient. Since all the structures simulated at room temperature, the 7 QW structure had a better device performance. For the structures that produced emissions near the 1550 nm range, the VCSEL with seven QWs emitted better power outputs for both the two mirror ratios.

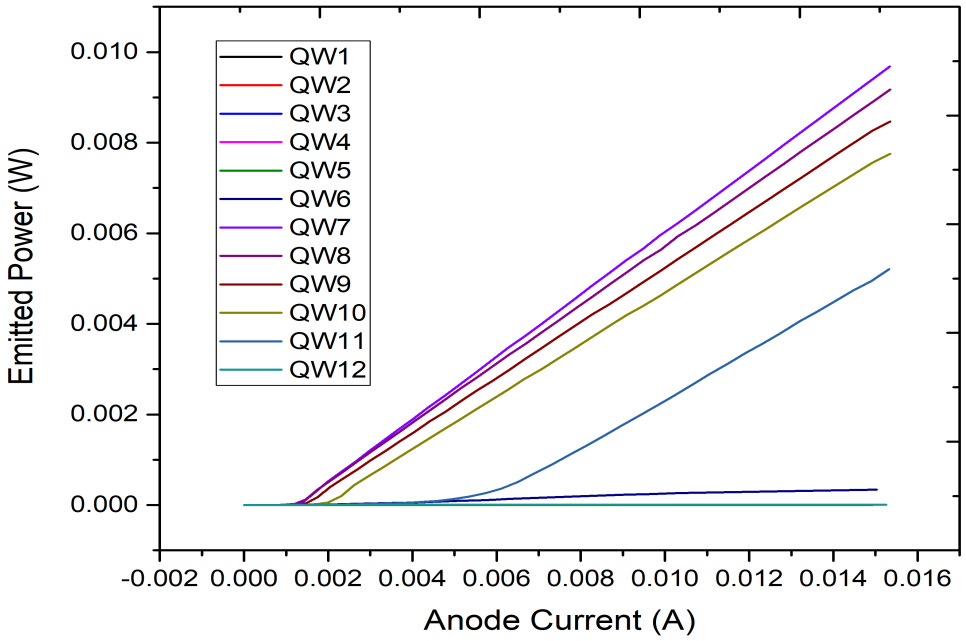


FIGURE 4.19: Emitted power vs anode current for 30:28 mirror ratio.

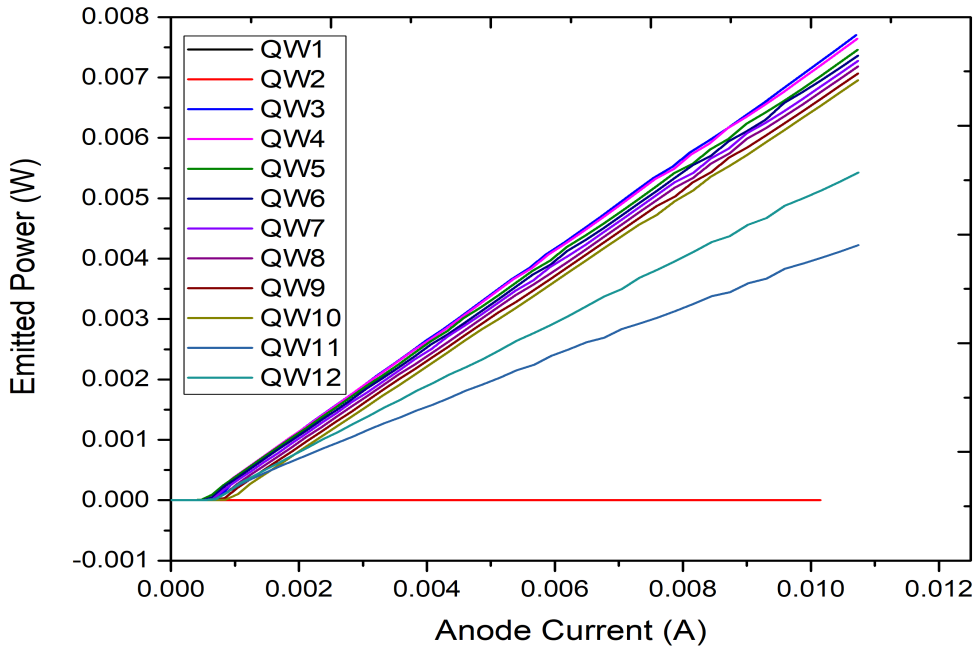


FIGURE 4.20: Emitted power vs anode current for 45:43 mirror ratio.

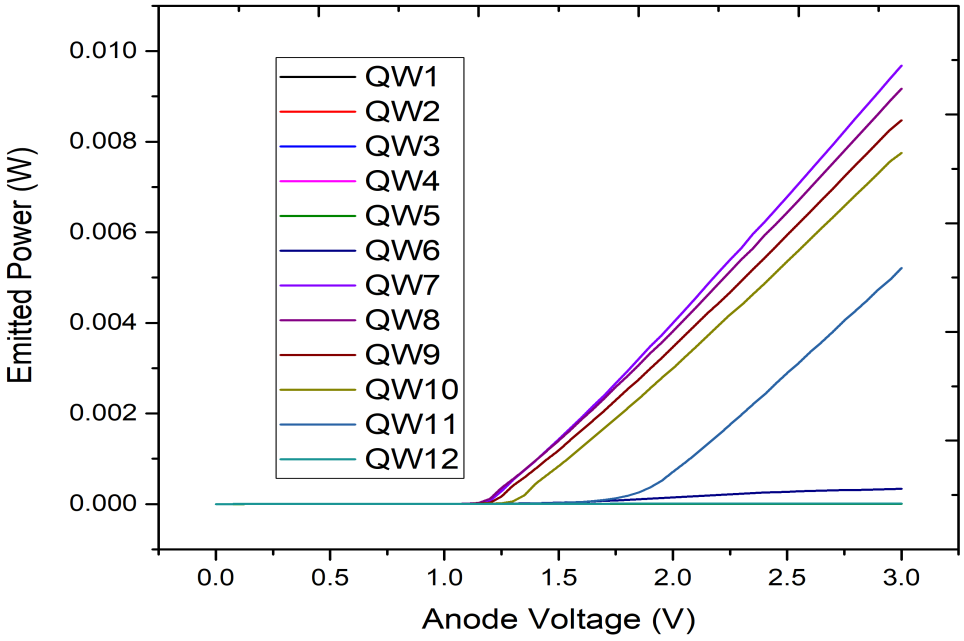


FIGURE 4.21: Emitted power vs anode voltage for 30:28 mirror ratio.

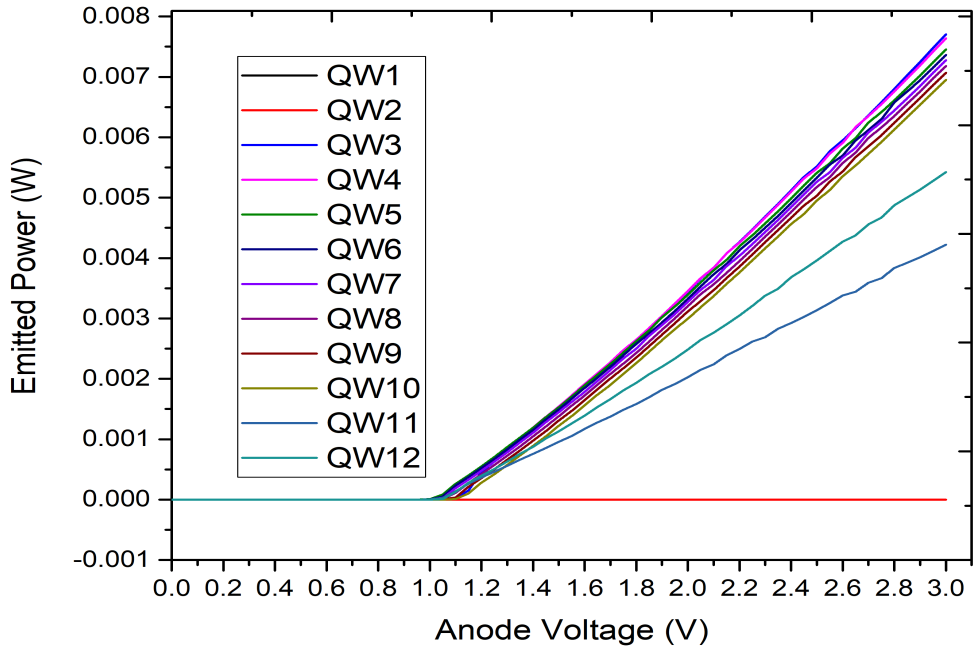


FIGURE 4.22: Emitted power vs anode voltage for 45:43 mirror ratio.

Other characteristics of the I-V device such as Voltage versus Current were plotted in figure 4.23 and 4.24. The characteristic behaviour of the structures was studied by varying the mirror periods and the number of QWs in order to select a structure with a lower warm-up voltage and current. From this, it can be concluded that VCSEL with an InGaAsP Active region has a threshold voltage range of 0.8 - 1 V.

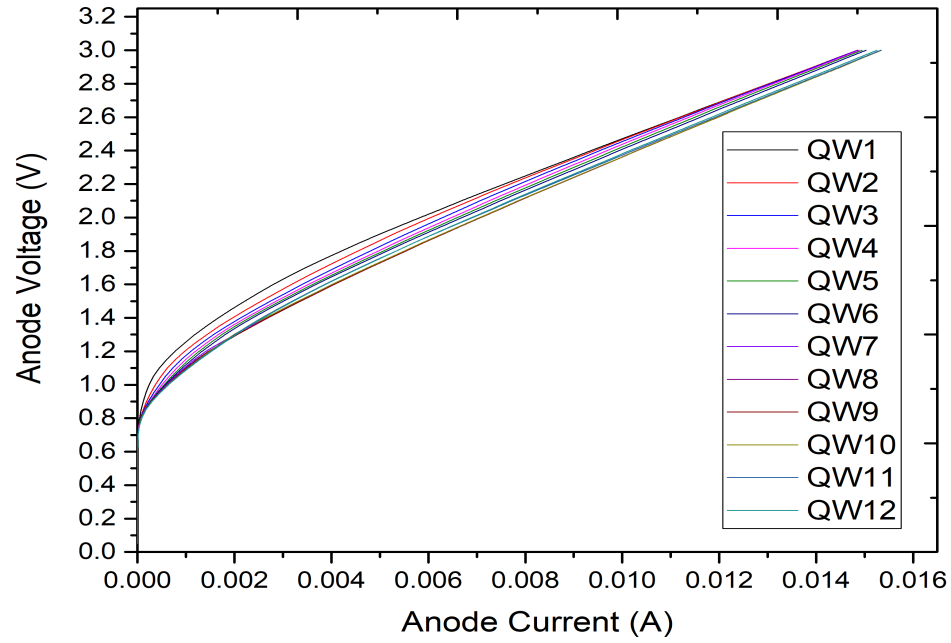


FIGURE 4.23: Anode voltage vs anode current for 30:28 mirror ratio.

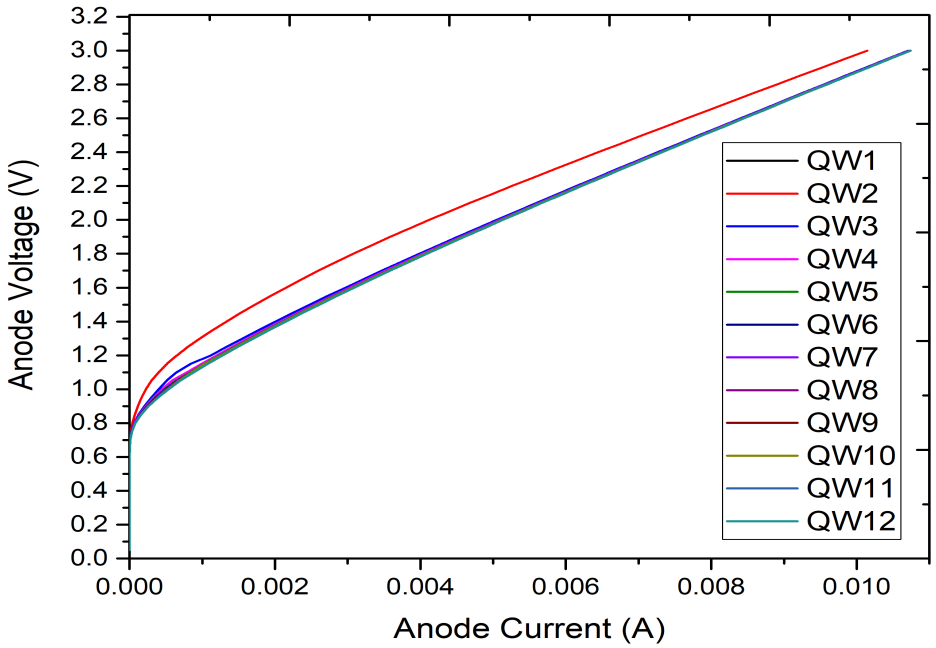


FIGURE 4.24: Anode voltage vs anode current for 45:43 mirror ratio.

4.4 Chapter summary

This Chapter of this thesis summarises the most important accomplishments and conclusions of this work. In addition to performance analysis such as power, current and voltage, the focus is still on the general principles of a laser for optical fibre communications. These principles are likely to lead to future improvements on the device. The study concludes with an outlook on the proposed future work that is dependent on the work done in this thesis.

Chapter 5

Conclusion

It can be concluded that for an interval of 0-1 V the device is in a warm state as seen from figure 4.4 that there is a deflection in wavelength before it becomes stable. This justifies that when the voltage rises, there is a little deviation from the operating emission wavelength. From figure 4.3, it can also be seen that in this voltage interval the device does not contribute to any output power, hence the term warm-up voltage. The threshold voltage of the device is 0.8 V. It was evident from the simulated QWs that it emits at different wavelengths, and it has been observed that higher wavelengths carry less power, so they require high frequencies for high power transmissions. The absorption and reflectivity values are vital for the operation of the de- vice as they control the output of the device. If the reflectivity is very close to 100%, then the light will be trapped, and if the reflectivity is less than 70%, there will be no lasing. If the absorption is low, the power depends on the voltage input and the device works like a Light emitting diode or a normal bulky laser. From the I-V curves, it can be concluded that the simulated device behaves like a nonlinear device that correlates with the theory as it is a family of semiconductor diodes. The seven VCSEL quantum wells with 30 periods in the top mirror and 28 periods in the bottom mirror gave an output power of 9.5 mW, which was compared with the previous works of [161], [199] and [21] . There is an increase in power that was noticed with comparison with the mentioned as their output power were 5 mW, 5.7 mW and 6.4 mW. Research shows that surface emitting lasers have shown better results than the edge emitters in the optical field. Currently, surface emitters that are used are the VCSELs with cavities built inside the structure of the device and vertical external cavity surface emitting lasers (VECSELs) having cavities built outside the structures [165, 200, 201]. Surface emitters have critical characteristics that leads to debates about which structure is best for optical communication. VCSELs can be modulated directly without any external modulator, unlike the bulky lasers. VCSELs can lase in ultraviolet to infrared regions. Lower power efficiency, high speed modulations (with over 50 Gbps data rates), low driving currents, 2-D

arrangements, beams that are narrow for simple coupling into fibre, easy packaging, single mode operation, tests at the wafer level are the qualities that have been demonstrated by the VCSELs. These semiconductor structures have shown higher power efficiencies of about 20% to 30% than the bulky lasers that has about 0.1% - 1 % efficiencies. VCSELs that had an oxide bound to the designs showed promising threshold currents [202] and higher power efficiencies of more than 50 % [203, 204]. The ability of VCSELs to be integrated with other optical electronic devices is another quality that has led to their success. The integration of VCSELs and PICs through the meta structure makes the chips compact, which results in better power performances, which is the future of electronics as the cabling is replaced by optical light. These laser designs have great applications used as sensors and in the optical field [68, 205]. Achieving low losses and coupling and between n-plane PICs and VCSELs has been hard during their introduction. A couple of adjustments have been made, depending on what the designers wants. of the has resulted in quality crystals with temperature attributes structures such as the highly strained GaInAs QW lasers [163].Surface emitters with single mode radiation having short spectral width has enabled long transmissions over HPCs and Multi-Mode Fibre (MMF) for server farms [206]. Various studies have shown that Discrete Multi-Tone (DMT) or CAP for VCSELs with higher speed transmissions can take data transmission rates of more than 100Gbps with higher spectral efficiencies [207, 208]. The spontaneous emission control in cavities has become one of the most novel and neglected topics in laser operations.

Appendix A

Final code

Define CYL on MESH statement for cylindrical symetry
options verbose
mesh cyl auto

CYL STATEMENT:
X=0
Y=0
AUTO=0
CYL STATEMENT ($X-in, Y-in, Auto-in$)
X=X-in ;
Y=Y-in ;
AUTO=Auto-in ;
Cyl-statement (mesh auto cyl) ;

TOP REGION:
X=0
Y=0
SPACE=0
TOP REGION (X-in, Y-in, Space-in)
X=X-in ;
Y=Y-in ;
SPACE=Space-in ;
TOP REGION region-1(0, 0, 0.5)
TOP REGION region-2(6, 0, 0.5) ;

SPACERS:
RM=0
THICK=0
Y=0

```
ACCE=0
SPACER (RM-in, THICK-in, Y-in, ACCE-in)
RM=RM-in ;
THICK=THICK-in ;
Y=Y-in ;
ACCE=ACEE-in ;
SPACERS spacer-1 (GaAs, 0.01, 0.005, 4e19)
SPACERS spacer-2 (GaAs, 0.02, 0.01, 4e17) ;

TOP DBR:
THICK=0
RM=0
N=0
X.COMP=0
ACCE=0
TOP DBR (THICK-in, RM-in, N-in, X.COMP-in, ACCE-in)
THICK=THICK-in ;
RM=RM-in ;
N=N-in ;
X.COMP=X.COMP-in ;
ACCE=ACCE-in ;
while (half.cyc < 30)
TOP DBR mat-1 (0.1157, GaAs, 3, 0.67, 4e17)
TOP DBR mat-2 (0.1273, AlGaAs, 3, 0.67, 4e17) ;
half.cyc++ ;

TOP CONTACT:
RM=0
THICK=0
Y=0
ACCE=0
TOP CONTACT (RM-in, THICK-in, Y-in, ACCE-in)
RM=RM-in ;
THICK=THICK-in ;
Y=Y-in ;
ACCE=ACEE-in ;
TOP CONTACT contact-1 (GaAs, 0.184, 0.02, 4e17)
TOP CONTACT contact-2 (GaAs,0.02, 0.01, 2e19) ;
```

ACCEPTOR REGION:
RM=0
THICK=0
Y=0
ACCE=0
ACCEPTOR REGION (RM-in, THICK-in, Y-in, ACCE-in)
RM=RM-in ;
THICK=THICK-in ;
Y=Y-in ;
ACCE=ACEE-in ;
ACCEPTOR REGION accept-1 (InP, 0.178, 0.04, 1e18)
ACCEPTOR REGION accept-2 (InP,0.1, 0.05, 1e16) ;

QWELL:
RM=0
THICK=0
Y=0
X.COMP=0
Y.COMP=0
NX=0
NY=0
QWELL(RM-in, THICK-in, Y-in, X.COMP-in, Y.COMP-in, NX-in, NY-in)
RM=0
THICK=THICK-in ;
Y=Y-in ;
X.COMP=X.COMP-in ;
Y.COMP=Y.COMP-in ;
NX=NX-in ;
NY=NY-in ;
I = 0
While (i < 7) QWELL active (InGaAsP, 0.008 0.001, 0.52, 0.82)
QWELL well (InGaAsP,0.0055, 0.001, 0.24, 0.82, 12, 99)
I++ ;

DONOR REGION:
RM=0
THICK=0

```
Y=0
DON=0
DONOR REGION (RM-in, THICK-in, Y-in, DON-in)
RM=RM-in ;
THICK=THICK-in ;
Y=Y-in ;
DON=DON-in ;
DONOR REGION donor-1 (InP, 0.258, 0.04, 5e18)
DONOR REGION donor-2 (GaAs,0.05, 0.025, 1e18) ;

BOTTOM DBR:
THICK=0
RM=0
N=0
DON=0
BOTTOM DBR (THICK-in, RM-in, N-in, DON-in)
THICK=THICK-in ;
RM=RM-in ;
N=N-in ;
DON=DON-in ;
while (half.cyc < 28)
BOTTOM DBR mat-1 (0.1157, GaAs, 3, 1e18)
BOTTOM DBR mat-2 (0.134, AlAs, 3, 1e18)
Half.cyc++ ;

BOTTOM CONTACT:
RM=0
THICK=0
Y=0
DON=0
BOTTOM CONTACT (RM-in, THICK-in, Y-in, DON-in)
RM=RM-in ;
THICK=THICK-in ;
Y=Y-in ;
DON=DON-in ;
BOTTOM CONTACT contact-1 (GaAs, 0.02, 0.005, 5e18) ;

ELECTRODES:
```

```
NAM=0
X=0
ELECTRODE (NAM-in, X-in)
NAM=NAM-in ;
X=X-in ;
ELECTRODES name-1(anode top, 6)
ELECTRODES name-2(cathode bottom) ;

saveout f = vcselex010.str
solvevstep = 0.05name = anodev final = 1.0
saveout f = vcselex011.str
vcselprojtauss = 0.01
solvevstep = 0.05name = anodev final = 1.2
saveout f = vcselex012.str
solvevstep = 0.05name = anodev final = 3.0
saveout f = vcselex013.str
tonyplotvcselex01.log-setvcselex010.set
tonyplotvcselex013.str-setvcselex011.set quit
```

Appendix B

List of publications

Journals

1. **Vertical Cavity Surface Emitting Lasers as Sources for Optical Communication Systems: A Review**
   O. O. Moatlhodi, N. M. J. Ditshego, and R.Samikannu, "Vertical Cavity Surface Emitting Lasers as Sources for Optical Communication Systems: A Review.," Journal of Nano Research, Vol. 65, pp 51-96, Dec. 2020.

2. **Simulation and Analysis of a Single Mode Indium Gallium Arsenide Phosphide Vertical Cavity Surface Emitting Laser for Optical Communication**
   O. O. Moatlhodi, N. M. J. Ditshego, and R.Samikannu, "Simulation and Analysis of a Single Mode Indium Gallium Arsenide Phosphide Vertical Cavity Surface Emitting Laser for Optical Communication.," Journal of Nano Research, Vol. 43, pp 93-109, July. 2021.

Bibliography

[1] K. F. Brennan, *The Physics of Semiconductors: With Applications to Optoelectronic Devices*. Cambridge University Press, 1999.

[2] B. G. Streetman, *Solid State Electronic Devices*. USA: Prentice-Hall, Inc., 1990.

[3] B. G. Streetman and B. Sanjay Kumar, "Solid state electronic devices," in *A Solid State Electronic Devices seventh edition*. Pearson Education Limited, 2016, pp. 21–42.

[4] V. Jain, H. Kaushal, and A.Vats, "Free space optical communication: laser sources, modulation schemes and detection techniques," 02 2013.

[5] K. F. Brennan, *Introduction to Semiconductor Devices: For Computing and Telecommunications Applications*. Cambridge University Press, 2005.

[6] J. C. Palais, *Fiber Optic Communication*. Prentice Hall: Engle wood Cliffs, 1992.

[7] C. P.K, *Fiber Optics and Optoelectronics*. Prentice Hall: Engle wood Cliffs, 1990.

[8] S. D. Personick, *Optical Sources and Transmitters*. Boston, MA: Springer US, 1985, pp. 46–70. [Online]. Available: https://doi.org/10.1007/978-1-4899-3478-9_3

[9] K. Iga, "Surface-emitting laser - its birth and generation of new optoelectronics field," *IEEE Journal on Selected Topics in Quantum Electronics*, vol. 6, no. 6, pp. 1201–1215, 2000.

[10] R. H. Johnson and D. M. Kuchta, "30 gb/s directly modulated 850 nm datacom vcsels," in *Conference on Lasers and Electro-Optics/Quantum Electronics and Laser Science Conference and Photonic Applications Systems Technologies*. Optical Society of America, 2008, p. CPDB2. [Online]. Available: http://www.osapublishing.org/abstract.cfm?URI=CLEO-2008-CPDB2

[11] S. B. Mer, "Ways to Improve the Throughput in Fiber Optic Communication - An Overview," *International Journal of Computer Science and Mobile Computing*, vol. 4, no. 4, pp. 858–862, 2015. [Online]. Available: www.ijcsmc.com

[12] P. Westbergh, J. Gustavsson, Haglund, A. Larsson, F. Hopfer, G. Fiol, D. Bimberg, and A. Joel, "32 gbit/s multimode fibre transmission using high-speed, low current density 850 nm vcsel," *Electronics Letters*, vol. 45, pp. 366 – 368, 04 2009.

[13] M. Vogel, "Masers and lasers, second edition: an historical approach," *Contemporary Physics*, vol. 57, pp. 1–1, 12 2015.

[14] C. H. Townes, *Maser*. McGraw-Hill, 1960.

[15] I. S. Chung and J. Moerk, "Vectorial analysis of dielectric photonic crystal VCSEL," *ICTON 2009: 11th International Conference on Transparent Optical Networks*, vol. 1, pp. 1–4, 2009.

[16] S. Spiga, C. Xie, P. Dong, M. C. Amann, and P. Winzer, "Ultra-high-bandwidth monolithic VCSEL arrays for high-speed metro networks," *International Conference on Transparent Optical Networks*, pp. 1–4, 2014.

[17] W. Gordy, "Early events and some later developments in microwave spectroscopy," *Journal of Molecular Structure*, vol. 97, pp. 17–32, 1983, determination of Molecular Structure by Microwave Spectroscopy and Electron Diffraction. [Online]. Available: https://www.sciencedirect.com/science/article/pii/0022286083901722

[18] R. Esman, "Fiber optics for microwave applications," in *Proceedings of Optical Fiber Communication Conference* (, 1997, pp. 254–.

[19] H. Casey and M. Panish, "Chapter 4 - heterojunctions," in *Heterostructure Lasers*, H. Casey and M. Panish, Eds. Academic Press, 1978, pp. 187 – 255. [Online]. Available: http://www.sciencedirect.com/science/article/pii/B9780121631017500116

[20] J. Hecht, "Short history of laser development," *Applied optics*, vol. 49, pp. F99–122, 09 2010.

[21] R. Faez, A. Marjani, and S. Marjani, "Design and simulation of a high power single mode 1550nm InGaAsP VCSELs," *IEICE Electronics Express*, vol. 8, no. 13, pp. 1096–1101, 2011.

[22] B. Lanz, "Compact current pulse-pumped gaas–algaas laser diode structures for generating high peak-power (1–50 watt) picosecond-range single optical pulses," Ph.D. dissertation, 10 2016.

[23] A. Kakuta, *Laser Printer Application*. Boston, MA: Springer US, 1990, pp. 155–171. [Online]. Available: https://doi.org/10.1007/978-1-4899-2046-1_12

[24] H. Jelínková and Z. Č. Kluiber, "8 . Laser Applications," pp. 201–212, 1961.

[25] V. Sypin, A. Volkov, D. Myasnikov, F. Shcherbina, and A. Mashkin, "QCW thulium fiber laser for medical application," *Proceedings - 2016 International Conference Laser Optics, LO 2016*, vol. 37, no. 1, p. S110, 2016.

[26] P. Sprangle, B. Hafizi, A. Ting, and R. Fischer, "High-power lasers for directed-energy applications," *Appl. Opt.*, vol. 54, no. 31, pp. F201–F209, Nov 2015. [Online]. Available: http://ao.osa.org/abstract.cfm?URI=ao-54-31-F201

[27] C. Burrus, E. Chinnock, D. Gloge, W. Holden, T. Li, R. Standley, and D. Keck, "Pulse dispersion and refractive-index profiles of some low-noise multimode optical fibers," *Proceedings of the IEEE*, vol. 61, no. 10, pp. 1498–1499, 1973.

[28] D. Keck, "A future full of light," *IEEE Journal of Selected Topics in Quantum Electronics*, vol. 6, no. 6, pp. 1254–1258, 2000.

[29] A. W. Smith, "John tyndall (1820-1893)," *The Scientific Monthly*, vol. 11, no. 4, pp. 331–340, 1920. [Online]. Available: http://www.jstor.org/stable/6497

[30] J. Flood, "Alexander graham bell and the invention of the telephone," *Electronics and Power*, vol. 22, no. 3, pp. 159–162, 1976.

[31] S. Hranilovic, L. Lampe, S. Hosur, and R. D. Roberts, "Visible light communications: the road to standardization and commercialization (part 2) [guest editorial]," *IEEE Communications Magazine*, vol. 52, no. 7, pp. 62–63, 2014.

[32] S. A. Mostofa, "Smart light pipe strategies in deep plan office building in dhaka, bangladesh," *NJEDP*, vol. 11, pp. 125–136, 2015.

[33] A. Méndez, *Optics in Medicine*. Cham: Springer International Publishing, 2016, pp. 299–333. [Online]. Available: https://doi.org/10.1007/978-3-319-31903-2_13

[34] A. B. Magoun, "The electrical engineer who clarified glass [scanning our past]," *Proceedings of the IEEE*, vol. 107, no. 5, pp. 928–932, 2019.

[35] P. Mishra, S. S. Rout, G. Palai, and L. Spandana, "Comparative analysis of a dispersion compensating fiber optic link using fbg based on different grating length and extinction ratio for long haul communication," in *Innovations in Bio-Inspired Computing and Applications*, A. Abraham, M. Panda, S. Pradhan,

L. Garcia-Hernandez, and K. Ma, Eds. Cham: Springer International Publishing, 2021, pp. 139–147.

[36] P. Steglich and F. De Matteis, *Introductory Chapter: Fiber Optics*, 03 2019.

[37] S. Addanki, I. Sadegh Amiri, and P. Yupapin, "Review of optical fibers-introduction and applications in fiber lasers," *Results in Physics*, vol. 10, 07 2018.

[38] C. J. Koester and E. Snitzer, "Amplification in a fiber laser," *Appl. Opt.*, vol. 3, no. 10, pp. 1182–1186, Oct 1964. [Online]. Available: http://ao.osa.org/abstract.cfm?URI=ao-3-10-1182

[39] H. Griffiths, K.-F. Tong, and Y. Yang, "Charles k. kao and other telecommunication pioneers," *Communications Magazine, IEEE*, vol. 48, pp. S20 – S27, 04 2010.

[40] M. Ohring, "Chapter 8 - epitaxy," in *Materials Science of Thin Films (Second Edition)*, second edition ed., M. Ohring, Ed. San Diego: Academic Press, 2002, pp. 417–494. [Online]. Available: https://www.sciencedirect.com/science/article/pii/B9780125249751500112

[41] G. P. Agrawal, *Optical Communication: Its History and Recent Progress*. Cham: Springer International Publishing, 2016, pp. 177–199. [Online]. Available: https://doi.org/10.1007/978-3-319-31903-2_8

[42] C. Levallois, A. L. Corre, O. Dehaese, H. Folliot, C. Paranthoen, C. Labbé, and S. Loualiche, "Design and fabrication of GaInAsP/InP VCSEL with two a-Si/a-SiNx Bragg reflectors," *Optical and Quantum Electronics*, vol. 38, no. 4-6, pp. 281–291, 2006.

[43] K.-L. Chi, J.-L. Yen, J.-M. Wun, J.-W. Jiang, I.-C. Lu, J. Chen, Y.-J. Yang, and J.-W. Shi, "Strong wavelength detuning of 850 nm vertical-cavity surface-emitting lasers for high-speed (>40 gbit/s) and low-energy consumption operation," *IEEE Journal of Selected Topics in Quantum Electronics*, vol. 21, pp. 1–1, 11 2015.

[44] P. Moser, J. A. Lott, P. Wolf, G. Larisch, H. Li, and D. Bimberg, "85-fj dissipated energy per bit at 30 gb/s across 500-m multimode fiber using 850-nm vcsels," *IEEE Photonics Technology Letters*, vol. 25, no. 16, pp. 1638–1641, 2013.

[45] R. Safaisini, E. Haglund, P. Westbergh, J. Gustavsson, and A. Larsson, "20 gbit/s data transmission over 2 km multimode fibre using 850 nm mode filter vcsel," *Electronics Letters*, vol. 50, pp. 40–42, 01 2014.

[46] G. Keiser, *Digital Optical Fiber Links*. Singapore: Springer Singapore, 2021, pp. 303–362. [Online]. Available: https://doi.org/10.1007/978-981-33-4665-9_8

[47] "Fiber optics applications and technology symposium (foats 93)," *Canadian Journal of Electrical and Computer Engineering*, vol. 18, no. 1, pp. 4–4, 1993.

[48] I. Tomkos, S. Azodolmolky, J. Solé-Pareta, D. Careglio, and E. Palkopoulou, "A tutorial on the flexible optical networking paradigm: State of the art, trends, and research challenges," *Proceedings of the IEEE*, vol. 102, no. 9, pp. 1317–1337, 2014.

[49] A. Safaai-Jazi, "Tutorial: holey fibers: fundamentals and applications," in *Optical Fiber Communication Conference and Exhibit*, 2002, pp. 19–.

[50] G. P. Agrawal, "Nonlinearity of optical fibers: A tutorial," in *2018 Optical Fiber Communications Conference and Exposition (OFC)*, 2018, pp. 1–3.

[51] A. Ciekurs, J. Porinš, and M. Klochana, "Assessment of lifetime of the fiber optic infrastructure based on attenuation measurements," in *2016 Advances in Wireless and Optical Communications (RTUWO)*, 2016, pp. 70–74.

[52] M. A. Melkumov, "Optical amplification in extended wavelength windows," in *2018 Optical Fiber Communications Conference and Exposition (OFC)*, 2018, pp. 1–72.

[53] Bhattacharya, *Semiconductor Optoelectronics Devices*. Prentice Hall: Engle wood Cliffs, 1994.

[54] N. N. Ledentsov, V. A. Shchukin, V. P. Kalosha, N. N. Ledentsov, J.-R. Kropp, M. Agustin, Ł. Chorchos, G. Stępniak, J. P. Turkiewicz, and J.-W. Shi, "Anti–waveguiding vertical–cavity surface–emitting laser at 850 nm: From concept to advances in high–speed data transmission," *Opt. Express*, vol. 26, no. 1, pp. 445–453, Jan 2018. [Online]. Available: http://www.opticsexpress.org/abstract.cfm?URI=oe-26-1-445

[55] G. Stepniak, A. Lewandowski, J. R. Kropp, N. N. Ledentsov, V. A. Shchukin, N. Ledentsov, G. Schaefer, M. Agustin, and J. P. Turkiewicz, "54 gbit/s ook transmission using single-mode vcsel up to 2.2 km mmf," *Electronics Letters*, vol. 52, no. 8, pp. 633–635, 2016.

[56] A. Liu, M. Xing, H. Qu, W. Chen, W. Zhou, and W. Zheng, "Reduced divergence angle of photonic crystal vertical-cavity surface-emitting laser," *Applied Physics Letters - APPL PHYS LETT*, vol. 94, 05 2009.

[57] A. Liu, W. Chen, H. Qu, B. Jiang, W. Zhou, M. Xing, and W. Zheng, "Single-mode holey vertical-cavity surface-emitting laser with ultra-narrow beam divergence," *Laser Physics Letters*, vol. 7, no. 3, pp. 213–217, mar 2010. [Online]. Available: https://doi.org/10.1002%2Flapl.200910130

[58] D. Huffaker, D. Deppe, K. Kumar, and T. Rogers, "Native-oxide ring contact for low threshold vertical-cavity lasers," *Applied Physics Letters*, vol. 65, pp. 97 – 99, 08 1994.

[59] K. D. Choquette, K. M. Geib, C. I. H. Ashby, R. D. Twesten, O. Blum, H. Q. Hou, D. M. Follstaedt, B. E. Hammons, D. Mathes, and R. Hull, "Advances in selective wet oxidation of algaas alloys," *IEEE Journal of Selected Topics in Quantum Electronics*, vol. 3, no. 3, pp. 916–926, 1997.

[60] I. Amiri, A. N. Z. Rashed, and P. Yupapin, "Interaction between optical sources and optical modulators for high-speed optical communication networks," *Journal of Optical Communications*, 2019. [Online]. Available: https://doi.org/10.1515/joc-2019-0041

[61] N. Robinson, "Optical transmission system design," in *Proceedings of Optical Fiber Communication Conference (*, 1997, pp. 161–162.

[62] F. Kerfoot, "Tutorial: forward error correction for optical transmission systems," in *Optical Fiber Communication Conference and Exhibit*, 2002, pp. 259–.

[63] C. Giles, "Tutorial on fiber gratings in lightwave network applications," in *Proceedings of Optical Fiber Communication Conference (*, 1997, pp. 64–.

[64] B. G. Streetman, *Solid State Electronic Devices*. USA: Prentice-Hall, Inc., 1990.

[65] J. Nilsson, "High power fiber sources: more than kilowatts," in *2007 Asia Optical Fiber Communication and Optoelectronics Conference*, 2007, pp. 364–366.

[66] S. Selberherr and A. Eringen, *Analysis and Simulation of Semiconductor Devices*. Springer-Verlag, 1984. [Online]. Available: https://books.google.co.bw/books?id=EE4HlRZTYi4C

[67] A. S. Arnold, J. S. Wilson, M. G. Boshier, and J. Smith, "A simple extended-cavity diode laser," *Review of Scientific Instruments*, vol. 69, no. 3, pp. 1236–1239, 3 1998. [Online]. Available: http://link.aip.org/link/?RSI/69/1236/1

[68] K. Li, Y. Rao, C. Chase, W. Yang, and C. J. Chang-Hasnain, "Monolithic high-contrast metastructure for beam-shaping vcsels," *Optica*, vol. 5, no. 1,

pp. 10–13, Jan 2018. [Online]. Available: http://www.osapublishing.org/optica/abstract.cfm?URI=optica-5-1-10

[69] *A Phenomenological Approach to Diode Lasers*. John Wiley Sons, Ltd, 2012, ch. Two, pp. 45–90. [Online]. Available: https://onlinelibrary.wiley.com/doi/abs/10.1002/9781118148167.ch2

[70] D. F. Welch, "A brief history of high-power semiconductor lasers," *IEEE Journal on Selected Topics in Quantum Electronics*, vol. 6, no. 6, pp. 1470–1477, 2000.

[71] P. Zak and J. Zalesak, "The influence of spectral properties of light in street lighting on visual perception," *Proceedings of 2016 IEEE Lighting Conference of the Visegrad Countries, Lumen V4 2016*, pp. 0–3, 2016.

[72] J. Dong, K. I. Ueda, and A. A. Kaminskii, "Optical properties and laser operation of Yb:Y3Sc 2Al3O12 crystal," *Pacific Rim Conference on Lasers and Electro-Optics, CLEO - Technical Digest*, pp. 1–2, 2009.

[73] K. A. E., *Laser Generation*. John Wiley Sons, Ltd, 2008, ch. 1, pp. 1–25. [Online]. Available: https://onlinelibrary.wiley.com/doi/abs/10.1002/9780470459300.ch1

[74] C. W. R. O'Shea, D. C. and W. T. Rhodes, *Introduction to Lasers and Their Applications*. Addison-Wesley, Reading, MA., 1977.

[75] J. T. Luxon and D. E. Parker, *Industrial Lasers and Their Applications*. Prentice Hall, Englewood Cliffs, NJ., 1985.

[76] P. Berlien and G. Müller, *Applied Laser Medicine*, 01 2003.

[77] G. Chryssolouris, *Laser machining - Theory and practice*, 01 1991.

[78] M. Goeppert-Mayer, "Annalenden physik," vol. 9, p. 273, 1931.

[79] A. R. Henderson, *A Guide to Laser Safety*. Chapman and Hall, London, 1997.

[80] B. B. Laud, *Lasers and Non-Linear Optics*. Wiley Eastern Limited, New Delhi, 1985.

[81] K. Shimoda, *Introduction to Laser Physics, 2nd edition*. Springer-Verlag, Berlin., 1986.

[82] K. Thyagarajan and A. K. Ghatak, *Lasers, Theory and Applications*. Plenum press,New York, 1981.

[83] J. Wilson and J. F. B. Hawkes, *Lasers: Principles and Applications*. Prentice Hall,New York, 1987.

[84] O. Svelto, *Principles of Lasers , 3rd edition*. Plenum press,New York, 1989.

[85] E. K.-A. Jr, *Principles of Laser Material Processing*. John Wiley Sons, inc., Hoboken, New Jersey, 2000.

[86] K. A. E., *Rate Equations*. John Wiley Sons, Ltd, 2008, ch. 4, pp. 71–82. [Online]. Available: https://onlinelibrary.wiley.com/doi/abs/10.1002/9780470459300.ch4

[87] N. W. Barret, C.R. and A. S. Tetelman, *The Principles of Engineering Materials*. Prentice Hall, Englewood Cliffs, NJ, 1973.

[88] *Overview of Semiconductor Device Trends*. John Wiley Sons, Ltd, 2002, ch. 1, pp. 1–13. [Online]. Available: https://onlinelibrary.wiley.com/doi/abs/10.1002/0471224618.ch1

[89] *Semiconductor Heterostructures*. John Wiley Sons, Ltd, 2002, ch. 2, pp. 14–83. [Online]. Available: https://onlinelibrary.wiley.com/doi/abs/10.1002/0471224618.ch2

[90] R. Pierret, *Semiconductor Device Fundamentals*. Addison-Wesley, 1996. [Online]. Available: https://books.google.co.bw/books?id=dh3CQgAACAAJ

[91] Y. Yamazoe, T. Nishino, Y. Hamakawa, and T. Kariya, "Bandgap energy of InGaAsP quaternary alloy," *Japanese Journal of Applied Physics*, vol. 19, no. 8, pp. 1473–1479, aug 1980. [Online]. Available: https://doi.org/10.1143

[92] M. Kondow, K. Uomi, A. Niwa, T. Kitatani, S. Watahiki, and Y. Yazawa, "GaInNAs: A novel material for long-wavelength-range laser diodes with excellent high-temperature performance," *Japanese Journal of Applied Physics*, vol. 35, no. Part 1, No. 2B, pp. 1273–1275, feb 1996. [Online]. Available: https://doi.org/10.1143%2Fjjap.35.1273

[93] M. Ohring, "Chapter 1 - a review of materials science," in *Materials Science of Thin Films (Second Edition)*, second edition ed., M. Ohring, Ed. San Diego: Academic Press, 2002, pp. 1–56. [Online]. Available: https://www.sciencedirect.com/science/article/pii/B9780125249751500045

[94] J. Harris, T. O'Sullivan, T. Sarmiento, M. Lee, and S. Vo, "Emerging applications for vertical cavity surface emitting lasers," *Semiconductor Science and Technology*, vol. 26, p. 014010, 11 2010.

[95] E. O. Odoh1 and A. S. Njapba2, "A review of semiconductor quantum well devices," *IRnova*, vol. 46, 2015.

[96] M. Ohring, "Chapter 7 - substrate surfaces and thin-film nucleation," in *Materials Science of Thin Films (Second Edition)*, second edition ed., M. Ohring, Ed. San Diego: Academic Press, 2002, pp. 357–415. [Online]. Available: https://www.sciencedirect.com/science/article/pii/B9780125249751500100

[97] W. Lin, H.-P. Shiao, C.-Y. Chang, T.-T. Shi, C.-T. Lee, and Y.-K. Tu, "Energy band structure tailoring of ingaasp/ingaasp quantum well prepared by organometallic vapor phase epitaxy and measured by photoluminescence," 02 1994, pp. 4–9.

[98] M. Ohring, "Chapter 6 - chemical vapor deposition," in *Materials Science of Thin Films (Second Edition)*, second edition ed., M. Ohring, Ed. San Diego: Academic Press, 2002, pp. 277–355. [Online]. Available: https://www.sciencedirect.com/science/article/pii/B9780125249751500094

[99] J. P. van der Ziel and M. Ilegems, "Multilayer gaas-al0.3ga0.7as dielectric quarter wave stacks grown by molecular beam epitaxy," *Appl. Opt.*, vol. 14, no. 11, pp. 2627–2630, Nov 1975. [Online]. Available: http://ao.osa.org/abstract.cfm?URI=ao-14-11-2627

[100] M. Ogura, T. Hata, N. J. Kawai, and T. Yao, "GaAs/AlxGa1-xAs multilayer reflector for surface emitting laser diode," *Japanese Journal of Applied Physics*, vol. 22, no. Part 2, No. 2, pp. L112–L114, feb 1983. [Online]. Available: https://doi.org/10.1143%2Fjjap.22.l112

[101] M. Ogura, T. Hata, and T. Yao, "Distributed feed back surface emitting laser diode with multilayered heterostructure," *Japanese Journal of Applied Physics*, vol. 23, no. Part 2, No. 7, pp. L512–L514, jul 1984. [Online]. Available: https://doi.org/10.1143%2Fjjap.23.l512

[102] M. Ogura and T. Yao, "Surface emitting laser diode with alxga1-xas /gaas multilayered heterostructure," *Journal of Vacuum Science Technology B: Microelectronics and Nanometer Structures*, vol. 3, pp. 784 – 787, 04 1985.

[103] K. Iga, S. Kinoshita, and F. Koyama, "Microcavity galaas/gaas surface-emitting laser with ith = 6 ma," *Electronics Letters*, vol. 23, no. 3, pp. 134–136, 1987.

[104] T. Sakaguchi, F. Koyama, and K. Iga, "Vertical cavity surface-emitting laser with an algaas/alas bragg reflector," *Electronics Letters*, vol. 24, no. 15, pp. 928–929, 1988.

[105] P. L. Gourley and T. J. Drummond, "Visible, room-temperature, surface-emitting laser using an epitaxial Fabry-Perot resonator with AlGaAs/AlAs quarter-wave high reflectors and AlGaAs/GaAs multiple quantum wells," *Applied Physics Letters*, vol. 50, no. 18, pp. 1225–1227, May 1987.

[106] J. L. Jewell, A. Scherer, S. L. McCall, Y. H. Lee, S. Walker, J. P. Harbison, and L. T. Florez, "Low-threshold electrically pumped vertical-cavity surface-emitting microlasers," *Electronics Letters*, vol. 25, no. 17, pp. 1123–1124, 1989.

[107] Y. H. Lee, J. L. Jewell, A. Scherer, S. L. McCall, J. P. Harbison, and L. T. Florez, "Room-temperature continuous-wave vertical-cavity single-quantum-well microlaser diodes," *Electronics Letters*, vol. 25, no. 20, pp. 1377–1378, 1989.

[108] Y. H. Lee, B. Tell, K. Brown-Goebeler, J. L. Jewell, and J. V. Hove, "Top-surface-emitting gaas four-quantum-well lasers emitting at 0.85 mu m," *Electronics Letters*, vol. 26, no. 11, pp. 710–711, 1990.

[109] R. S. Geels, S. W. Corzine, J. W. Scott, D. B. Young, and L. A. Coldren, "Low threshold planarized vertical-cavity surface-emitting lasers," *IEEE Photonics Technology Letters*, vol. 2, no. 4, pp. 234–236, 1990.

[110] J. Dallesasse, N. Holonyak, A. Sugg, T. Richard, and N. El-Zein, "Hydrolyzation oxidation of alxga1-xas-alas-gaas quantum well heterostructures and superlattices," *Applied Physics Letters*, vol. 57, pp. 2844 – 2846, 01 1991.

[111] J. Dallesasse and J. Holonyak, "Oxidation of al-bearing iii-v materials: A review of key progress," *Journal of Applied Physics*, vol. 113, 02 2013.

[112] A. Liu, P. Wolf, J. Lott, and D. Bimberg, "Vertical-cavity surface-emitting lasers for data communication and sensing," *Photonics Research*, vol. 7, p. 121, 02 2019.

[113] I. Melngailis, "Longitudinal Injection-Plasma Laser of InSb," *Applied Physics Letters*, vol. 6, no. 3, pp. 59–60, Feb. 1965.

[114] K. Iga, "Surface-emitting laser-its birth and generation of new optoelectronics field," *IEEE Journal of Selected Topics in Quantum Electronics*, vol. 6, no. 6, pp. 1201–1215, 2000.

[115] J. S. Eng and C. Kocot, "Surface emitting laser," *IEICE, C-I*, pp. 483–493, 9 1998.

[116] H. Soda, K. ichi Iga, C. Kitahara, and Y. Suematsu, "GaInAsP/InP surface emitting injection lasers," *Japanese Journal of Applied Physics*, vol. 18, no. 12, pp. 2329–2330, dec 1979. [Online]. Available: https://doi.org/10.1143%2Fjjap.18.2329

[117] D. Schlenker, T. Miyamoto, Z. Chen, F. Koyama, and K. Iga, "1.17-m highly strained gainas-gaas quantum-well laser," *IEEE Photonics Technology Letters*, vol. 11, pp. 946–948, 1999.

[118] P. G. S. P. A. C. J.-M. G. G. B. R. S. R. H. M. H. J. B. E. Pougeoise, Ph. Gilet and P. Sundgren, "Strained ingaas quantum well vertical cavity surface emitting lasers emitting at 1.3 m," *Electron Letters*, vol. 42, pp. 584–586, 05 2006.

[119] N. Niskiyama, M. Arai, S. Shinada, M. Azuchi, T. Miyamoto, F. Koyama, and K. Iga, "Highly strained gainas-gaas quantum-well vertical-cavity surface-emitting laser on gaas (311)b substrate for stable polarization operation," *IEEE Journal of Selected Topics in Quantum Electronics*, vol. 7, no. 2, pp. 242–248, 2001.

[120] C. Asplund, P. Sundgren, S. Mogg, M. Hammar, U. Christiansson, V. Oscarsson, C. Runnstrm, E. Odling, and J. Malmquist, "1260 nm ingaas vertical-cavity lasers," *Electronics Letters*, vol. 38, no. 13, pp. 635–636, 2002.

[121] H.-C. Kuo, Y. Chang, H. Yao, Y. Chang, F.-I. Lai, M. Tsai, and S.-C. Wang, "High-speed modulation of ingaas: Sb-gaas-gaasp quantum-well vertical-cavity surface-emitting lasers with 1.27-m emission wavelength," *Photonics Technology Letters, IEEE*, vol. 17, pp. 528 – 530, 04 2005.

[122] R. Marcks von Würtemberg, P. Maly Sundgren, J. Berggren, M. Hammar, M. Ghisoni, E. Ödling, V. Oscarsson, and J. Malmquist, "1.3 m ingaas vertical-cavity surface-emitting lasers with mode filter for single mode operation," *Applied Physics Letters*, vol. 85, pp. 4851–4853, 11 2004.

[123] D. Babic, K. Streubel, R. Mirin, N. Margalit, J. Bowers, E. Hu, D. Mars, L. Yang, and K. Carey, "Room-temperature continuous-wave operation of 1.54-m vertical-cavity lasers," *Photonics Technology Letters, IEEE*, vol. 7, pp. 1225 – 1227, 12 1995.

[124] M. Ortsiefer, R. Shau, G. Böhm, F. Köhler, and M.-C. Amann, "Low-threshold index-guided 1.5 m long-wavelength vertical-cavity surface-emitting laser with high efficiency," *Applied Physics Letters*, vol. 76, pp. 2179–2181, 04 2000.

[125] V. Jayaraman, M. Mehta, A. W. Jackson, S. Wu, Y. Okuno, J. Piprek, and J. E. Bowers, "High-power 1320-nm wafer-bonded vcsels with tunnel junctions," *IEEE Photonics Technology Letters*, vol. 15, no. 11, pp. 1495–1497, 2003.

[126] C.-K. Lin, D. P. Bour, J. Zhu, W. Perez, M. H. Leary, A. Tandon, S. Corzine, and M. R. T. Tan, "High temperature continuous-wave operation of 1.3-1.55 /spl mu/m vcsels with inp/air-gap dbrs," *IEEE 18th International Semiconductor Laser Conference*, pp. 145–146, 2002.

[127] N. Nishiyama, C. Caneau, B. Hall, G. Guryanov, M. H. Hu, X. S. Liu, M. . Li, R. Bhat, and C. E. Zah, "Long-wavelength vertical-cavity surface-emitting lasers on inp with lattice matched algainas–inp dbr grown by mocvd," *IEEE Journal of Selected Topics in Quantum Electronics*, vol. 11, no. 5, pp. 990–998, 2005.

[128] Julian Cheng, Chan-Long Shieh, Xiaodong Huang, Guoli Liu, M. V. R. Murty, C. C. Lin, and D. X. Xu, "Efficient cw lasing and high-speed modulation of 1.3-m algainas vcsels with good high temperature lasing performance," *IEEE Photonics Technology Letters*, vol. 17, no. 1, pp. 7–9, 2005.

[129] M. V. R. Murty, X. D. Huang, G. L. Liu, C. C. Lin, D. Xu, C. L. Shieh, H. C. Lee, and J. Cheng, "Long-wavelength vcsel-based cwdm scheme for 10-gbe links," *IEEE Photonics Technology Letters*, vol. 17, no. 6, pp. 1286–1288, 2005.

[130] V. Iakovlev, G. Suruceanu, A. Caliman, A. Mereuta, A. Mircea, C. . Berseth, A. Syrbu, A. Rudra, and E. Kapon, "High-performance single-mode vcsels in the 1310-nm waveband," *IEEE Photonics Technology Letters*, vol. 17, no. 5, pp. 947–949, 2005.

[131] W. Hofmann, N. H. Zhu, M. Ortsiefer, G. Bohm, J. Rosskopf, L. Chao, S. Zhang, M. Maute, and M. . Amann, "10-gb/s data transmission using bcb passivated 1.55-m ingaalas-inp vcsels," *IEEE Photonics Technology Letters*, vol. 18, no. 2, pp. 424–426, 2006.

[132] J. Boucart, G. Suruceanu, P. Royo, V. I. Iakovlev, A. Syrbu, A. Caliman, A. Mereuta, A. Mircea, C. . Berseth, A. Rudra, and E. Kapon, "3.125-gb/s modulation up to 70/spl deg/c using 1.3-/spl mu/m vcsels fabricated with localized wafer fusion for 10gbase lx4 applications," *IEEE Photonics Technology Letters*, vol. 18, no. 4, pp. 571–573, 2006.

[133] T. Anan, M. Yamada, K. Nishi, K. Kurihara, K. Tokutome, A. Kamei, and S. Sugou, "Continuous-wave operation of 1.30 [micro sign]m gaassb/gaas vcsels," *Electronics Letters*, vol. 37, pp. 566 – 567, 05 2001.

[134] D. C. Kilper, F. Quochi, J. E. Cunningham, and M. Dinu, "High-speed dynamics of gaassb vertical-cavity lasers," *IEEE Photonics Technology Letters*, vol. 14, no. 4, pp. 438–440, 2002.

[135] P. Dowd, S. R. Johnson, S. A. Feld, M. Adamcyk, S. A. Chaparro, J. Joseph, K. Hilgers, M. P. Horning, K. Shiralagi, and Y. . Zhang, "Long wavelength gaasp/gaas/gaassb vcsels on gaas substrates for communications applications," *Electronics Letters*, vol. 39, no. 13, pp. 987–988, 2003.

[136] K. Choquette, J. Klem, A. Fischer, O. Blum, A. Allerman, I. Fritz, S. Kurtz, W. Breiland, R. Sieg, K. Geib, J. Scott, and R. Naone, "Room temperature continuous wave ingaasn quantum well vertical-cavity lasers emitting at 1.3 ??m," *Electronics Letters*, vol. 36, pp. 1388 – 1390, 09 2000.

[137] T. Kageyama, T. Miyamoto, S. Makino, N. Nishiyama, F. Koyama, and K. Iga, "High-temperature operation up to 170 °c of gainnas-gaas quantum-well lasers grown by chemical beam epitaxy," *Photonics Technology Letters, IEEE*, vol. 12, pp. 10 – 12, 02 2000.

[138] A. W. Jackson, R. L. Naone, M. J. Dalberth, J. M. Smith, K. J. Malone, D. W. Kisker, J. F. Klem, K. D. Choquette, D. K. Serkland, and K. M. Geib, "Oc-48 capable ingaasn vertical cavity lasers," *Electronics Letters*, vol. 37, no. 6, pp. 355–356, 2001.

[139] A. Ramakrishnan, G. Steinle, D. Supper, C. Degen, and G. Ebbinghaus, "Electrically pumped 10 gbit/s movpe-grown monolithic 1.3 mu m vcsel with gainnas active region," *Electronics Letters*, vol. 38, pp. 322 – 324, 04 2002.

[140] T. Takeuchi, Y.-L. Chang, M. Leary, A. Tandon, H. Luan, D. Bour, S. Corzine, R. Twist, and M. Tan, "1.3 m ingaasn vertical cavity surface emitting lasers grown by mocvd," *Electronics Letters*, vol. 38, pp. 1438 – 1440, 12 2002.

[141] T. Nishida, M. Takaya, S. Kakinuma, and T. Kaneko, "4.2-mw gainnas long-wavelength vcsel grown by metalorganic chemical vapor deposition," *IEEE Journal of Selected Topics in Quantum Electronics*, vol. 11, no. 5, pp. 958–961, 2005.

[142] J. Jewell, L. Graham, M. Crom, K. Maranowski, J. Smith, and T. Fanning, "1310nm vcsels in 1-10gb/s commercial applications," *Proc. SPIE*, vol. 6132, 02 2006.

[143] M. A. Wistey, S. R. Bank, H. P. Bae, H. B. Yuen, E. R. Pickett, L. L. Goddard, and J. S. Harris, "Gainnassb/gaas vertical cavity surface emitting lasers at 1534 nm," *Electronics Letters*, vol. 42, no. 5, pp. 282–283, 2006.

[144] J. Lott, N. Ledentsov, V. Ustinov, N. Maleev, A. Zhukov, A. Kovsh, M. Maximov, B. Volovik, Z. Alferov, and D. Bimberg, "Inas-ingaas quantum dot vcsels on gaas substrates emitting at 1.3 [micro sign]m," *Electronics Letters*, vol. 36, pp. 1384 – 1385, 09 2000.

[145] A. N. AL-Omari and K. L. Lear, "Polyimide-planarized vertical-cavity surface-emitting lasers with 17.0-ghz bandwidth," *IEEE Photonics Technology Letters*, vol. 16, no. 4, pp. 969–971, 2004.

[146] D. M. Kuchta, P. Pepeljugoski, and Y. Kwark, "Vcsel modulation at 20 gb/s over 200 m of multimode fiber using a 3.3 v sige laser driver ic," in *2001 Digest of LEOS Summer Topical Meetings: Advanced Semiconductor Lasers and Applications/Ultraviolet and Blue Lasers and Their Applications/Ultralong Haul DWDM Transmission and Networking/WDM Compo*, 2001, pp. 2 pp.–.

[147] P. Pepeljugoski, D. Kuchta, Y. Kwark, P. Pleunis, and G. Kuyt, "15.6-gb/s transmission over 1 km of next generation multimode fiber," *IEEE Photonics Technology Letters*, vol. 14, no. 5, pp. 717–719, 2002.

[148] C. J. Chang-Hasnain, J. P. Harbison, C. . Zah, M. W. Maeda, L. T. Florez, N. G. Stoffel, and T. . Lee, "Multiple wavelength tunable surface-emitting laser arrays," *IEEE Journal of Quantum Electronics*, vol. 27, no. 6, pp. 1368–1376, 1991.

[149] F. Koyama, T. Mukaihara, Y. Hayashi, N. Ohnoki, N. Hatori, and K. Iga, "Wavelength control of vertical cavity surface-emitting lasers by using nonplanar mocvd," *IEEE Photonics Technology Letters*, vol. 7, no. 1, pp. 10–12, 1995.

[150] L. E. Eng, K. Bacher, Wupen Yuen, J. S. Harris, and C. J. Chang-Hasnain, "Multiple-wavelength vertical cavity laser arrays on patterned substrates," *IEEE Journal of Selected Topics in Quantum Electronics*, vol. 1, no. 2, pp. 624–628, 1995.

[151] G. G. Ortiz, S. Q. Luong, S. Z. Sun, J. Cheng, H. Q. Hou, G. A. Vawter, and B. E. Hammons, "Monolithic, multiple-wavelength vertical-cavity surface-emitting laser arrays by surface-controlled mocvd growth rate enhancement and reduction," *IEEE Photonics Technology Letters*, vol. 9, no. 8, pp. 1069–1071, 1997.

[152] Kai Yang, Yuxin Zhou, X. D. Huang, C. P. Hains, and Julian Cheng, "Monolithic oxide-confined multiple-wavelength vertical-cavity surface-emitting laser arrays with a 57-nm wavelength grading range using an oxidized upper bragg mirror," *IEEE Photonics Technology Letters*, vol. 12, no. 4, pp. 377–379, 2000.

[153] F. Koyama, "Recent advances of vcsel photonics," *Journal of Lightwave Technology*, vol. 24, no. 12, pp. 4502–4513, 2006.

[154] H. Li, P. Wolf, P. Moser, G. Larisch, J. Lott, and D. Bimberg, "Vertical-cavity surface-emitting lasers for optical interconnects," *SPIE Newsroom*, 11 2014.

[155] C. G. Van de Walle, "Band lineups and deformation potentials in the model-solid theory," *Phys. Rev. B*, vol. 39, pp. 1871–1883, Jan 1989. [Online]. Available: https://link.aps.org/doi/10.1103/PhysRevB.39.1871

[156] Y. K. T. W. Lin, "Internal technical report." [Online]. Available: https://scholar.google.com/scholar?q=W.+Lin,+Y.k+tu,+internal+technical+report,+telecommunication+labs.&hl=en&as_sdt=0&as_vis=1&oi=scholart

[157] T. A. D. W. J. H.-G. Y. L. W. Lin, Y. K. Tu and J. H. P, Shiao, "Cryst growth," vol. 123, 1992.

[158] N. El-Zein and B. McDermott, "Interface and material-quality study of ingaasp/inp and ingaasp1/ingaasp2 superlattices," *Conference Proceedings - International Conference on Indium Phosphide and Related Materials*, 01 2003.

[159] S. Pradana, A. Syahriar, A. H. Lubis, and S. Rahardjo, "Comparison power of semiconductor lasers at wavelength 1480nm using ingaas ingaasp materials for edfa pumping scheme," in *2018 International Conference on Smart Computing and Electronic Enterprise (ICSCEE)*, 2018, pp. 1–5.

[160] J. Piprek, D. Babic, and J. Bowers, "Simulation and analysis of 1.55 m double-fused vertical-cavity lasers," *Journal of Applied Physics*, vol. 81, pp. 3382 – 3390, 05 1997.

[161] K. Kandiah, P. S. Menon, S. Shaari, and B. Majlis, "Design and modeling of a vertical-cavity surface-emitting laser (vcsel)," 12 2008, pp. 297 – 301.

[162] D. B. Werner Hofmann, "Vcsel-based light sources-scalability challenges for vcsel-based multi-100-gb/s systems," *IEEE Photonics Journal*, vol. 4, October 2012.

[163] N. Nishiyama, M. Arai, S. Shinada, T. Miyamoto, F. Koyama, and K. Iga, "Growth and optical properties of highly strained gainas/gaas quantum wells on (3 1 1)b gaas by mocvd," *Journal of Crystal Growth - J CRYST GROWTH*, vol. 221, pp. 530–534, 12 2000.

[164] W. Hofmann, E. Wong, G. Bohm, M. Ortsiefer, N. H. Zhu, and M. C. Amann, "1.55-μm vcsel arrays for high-bandwidth wdm-pons," *IEEE Photonics Technology Letters*, vol. 20, no. 4, pp. 291–293, 2008.

[165] G. Keeler, D. Serkland, K. Geib, G. Peake, and A. Mar, "Single transverse mode operation of electrically pumped vertical-external-cavity surface-emitting lasers with micromirrors," *IEEE Photonics Technology Letters*, vol. 17, no. 3, pp. 522–524, 2005.

[166] E. Kotelnikov, A. Katsnelson, K. Patel, and I. Kudryashov, "High-power single-mode ingaasp/inp laser diodes for pulsed operation," *Proceedings of SPIE - The International Society for Optical Engineering*, pp. 22–, 02 2012.

[167] P. Doussiere, C.-L. Shieh, S. DeMars, and K. Dzurko, "Very high power 1310nm inp single mode distributed feed back laser diode with reduced linewidth - art. no. 64850g," *Proc SPIE*, vol. 6485, 03 2007.

[168] N. Das, H. Hsen, P. Newman, M. Lara, and W. Chang, "Design and fabrication of 850 and 980 nm vertical cavity surface emitting laser," p. 22, 03 2004.

[169] C.-K. Lin, D. Bour, J. Zhu, W. Perez, M. Leary, A. Tandon, S. Corzine, and M. Tan, "High temperature continuous-wave operation of 1.3- and 1.55-m vcsels with inp/air-gap dbrs," *Selected Topics in Quantum Electronics, IEEE Journal of*, vol. 9, pp. 1415 – 1421, 10 2003.

[170] F. Marino, S. Barland, and S. Balle, "Single-mode operation and transverse-mode control in VCSELs induced by frequency-selective feedback," *IEEE Photonics Technology Letters*, vol. 15, no. 6, pp. 789–791, 2003.

[171] S. Y. Hu, J. Ko, and L. A. Coldren, "High-performance densely packed vertical-cavity photonic integrated emitter arrays for direct-coupled WDM applications," *IEEE Photonics Technology Letters*, vol. 10, no. 6, pp. 766–768, 1998.

[172] N. Nishiyama, A. Mizutani, N. Hatori, M. Arai, F. Koyama, and K. Iga, "Single-transverse mode and stable-polarization operation under high-speed modulation of inGaAs-GaAs vertical-cavity surface-emitting laser grown on GaAs (311) B substrate," *IEEE Photonics Technology Letters*, vol. 10, no. 12, pp. 1676–1678, 1998.

[173] P. Westbergh, R. Safaisini, E. Haglund, B. Kögel, J. S. Gustavsson, A. Larsson, M. Geen, R. Lawrence, and A. Joel, "High-speed 850 nm vcsels with 28 ghz modulation bandwidth operating error-free up to 44 gbit/s," *Electronics Letters*, vol. 48, no. 18, pp. 1145–1147, 2012.

[174] D. M. Kuchta, A. V. Rylyakov, F. E. Doany, C. L. Schow, J. E. Proesel, C. W. Baks, P. Westbergh, J. S. Gustavsson, and A. Larsson, "A 71-gb/s nrz modulated 850-nm vcsel-based optical link," *IEEE Photonics Technology Letters*, vol. 27, no. 6, pp. 577–580, 2015.

[175] E. Haglund, P. Westbergh, J. S. Gustavsson, E. P. Haglund, and A. Larsson, "High-speed vcsels with strong confinement of optical fields and carriers," *Journal of Lightwave Technology*, vol. 34, no. 2, pp. 269–277, 2016.

[176] E. Haglund, P. Westbergh, J. S. Gustavsson, E. P. Haglund, A. Larsson, M. Geen, and A. Joel, "30 ghz bandwidth 850 nm vcsel with sub-100 fj/bit energy dissipation at 25–50 gbit/s," *Electronics Letters*, vol. 51, no. 14, pp. 1096–1098, 2015.

[177] Y. . Chang, C. S. Wang, and L. A. Coldren, "High-efficiency, high-speed vcsels with 35 gbit=s error-free operation," *Electronics Letters*, vol. 43, no. 19, pp. 1022–1023, 2007.

[178] W. Hofmann, P. Moser, P. Wolf, A. Mutig, M. Kroh, and D. Bimberg, "44 gb/s vcsel for optical interconnects," 03 2011.

[179] P. Wolf, P. Moser, G. Larisch, W. Hofmann, and D. Bimberg, "High-speed and temperature-stable, oxide-confined 980-nm vcsels for optical interconnects," *IEEE Journal of Selected Topics in Quantum Electronics*, vol. 19, no. 4, pp. 1 701 207–1 701 207, 2013.

[180] P. Moser, J. A. Lott, G. Larisch, and D. Bimberg, "Impact of the oxide-aperture diameter on the energy efficiency, bandwidth, and temperature stability of 980-nm vcsels," *Journal of Lightwave Technology*, vol. 33, no. 4, pp. 825–831, 2015.

[181] R. Rosales, M. Zorn, and J. A. Lott, "30-ghz bandwidth with directly current-modulated 980-nm oxide-aperture vcsels," *IEEE Photonics Technology Letters*, vol. 29, no. 23, pp. 2107–2110, 2017.

[182] N. Haghighi, R. Rosales, G. Larisch, M. Gębski, L. Frasunkiewicz, T. Czyszanowski, and J. A. Lott, "Simplicity VCSELs," in *Vertical-Cavity*

Surface-Emitting Lasers XXII, C. Lei and K. D. Choquette, Eds., vol. 10552, International Society for Optics and Photonics. SPIE, 2018, pp. 119 – 127. [Online]. Available: https://doi.org/10.1117/12.2295028

[183] K. Yashiki, N. Suzuki, K. Fukatsu, T. Anan, H. Hatakeyama, and M. Tsuji, "1.1-$\mu$$m - rangehigh - speedtunneljunctionvertical - cavitysurface - emittinglasers," *IEEE Photonics Technology Letters, vol.* 19, *pp.*1883 - -1885, 2007.

[184] N. Suzuki, T. Anan, H. Hatakeyama, K. Fukatsu, K. Yashiki, K. Tokutome, T. Akagawa, and M. Tsuji, "High speed 1.1-m-range ingaas-based vcsels," *IEICE Transactions*, vol. 92-C, pp. 942–950, 07 2009.

[185] P. Westbergh, J. S. Gustavsson, Haglund, M. Skold, A. Joel, and A. Larsson, "High-speed, low-current-density 850 nm vcsels," *IEEE Journal of Selected Topics in Quantum Electronics*, vol. 15, no. 3, pp. 694–703, 2009.

[186] S. Healy, E. O'Reilly, J. Gustavsson, P. Westbergh, Haglund, A. Larsson, and A. Joel, "Active region design for high-speed 850-nm vcsels," *Quantum Electronics, IEEE Journal of*, vol. 46, pp. 506 – 512, 05 2010.

[187] N. Haghighi, G. Larisch, R. Rosales, M. Zorn, and J. A. Lott, "35 ghz bandwidth with directly current modulated 980 nm oxide aperture single cavity vcsels," in *2018 IEEE International Semiconductor Laser Conference (ISLC)*, 2018, pp. 1–2.

[188] D. Mahgerefteh, C. Thompson, C. Cole, G. Denoyer, T. Nguyen, I. Lyubomirsky, C. Kocot, and J. Tatum, "Techno-economic comparison of silicon photonics and multimode vcsels," *J. Lightwave Technol.*, vol. 34, no. 2, pp. 233–242, Jan 2016. [Online]. Available: http://jlt.osa.org/abstract.cfm?URI=jlt-34-2-233

[189] H. Liu, C. F. Lam, and C. Johnson, "Scaling optical interconnects in datacenter networks opportunities and challenges for wdm," in *2010 18th IEEE Symposium on High Performance Interconnects*, 2010, pp. 113–116.

[190] Silvaco, "DevEdit Manual," no. 408, pp. 1–2, 2010.

[191] S. Clara, "ATHENA User ' s Manual 2D PROCESS SIMULATION SOFTWARE," vol. 95054, no. August, 2004.

[192] D. A. B. Miller, "Device requirements for optical interconnects to silicon chips," *Proceedings of the IEEE*, vol. 97, no. 7, pp. 1166–1185, 2009.

[193] H. Li, P. Wolf, P. Moser, G. Larisch, J. Lott, and D. Bimberg, "Temperature-stable, energy-efficient, and high-bit rate oxide-confined 980-nm vcsels for optical interconnects," *IEEE Journal of Selected Topics in Quantum Electronics*, vol. 21, pp. 1–9, 11 2015.

[194] H. Li, P. Wolf, P. Moser, G. Larisch, A. Mutig, J. A. Lott, and D. H. Bimberg, "Impact of the quantum well gain-to-cavity etalon wavelength offset on the high temperature performance of high bit rate 980-nm vcsels," *IEEE Journal of Quantum Electronics*, vol. 50, no. 8, pp. 613–621, 2014.

[195] S. Selmic, T.-M. Chou, J. Sih, J. Kirk, A. Mantle, J. Butler, D. Bour, and G. Evans, "Design and characterization of 1.3-/spl mu/m algainas-inp multiple-quantum-well lasers," *IEEE Journal of Selected Topics in Quantum Electronics*, vol. 7, no. 2, pp. 340–349, 2001.

[196] P. R. Moser, W. Hofmann, P. Wolf, J. A. Lott, G. Larisch, A. Payusov, N. N. Ledentsov, and D. Bimberg, "81 fj/bit energy-to-data ratio of 850 nm vertical-cavity surface-emitting lasers for optical interconnects," 2011.

[197] A. Mutig, J. Lott, S. Blokhin, P. Moser, P. Wolf, W. Hofmann, A. Nadtochiy, and D. Bimberg, "High speed 980 nm vcsels for short reach optical interconnects operating error-free at 25 gbit/s up to 85 °c," 05 2011.

[198] P. Westbergh, J. S. Gustavsson, B. Kögel, Haglund, and A. Larsson, "Impact of photon lifetime on high-speed vcsel performance," *IEEE Journal of Selected Topics in Quantum Electronics*, vol. 17, no. 6, pp. 1603–1613, 2011.

[199] P. Goyal, M. Sharma, A. Jha, M. Kumari, S. P. Singh, N. Singh, and G. Kaur, "Design and analysis of vcsel laser for third window of optical communication system," in *2016 International Conference on Electrical, Electronics, and Optimization Techniques (ICEEOT)*, 2016, pp. 4220–4224.

[200] M. Kuznetsov, F. Hakimi, R. Sprague, and A. Mooradian, "Design and characteristics of high-power (>0.5-w cw) diode-pumped vertical-external-cavity surface-emitting semiconductor lasers with circular tem/sub 00/ beams," *IEEE Journal of Selected Topics in Quantum Electronics*, vol. 5, no. 3, pp. 561–573, 1999.

[201] A. Shchegrov, A. Umbrasas, J. Watson, D. Lee, C. Amsden, W. Ha, G. Carey, V. Doan, B. Moran, A. Lewis, and A. Mooradian, "532-nm laser sources based on intracavity frequency doubling of extended-cavity surface-emitting diode lasers," *Proc SPIE*, vol. 5332, pp. 151–156, 07 2004.

[202] Y. Hayashi, T. Mukaihara, N. Hatori, N. Ohnoki, A. Matsutani, F. Koyama, and K. Iga, "Lasing characteristics of low-threshold oxide confinement ingaas-gaalas vertical-cavity surface-emitting lasers," *IEEE Photonics Technology Letters*, vol. 7, no. 11, pp. 1234–1236, 1995.

[203] K. L. Lear, K. D. Choquette, R. P. Schneider, S. P. Kilcoyne, and K. M. Geib, "Selectively oxidised vertical cavity surface emitting lasers with 50 % power conversion efficiency," *Electronics Letters*, vol. 31, no. 3, pp. 208–209, 1995.

[204] R. Jager, M. Grabherr, C. Jung, R. Michalzik, G. Reiner, B. Weigl, and K. J. Ebeling, "57wavelength gaas vcsels," *Electronics Letters*, vol. 33, no. 4, pp. 330–331, 1997.

[205] H. Li, D. B. Phillips, X. Wang, Y.-L. D. Ho, L. Chen, X. Zhou, J. Zhu, S. Yu, and X. Cai, "Orbital angular momentum vertical-cavity surface-emitting lasers," *Optica*, vol. 2, no. 6, pp. 547–552, Jun 2015. [Online]. Available: http://www.osapublishing.org/optica/abstract.cfm?URI=optica-2-6-547

[206] A.-J. Liu, W. Chen, W.-J. Zhou, B. Jiang, F. Fu, H.-W. Qu, and W.-H. Zheng, "Squeeze effect and coherent coupling behaviour in photonic crystal vertical-cavity surface-emitting lasers," *Journal of Physics D: Applied Physics*, vol. 44, no. 23, p. 239501, may 2011. [Online]. Available: https://doi.org/10.1088%2F0022-3727%2F44%2F23%2F239501

[207] R. Puerta, M. Agustin, Chorchos, J. Toński, J. R. Kropp, N. Ledentsov, V. A. Shchukin, N. N. Ledentsov, R. Henker, I. T. Monroy, J. J. V. Olmos, and J. P. Turkiewicz, "Effective 100 gb/s im/dd 850-nm multi- and single-mode vcsel transmission through om4 mmf," *Journal of Lightwave Technology*, vol. 35, no. 3, pp. 423–429, 2017.

[208] I. Lu, C. Wei, H. Chen, K. Chen, C. Huang, K. Chi, J. Shi, F. Lai, D. Hsieh, H. Kuo, W. Lin, S. Chiu, and J. Chen, "Very high bit-rate distance product using high-power single-mode 850-nm vcsel with discrete multitone modulation formats through om4 multimode fiber," *IEEE Journal of Selected Topics in Quantum Electronics*, vol. 21, no. 6, pp. 444–452, 2015.